

ESTIMATION OF SONOBUOY POSITION
RELATIVE TO AN AIRCRAFT
USING EXTENDED KALMAN FILTERS

Nicholas Mason Brownsberger

NAVAL POSTGRADUATE SCHOOL

Monterey, California



THESIS

Estimation of Sonobuoy Position
Relative to an Aircraft
Using Extended Kalman Filters

by

Nicholas Mason Brownsberger

September 1979

Thesis Advisor:

D. J. Collins

Approved for public release; distribution unlimited

T189584

REPORT DOCUMENTATION PAGE		READ INSTRUCTIONS BEFORE COMPLETING FORM
1. REPORT NUMBER	2. GOVT ACCESSION NO.	3. RECIPIENT'S CATALOG NUMBER
4. TITLE (and Subtitle) Estimation of Sonobuoy Position Relative to an Aircraft Using Extended Kalman Filters		5. TYPE OF REPORT & PERIOD COVERED Master's and Engineer's Thesis; September 1979
7. AUTHOR(s) Nicholas Mason Brownsberger		6. PERFORMING ORG. REPORT NUMBER
9. PERFORMING ORGANIZATION NAME AND ADDRESS Naval Postgraduate School Monterey, California 93940		8. CONTRACT OR GRANT NUMBER(s)
11. CONTROLLING OFFICE NAME AND ADDRESS Naval Postgraduate School Monterey, California 93940		10. PROGRAM ELEMENT, PROJECT, TASK AREA & WORK UNIT NUMBERS
14. MONITORING AGENCY NAME & ADDRESS (if different from Controlling Office) Naval Postgraduate School Monterey, California 93940		12. REPORT DATE September 1979
		13. NUMBER OF PAGES
		15. SECURITY CLASS. (of this report) Unclassified
16. DISTRIBUTION STATEMENT (of this Report) Approved for public release; distribution unlimited		15a. DECLASSIFICATION/DOWNGRADING SCHEDULE
17. DISTRIBUTION STATEMENT (of the abstract entered in Block 20, if different from Report)		
18. SUPPLEMENTARY NOTES		
19. KEY WORDS (Continue on reverse side if necessary and identify by block number) SRS (Sonobuoy Reference System) Kalman Filter Sonobuoy		
20. ABSTRACT (Continue on reverse side if necessary and identify by block number) In airborne anti-submarine warfare there is a need to more accurately determine the positions of sonobuoys on the surface of the water. This report develops two algorithms which employ extended Kalman filters to determine estimated position. The bearing from the aircraft to the sonobuoy is the primary measurement. Range information is not available. The first algorithm is a six-state filter which was reduced from the		

13-state system developed by the Orincon Corporation. Its states include relative position, relative velocity, and inertial misalignments. The second algorithm includes two cascaded Kalman filters. The primary two-state filter estimates sonobuoy position. A secondary filter estimates drift from information obtained from the primary filter. Both algorithms successfully estimated sonobuoy position for simulated aircraft data. The effect of aircraft-to-sonobuoy range, the frequency of measurement, and changes in altitude are also analyzed.

Approved for public release; distribution unlimited

Estimation of Sonobuoy Position
Relative to an Aircraft
Using Extended Kalman Filters

by

Nicholas Mason Brownsberger
Lieutenant, United States Navy
B.S., United States Naval Academy, 1972

Submitted in partial fulfillment of the
requirements for the degrees of

MASTER OF SCIENCE IN AERONAUTICAL ENGINEERING
AND
AERONAUTICAL ENGINEER

from the

NAVAL POSTGRADUATE SCHOOL
September 1979

ABSTRACT

In airborne anti-submarine warfare there is a need to more accurately determine the positions of sonobuoys on the surface of the water. This report develops two algorithms which employ extended Kalman filters to determine estimated position. The bearing from the aircraft to the sonobuoy is the primary measurement. Range information is not available. The first algorithm is a six-state filter which was reduced from the 13-state system developed by the Orincon Corporation. Its states include relative position, relative velocity, and inertial misalignments. The second algorithm includes two cascaded Kalman filters. The primary two-state filter estimates sonobuoy position. A secondary filter estimates drift from information obtained from the primary filter. Both algorithms successfully estimated sonobuoy position for simulated aircraft data. The effect of aircraft-to-sonobuoy range, the frequency of measurement, and changes in altitude are also analyzed.

TABLE OF CONTENTS

I.	INTRODUCTION - - - - -	10
II.	FILTERS - - - - -	13
III.	MODELS - - - - -	20
	A. GENERAL APPROACHES TO SYSTEM MODELING - - - -	20
	B. THE COORDINATE SYSTEM - - - - -	22
	C. THE SIX-STATE SYSTEM - - - - -	23
	D. THE TWO-STATE SYSTEM - - - - -	37
IV.	ANAYLSIS - - - - -	43
	A. THE SIMULATION - - - - -	43
	B. THE RESULTS - - - - -	56
V.	CONCULSION - - - - -	27
VI.	SUMMARY - - - - -	89
	APPENDIX A: THE COMPUTER PROGRAMS - - - - -	92
	APPENDIX B: COMPUTER PROGRAM FOR DATA GENERATION - - -	127
	APPENDIX C: RMS POSITION ERRORS FOR RANGE, FREQUENCY, AND ALTITUDE ANALYSIS - - - - -	140
	BIBLIOGRAPHY - - - - -	149
	INITIAL DISTRIBUTION LIST - - - - -	150

LIST OF FIGURES

1.	Kalman filter notation -----	15
2.	Divergence -----	18
3.	Earth fixed coordinate system -----	22
4.	Aircraft fixed coordinate system -----	22
5.	Cascaded Kalman filters -----	38
6.	Aircraft track for the 15 NM circular pattern with initial sonobuoy location and direction of drift indicated -----	46
7.	Aircraft track for the 15 NM square pattern with initial sonobuoy location and direction of drift indicated -----	47
8.	Aircraft's navigational output for the 15 NM square; navigational drift is 2.5 NM/Hr to the north -----	48
9.	Aircraft's navigational output for the 15 NM square; navigational drift is 2.5 NM/Hr north with a Schuler cycle -----	49
10.	The effect of drift in the aircraft navigational plot -----	52
11.	RMS statistics at time = k -----	55
12.	Orincon's simulation flight path -----	57
13.	Estimated position and relative errors for the six-state system using Orincon's pattern -----	67
14.	Estimated position and relative errors for the two-state system using Orincon's pattern -----	68
15.	Estimated position and relative errors for the two-state system using Orincon's pattern -----	69
16.	RMS position errors for the six-state system while flying the circular pattern developed by Orincon Corp. -----	70

17.	RMS position errors for the two-state system while flying the circular pattern developed by Orincon Corp. -----	71
18.	RMS position errors for the two-state system while flying the circular pattern developed by Orincon Corp. -----	72
19.	Estimated position and relative errors for the six-state system using circular pattern at 15 NM -----	73
20.	Estimated position and relative errors for the two-state system using circular pattern at 15 NM -	74
21.	Estimated position and relative errors for the two-state system using circular pattern at 15 NM -	75
22.	RMS position errors for the six-state system while flying a 15 NM circular pattern around the sonobuoy	76
23.	RMS position errors for the two-state system while flying a 15 NM circular pattern around the sonobuoy -----	77
24.	RMS position errors for the two-state system while flying a 15 NM circular pattern around the sonobuoy -----	78
25.	Estimated position and relative errors for the six-state system using square pattern at 15 NM ---	79
26.	Estimated position and relative errors for the two-state system using square pattern at 15 NM ---	80
27.	Estimated position and relative errors for the two-state system using square pattern at 15 NM ---	81
28.	RMS position errors for the six-state system while flying a 15 NM square pattern around the sonobuoy -----	82
29.	RMS position errors for the two-state system while flying a 15 NM square pattern around the sonobuoy -----	83
30.	RMS position errors for the two-state system while flying a 15 NM square pattern around the sonobuoy -----	84
31.	RMS position error as a function of aircraft-to-sonobuoy range, Δx , for the six-state and two-state systems -----	85

32.	RMS position error as a function of measurement interval, Δt , for the six-state and two-state systems -----	86
33.	Factors which influence the covariance -----	64
34.	Flow chart: main program -----	92
35.	Flow chart: subroutine FILTER six-state -----	93
36.	Flow chart: subroutine FILTER two-state -----	94
37.	Flow chart: data generation program -----	127
38.	RMS errors for two-state system and six-state system using circular pattern at 5 NM -----	140
39.	RMS errors for two-state system and six-state system using circular pattern at 30 NM -----	141
40.	RMS errors for two-state system and six-state system using circular pattern at 45 NM -----	142
41.	RMS errors for two-state system and six-state system using square pattern with $\Delta t = 4$ sec. -----	143
42.	RMS errors for two-state system and six-state system using square pattern with $\Delta t = 10$ sec. -----	144
43.	RMS errors for two-state system and six-state system using square pattern with $\Delta t = 30$ sec. -----	145
44.	RMS errors for two-state system and six-state system using circular pattern, Alt = 300' -----	146
45.	RMS errors for two-state system and six-state system using circular pattern, Alt = 10,000' -----	147
46.	RMS errors for two-state system and six-state system using circular pattern, Alt = 20,000' -----	148

ACKNOWLEDGEMENT

I would like to thank Dr. Birnbaum and Ms. Peggy Pembroke of NADC for their responsiveness in answering questions and supplying computer information. And to Dr. Collins I would like to express my gratitude for his help and guidance without which this thesis could not have been completed. To my wife I would like to offer my special thanks and love for her patience, understanding, and fortitude during a time which tested both of us.

Nick Brownsberger

I. INTRODUCTION

The P3 Orion is the U.S. Navy's primary long range anti-submarine warfare (ASW) aircraft. It is outfitted with equipment which allows it to search for, locate, and track submarines. The aircraft carries a Univac digital computer, the CP 901, which performs much of the navigational and tactical plotting chores. The primary sensor used by this and many other ASW aircraft is an airdropped listening device known as a sonobuoy. The Orion generally deploys several sonobuoys (4 to 20) in patterns which can cover a thousand square miles of ocean while searching for the submarine. Once contact has been made, these sonobuoys provide information which locates the submarine. The target can then be tracked (or attacked if required) until the Orion's mission is complete.

The sonobuoy is dropped from the aircraft at the geographical location designated by the aircrew. Once in the water the sonobuoy floats and deploys a hydrophone to depths varying from 50 to 500 feet. The information picked up is transmitted back to the aircraft where it is analyzed. This information can consist of the relative intensity of target noise, bearings and sometimes ranges to the target, all of which are used to fix the current position of the submarine. In order to maintain close, accurate tracking and be able to launch an attack, the submarine's position must

be accurate to within several hundred yards. The information received from the sonobuoys has some error inherent in the nature of the measurements made by the hydrophone. Sonobuoy position error also contributes significantly to the submarine tracking inaccuracies.

Historically, the positions of the sonobuoys were determined and updated by "mark-on-top"s. This required the aircraft to home on the transmitting sonobuoy until the buoy was overflown. At that instant the aircraft's position was entered into the on-board computer which slewed the buoy to this updated position. After many of these updates the computer was able to develop a bias which was applied to the sonobuoy positions in the computer effectively allowing them to drift. The method had several disadvantages. Error in the updated position was at least as great as the aircraft altitude at the time of the "mark" which could vary from 300 to 20,000 feet. The accuracy also depended on the consistency of the several pilots who might be making the mark-on-tops during the flight. The updating was not continuous in that it was several minutes between consecutive marks on one buoy at best, and more likely 30 to 60 minutes. Not all buoys were even updated. Furthermore, this method required the aircraft to overfly the submarine many times in order to make the mark-on-tops. This should be avoided.

The purpose of this thesis was to investigate some alternative methods for accurately fixing the position of

sonobuoys. They should allow the aircraft to stand-off from the sonobuoy field and still produce more accurate fixing than the historical method provided. The Naval Air Development Center (NADC) at Warminster, PA. had already partially developed such a system. This thesis was undertaken in support of their work but was conducted independently. Their system, the Sonobuoy Reference System (SRS), was already installed on the aircraft and had the capability of measuring the relative bearing to any transmitting sonobuoy. Additional information available for use included aircraft heading, altitude, and airspeed as well as doppler velocity and drift angle. Also, the aircraft's Inertial Navigational System (INS) provided geographical position although the Schuler cycle and inertial drifts could make this position several nautical miles in error. On the other hand, aircraft-to-sonobuoy range and sea surface drift information were assumed not to be available. An attempt was made to determine sonobuoy position at least relative to the aircraft with a less accurate geographical position as a secondary objective. Kalman filtering techniques were used based primarily on measurements of bearing from the aircraft to the sonobuoy.

II. FILTERS

Kalman filtering is a recursive technique for estimating the state of a system. It was developed in the 1960's by R. E. Kalman and improved upon previous methods by Wiener and others. The Wiener filter is based on frequency domain designs which are statistically optimal but are only applicable to stationary processes. The Kalman filter is based on state-space, time domain formulations and is especially suited to digital computers. From a simplistic, one-dimensional point of view, the Kalman filter recursively averages noisy measurements to provide a more precise estimate of the actual value.

Assume that a system can be linearly modeled with state equations in matrix form as

$$X_k = \Phi_{k-1} X_{k-1} + \Lambda_{k-1} U_{k-1} + \Gamma_{k-1} W_{k-1} \quad (1)$$

where X_k represents the states of the system at the k th interval. (Only the discrete case was considered in this study.) Φ_k is the transition matrix and is used to "propagate" the system from k to $k+1$. U_k represents the control input to the system and W_k represents white, gaussian noise with 0 mean and Q_k variance, written $N(0, Q_k)$. Measurements are required to update the system and are

described by the linear matrix equation

$$Z_k = H_k X_k + V_k \quad (2)$$

where Z_k is the measurement. H_k describes the relationship between the states and the measurement and V_k is measurement noise described by $N(0, R_k)$.

The discrete Kalman filter equations are:

Propagate

$$\hat{X}_k(-) = \Phi_{k-1} \hat{X}_{k-1}(+) \quad (3)$$

$$P_k(-) = \Phi_{k-1} P_{k-1}(+) \Phi_{k-1}^T + Q_{k-1} \quad (4)$$

Update

$$G_k = P_k(-) H_k^T \left[H_k P_k(-) H_k^T + R_k \right]^{-1} \quad (5)$$

$$\hat{X}_k(+) = \hat{X}_k(-) + G_k \left[Z_k - H_k \hat{X}_k(-) \right] \quad (6)$$

$$P_k(+) = \left[I - G_k H_k \right] P_k(-) \quad (7)$$

where

\hat{X}_k = estimate of the state X_k

P_k = covariance

G_k = Kalman gain

The estimate prior to the measurement is denoted by $\hat{X}_k(-)$ and can be updated after the measurement to a new estimate denoted $\hat{X}_k(+)$. This notation is shown in figure 1. The covariance matrix provides a statistical measure of the uncertainty of \hat{X} . Consider a 2 x 2 covariance matrix where the error \tilde{X} in the estimate is defined as $\hat{X} - x$:

$$P = \begin{bmatrix} E(\tilde{X}_1^2) & E(\tilde{X}_1, \tilde{X}_2) \\ E(\tilde{X}_1, \tilde{X}_2) & E(\tilde{X}_2^2) \end{bmatrix} = \begin{bmatrix} \sigma_1^2 & \sigma_1 \sigma_2 \\ \sigma_1 \sigma_2 & \sigma_2^2 \end{bmatrix} \quad (8)$$

The diagonal elements represent the mean square errors of the corresponding state variables x_1 and x_2 . The off-diagonal elements are indicators of cross-correlation between the states. The Kalman gain G is an optimal gain chosen so as to minimize the sum of the diagonal terms of the covariance matrix.

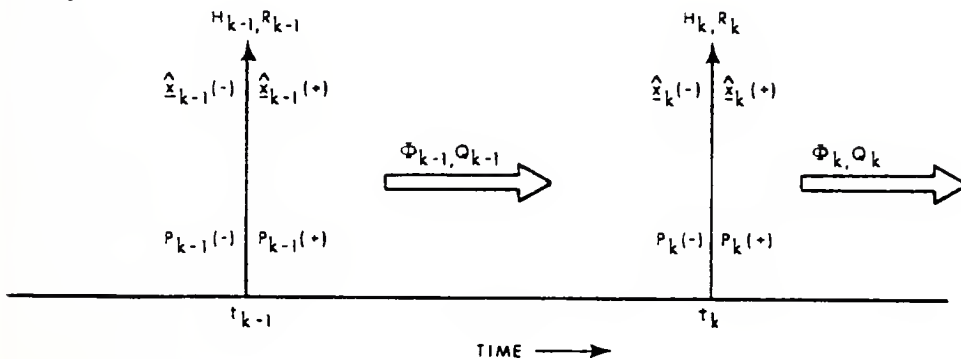


Figure 1. Kalman filter notation

If either the system model or the measurement model is non-linear, then non-linear filters must be used. Let the non-linear system be described by

$$X_k = \phi(X_{k-1}) + W_{k-1} \quad ; \quad W_k \sim N(0, Q_k) \quad (9)$$

$$Z_k = h(X_k) + V_k \quad ; \quad V_k \sim N(0, R_k) \quad (10)$$

where $\phi(\hat{X}_{k-1})$ represents the non-linear equations of the system. They can be linearized by a Taylor series expansion around the latest estimate of the state to obtain $\Phi(\hat{X}_{k-1})$. Likewise, $h(X_k)$ represents the non-linear measurement equations and by a Taylor series expansion yields $H(\hat{X}_k)$.

$$\phi(X_k) = \phi(\hat{X}_k) + \Phi(\hat{X}_k) [X_k - \hat{X}_k] + \dots \quad (11)$$

$$h(X_k) = h(\hat{X}_k) + H(\hat{X}_k) [X_k - \hat{X}_k] + \dots \quad (12)$$

where

$$\Phi(\hat{X}_k) = \frac{\partial}{\partial \mathbf{x}} \left[\phi(X_k) \right]_{\mathbf{x}=\hat{\mathbf{x}}} \quad (13)$$

$$H(\hat{X}_k) = \frac{\partial}{\partial \mathbf{x}} \left[h(X_k) \right]_{\mathbf{x}=\hat{\mathbf{x}}} \quad (14)$$

Second order Taylor series terms are neglected. Now, the extended Kalman filter can be implemented with the following equations:

Propagate

$$\hat{X}_k(-) = \phi(\hat{X}_{k-1}) \quad (15)$$

$$P_k(-) = \Phi(\hat{X}_{k-1}(-)) P_{k-1}(+) \bar{\Phi}(\hat{X}_{k-1}(-))^T + Q_{k-1} \quad (16)$$

Update

$$G = P_k(-) H(\hat{X}_k(-))^T \left[H(\hat{X}_k(-)) P_k(-) H(\hat{X}_k(-))^T + R_k \right]^{-1} \quad (17)$$

$$\hat{X}_k(+) = \hat{X}_k(-) + G_k \left[Z_k - H(\hat{X}_k(-)) \right] \quad (18)$$

$$P_k(+) = \left[I - G_k H(\hat{X}_k(-)) \right] P_k(-) \quad (19)$$

Higher order filters can be used if the linearization errors are large. The second order Kalman filter employs one more term in the Taylor series expansion by modifying the update equations of the extended Kalman filter to account for this term. The iterated extended Kalman filter uses the same equations as does the extended Kalman filter. However, the calculations are repeated, each time linearizing about the most recent estimate, until there is little further improvement with each new iteration. The iterated extended filter can greatly reduce the errors due to non-linearities, more so than the second order filter.

Kalman filters should be based on correctly modeled systems and accurate noise statistics to ensure proper

performance. This is not always possible either due to ignorance about the system or lack of sufficient statistical information. A filter which is not operating properly may diverge. Apparent divergence describes that situation where the true estimation errors are larger than the filter predicted errors although they are bounded. True divergence is characterized by errors which continue to grow with time and eventually become infinite. These divergence phenomenon are depicted in figure 2.

There are several ways to overcome the divergence problem when the modeling is not completely accurate such as adding fictitious noise. This allows the filter a little more freedom to adjust to whatever modeling inconsistencies may exist, but makes the filter estimate appear more erratic. Another method which helps overcome divergence is finite memory filtering. Since Kalman gains tend to grow smaller and smaller as time passes, they may reach a point

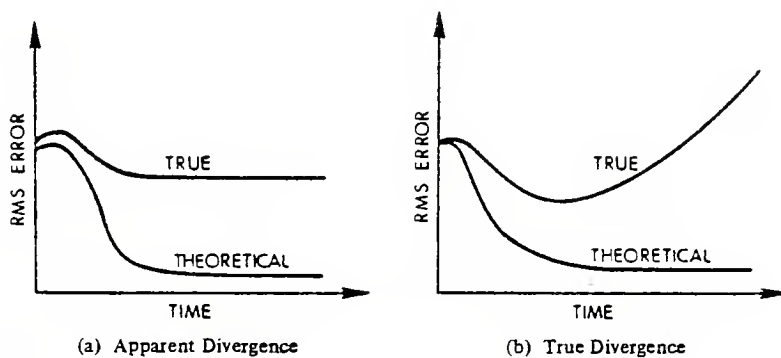


Figure 2. Divergence

where new measurement information has no effect on the estimates. Finite memory filtering effectively eliminates old data which is no longer useful by keeping the gains significant. This is sometimes called a "moving window".

Some simplifying techniques used in Kalman filters include precomputed gains. Although forfeiting the optimal Kalman gains, this has the advantage of reducing computational burden. More importantly, the gains can be controlled to overcome modeling weaknesses if necessary. Another technique which can be used when more than one measurement is provided to a filter is processing them one at a time. This avoids taking the inverse of more than a scalar when computing the updated covariance matrix $P_k(+)$. This is possible if the simultaneous measurements are considered to be taken sequentially over a zero time span.

III. MODELS

A. GENERAL APPROACHES TO SYSTEM MODELING

The aircraft-sonobuoy system must be modeled in state-space for use with the Kalman filter. There are at least two approaches to the modeling of this problem depending on the point of view. One intuitive approach is to assume the sonobuoy drifts at a constant velocity and then use aircraft-to-sonobuoy bearing measurements to locate the sonobuoy. The states become sonobuoy position and sonobuoy velocity. Unfortunately, this problem is not observable. The bearing measurements provide only information about position; there is no rate of change information in the bearings themselves. In addition, the aircraft must maintain a track of its geographical position between updates in order to determine the next expected measurement for the Kalman filter. As mentioned before, this aircraft position is subject to non-linear as well as linear navigational drifts which are not taken into account in this model. However, an observable system can be obtained by reducing the number of states to sonobuoy position only and introducing fictitious process noise to account for the drift. This noise effectively allows sonobuoy position to update so as to keep up with the drift. One approach developed by this thesis is a variation of this concept.

Another approach considers only the relative position of the sonobuoy with respect to the aircraft. Relative velocities and relative accelerations must be taken into account and these change radically as the aircraft flies in the tactical situation. Sonobuoy position is not obtained directly. (When only the word "position" is used it will indicate the position relative to an earth fixed coordinate system, such as latitude and longitude. "Relative position" will always mean the location with respect to an aircraft fixed coordinate system.)

There are some other considerations which should be addressed. The sonobuoy drift is generally slow (less than 5 NM/Hr most of the time) and constant. It is not unreasonable to assume that the entire sonobuoy field drifts at the same velocity. Another point is that aircraft navigational drift can not be distinguished from sonobuoy drift. In other words, the drift that is perceived by the aircraft is the combination of sonobuoy drift and aircraft navigational drift. If this navigational drift is linear and not excessive it causes few problems. However, non-linear navigational drifts, such as the Schuler cycle, can cause large errors.

B. THE COORDINATE SYSTEM

A right-handed coordinate system was chosen as depicted in figures 3 and 4. This is a departure from the work of Orincon Corporation which is described in the next section. This system allows all angles to be measured positive in the direction they are normally defined, i.e., aircraft heading measured clockwise from north. It also coincides with the usual aerodynamic coordinate system.

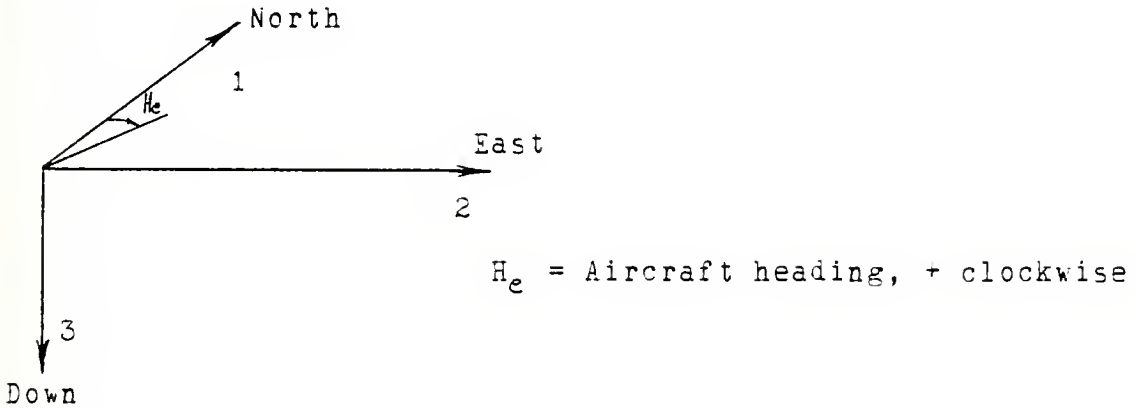


Figure 3. Earth fixed

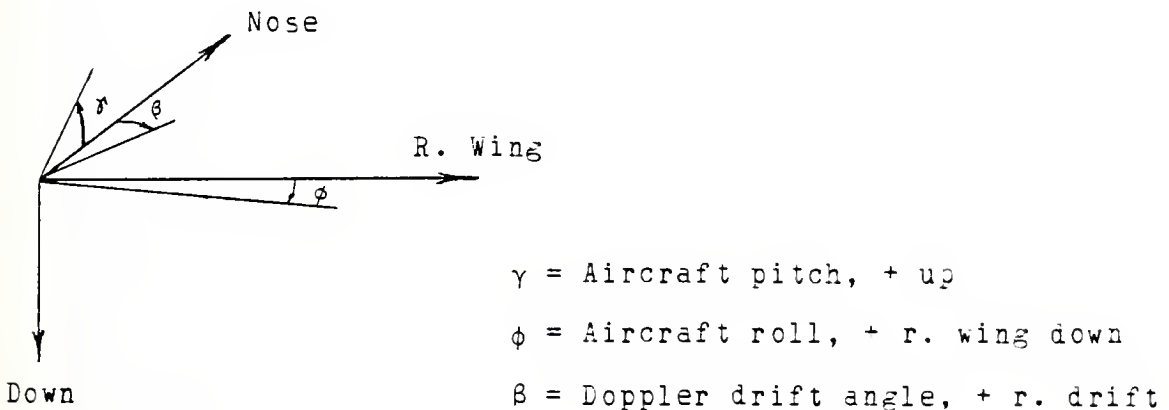


Figure 4. Aircraft fixed

C. THE SIX-STATE SYSTEM

Orincon Corporation of La Jolla, CA., completed a technical report in December of 1978 concerning the Sonobuoy Reference System. They were contracted by NADC to investigate the effect of errors in the aircraft navigational system on the performance of the sonobuoy tracking procedure. As a result of their work they developed a 13-state mathematical model which successfully determined sonobuoy positions in spite of these navigational errors. The complete state vector was

$$\mathbf{x}^T = \left[\Delta x_1 \ \Delta x_2 \ \Delta v_1 \ \Delta v_2 \ x_1 \ x_2 \ v_1 \ v_2 \ \psi_1 \ \psi_2 \ \psi_3 \ m_1 \ m_2 \right] \quad (20)$$

where

Δx = relative position of the sonobuoy from the aircraft;

Δv = relative velocity of the sonobuoy from the aircraft;

x = position of the sonobuoy on the ocean surface;

v = velocity of the sonobuoy on the ocean surface;

ψ = inertial system's platform azimuth alignment errors

m = inertial system's gyro drift rates assumed constant.

(Subscripts 1, 2, and 3 represent North, East, and down respectively.) The model was developed using state equations which described sonobuoy motion relative to the aircraft and relative to the ocean's surface. These were derived by

Orincon from

$$\Delta X = X - (X_a^I + E) \quad (21)$$

and other mechanization equations to obtain

$$\begin{aligned} \Delta \dot{x}_1 &= \Delta v_1 \\ \Delta \dot{x}_2 &= \Delta v_2 \\ \Delta \dot{v}_1 &= -\ddot{R}_1 + \omega^2 (x_1 - x_{a1}^I - \Delta x_1) - \psi_3 A_2 + \psi_2 g \\ \Delta \dot{v}_2 &= -\ddot{R}_2 + \omega^2 (x_2 - x_{a2}^I - \Delta x_2) - \psi_3 A_1 - \psi_1 g \\ \dot{x}_1 &= v_1 \\ \dot{x}_2 &= v_2 \\ \dot{v}_1 &= 0 \\ \dot{v}_2 &= 0 \end{aligned} \quad (22)$$

where

X_a^I = aircraft inertial navigation system position

E = aircraft inertial navigation system error

R = vector from the center of the earth to the aircraft

g = acceleration due to gravity (assumed constant)

ω = Schuler frequency $\sqrt{g/R}$

A = aircraft accelerometer outputs

The sonobuoys were assumed to drift at a constant velocity and the aircraft was assumed to fly at a constant altitude.

The inertial alignment errors were described by

$$\begin{aligned}
\dot{\psi}_1 &= \psi_2 \Omega \sin \lambda - \psi_3 \Omega \cos \lambda + m_1 \\
\dot{\psi}_2 &= -\psi_1 \Omega \sin \lambda + m_2 \\
\dot{\psi}_3 &= \psi_1 \Omega \cos \lambda
\end{aligned}
\tag{23}$$

where

Ω = earth rate

λ = latitude

There were several sources of measurement information. Aircraft to sonobuoy bearing was available from the aircraft interferometer system in the form of $\cos \theta$ where θ is the angle between the direction to the sonobuoy and the base line of the antenna. Doppler velocity and drift angle from the aircraft doppler radar system provided information about Δv_1 and Δv_2 . The only other relevant source of measurement information would have come from GPS (Global Positioning System) which would have provided error free aircraft position.

Orincon performed a numerical observability analysis on this system based on the observability matrix M_k given by

$$M_k = \sum_{i=1}^N \phi_k^T H_k^T R^{-1} H_k \phi_k
\tag{24}$$

If this matrix is positive definite for $N \geq 2$ then the system is considered observable. In addition, an eigenvalue analysis provided information as to the conditioning of the system. The result of their analysis indicated that the

system was not fully observable with measurements from the interferometer and doppler systems alone. Only ten states were observable; sonobuoy position most likely was not observable and ψ_3 , m_1 , m_2 , v_1 and v_2 were weakly observable at best. They also noted that "observability is reduced when the aircraft pursues a straight flight path". By removing sonobuoy positions and gyro drifts from the system they found the observability improved. Further, the system became fully observable if sonobuoy velocity was also removed from the state vector.

The Orincon report presented the results of a Monte-Carlo simulation on the 13-state system. However, they concluded that a reduced state filter made up of

$$X^T = \left[\Delta x_1 \quad \Delta x_2 \quad \Delta v_1 \quad \Delta v_2 \quad \psi_1 \quad \psi_2 \right] \quad (25)$$

would provide a workable solution to the problem although they noted that it had a tendency toward divergence. It was partly the intention of this report to further the investigation of this reduced state filter.

The state equations for the reduced six-state filter can be obtained directly from Equations (22) and (23).

$$\begin{aligned}
 \Delta \dot{x}_1 &= \Delta v_1 \\
 \Delta \dot{x}_2 &= \Delta v_2 \\
 \Delta \dot{v}_1 &= -\ddot{R}_1 + \omega^2(x_1 - x_{a1}^I - \Delta x_1) + \psi_2 g \\
 \Delta \dot{v}_2 &= -\ddot{R}_2 + \omega^2(x_2 - x_{a2}^I - \Delta x_2) - \psi_1 g \\
 \dot{\psi}_1 &= \psi_2 \sin \lambda \\
 \dot{\psi}_2 &= -\psi_1 \sin \lambda
 \end{aligned} \tag{26}$$

where ψ_3 , m_1 , and m_2 are set to zero. In matrix form

$$\dot{X} = \begin{bmatrix} \Delta \dot{x}_1 \\ \Delta \dot{x}_2 \\ \Delta \dot{v}_1 \\ \Delta \dot{v}_2 \\ \dot{\psi}_1 \\ \dot{\psi}_2 \end{bmatrix} = \begin{bmatrix} \emptyset & \emptyset & 1 & \emptyset & \emptyset & \emptyset \\ \emptyset & \emptyset & \emptyset & 1 & \emptyset & \emptyset \\ -\omega^2 & \emptyset & \emptyset & \emptyset & \emptyset & -g \\ \emptyset & -\omega^2 & \emptyset & \emptyset & g & \emptyset \\ \hline \emptyset & \emptyset & \emptyset & \emptyset & \emptyset & -\Omega \sin \lambda \\ \emptyset & \emptyset & \emptyset & \emptyset & \Omega \sin \lambda & \emptyset \end{bmatrix} \begin{bmatrix} \Delta x_1 \\ \Delta x_2 \\ \Delta v_1 \\ \Delta v_2 \\ \psi_1 \\ \psi_2 \end{bmatrix} + \begin{bmatrix} \emptyset \\ \emptyset \\ -\ddot{R}_1 + \omega^2(x_1 - x_{a1}^I) \\ -\ddot{R}_2 + \omega^2(x_2 - x_{a2}^I) \\ \emptyset \\ \emptyset \end{bmatrix}$$

which can be abbreviated

$$\dot{X} = \begin{bmatrix} A^\Delta & | & A^\Delta \psi \\ \hline \emptyset & | & A^\psi \end{bmatrix} X + B \tag{27}$$

Expressed in discrete time the state equation is

$$X_{k+1} = \bar{\Phi} X_k + \Lambda_k + W_k \tag{28}$$

The discrete formulation of the plant matrix can be obtained from

$$\Phi = \mathcal{L}^{-1} \left\{ (sI - A)^{-1} \right\} = e^{At} \quad (29)$$

Developing this

$$[sI - A] = \left[\begin{array}{cccc|cc} s & 0 & 1 & 0 & 0 & 0 \\ 0 & s & 0 & 1 & 0 & 0 \\ \omega^2 & 0 & s & 0 & 0 & g \\ 0 & \omega^2 & 0 & s & -g & 0 \\ \hline 0 & 0 & 0 & 0 & s & \Omega \sin \lambda \\ 0 & 0 & 0 & 0 & -\Omega \sin \lambda & s \end{array} \right] \quad (30)$$

from which the determinant of the system is

$$|sI - A| = (s^2 + \omega^2)^2 (s^2 + \Omega^2 \sin^2 \lambda)^2 \quad (31)$$

The inverse of this matrix and its Laplace transform are presented on the following pages as Equations (32) and (33) respectively.

$$[sI - A]^{-1} =$$

(32)

$\frac{s}{s^2 + \omega^2}$	0	$\frac{1}{s^2 + \omega^2}$	0	$\frac{-g \Omega \sin \lambda}{(s^2 + \omega^2)(s^2 + \Omega^2 \sin^2 \lambda)}$	$\frac{-g s}{(s^2 + \omega^2)(s^2 + \Omega^2 \sin^2 \lambda)}$
0	$\frac{s}{s^2 + \omega^2}$	0	$\frac{1}{s^2 + \omega^2}$	$\frac{g s}{(s^2 + \omega^2)(s^2 + \Omega^2 \sin^2 \lambda)}$	$\frac{-g \sin \lambda}{(s^2 + \omega^2)(s^2 + \Omega^2 \sin^2 \lambda)}$
$\frac{-\omega}{s^2 + \omega^2}$	0	$\frac{s}{s^2 + \omega^2}$	0	$\frac{-g s \Omega \sin \lambda}{(s^2 + \omega^2)(s^2 + \Omega^2 \sin^2 \lambda)}$	$\frac{-g s^2}{(s^2 + \omega^2)(s^2 + \Omega^2 \sin^2 \lambda)}$
0	$\frac{-\omega^2}{s^2 + \omega^2}$	0	$\frac{s}{s^2 + \omega^2}$	$\frac{g s^2}{(s^2 + \omega^2)(s^2 + \Omega^2 \sin^2 \lambda)}$	$\frac{-g s \Omega \sin \lambda}{(s^2 + \omega^2)(s^2 + \Omega^2 \sin^2 \lambda)}$

0	0	0	0	$\frac{s}{s^2 + \Omega^2 \sin^2 \lambda}$	$\frac{-\Omega \sin \lambda}{s^2 + \Omega^2 \sin^2 \lambda}$
0	0	0	0	$\frac{\Omega \sin \lambda}{s^2 + \Omega^2 \sin^2 \lambda}$	$\frac{s}{s^2 + \Omega^2 \sin^2 \lambda}$

$\cos \omega t$	0	$\frac{1}{\omega} \sin \omega t$	0	$-\frac{g}{\Omega^2 \sin^2 \lambda - \omega^2} \left[\frac{\Omega \sin \lambda}{\omega} \sin \omega t - \sin(\Omega \sin \lambda) t \right]$
0	$\cos \omega t$	0	$\frac{1}{\omega} \sin \omega t$	$-\frac{g}{\Omega^2 \sin^2 \lambda - \omega^2} \left[\frac{\Omega \sin \lambda}{\omega} \sin \omega t - \sin(\Omega \sin \lambda) t \right]$
$-\omega \sin \omega t$	0	$\cos \omega t$	0	$\frac{g}{\Omega^2 \sin^2 \lambda - \omega^2} \left[\omega \sin \omega t - \Omega \sin \lambda \sin(\Omega \sin \lambda) t \right]$
0	$-\omega \sin \omega t$	0	$\cos \omega t$	$-\frac{g}{\Omega^2 \sin^2 \lambda - \omega^2} \left[\omega \sin \omega t - \Omega \sin \lambda \sin(\Omega \sin \lambda) t \right]$
0	0	0	0	$\cos(\Omega \sin \lambda) t$
0	0	0	0	$-\sin(\Omega \sin \lambda) t$
0	0	0	0	$\cos(\Omega \sin \lambda) t$

The discrete formulation of the continuous matrix B is

$$\Lambda_k = \int_{t_k}^{t_{k+1}} e^{A\lambda} d\lambda B \quad \text{where } \lambda = \Delta t - \tau \quad (34)$$

Hence

$$\Lambda_k = \begin{bmatrix} \left\{ -\frac{\ddot{R}_1}{\omega^2} + (x_1 - x_{a1}^I) \right\} (1 - \cos\omega\Delta t) \\ \left\{ -\frac{\ddot{R}_2}{\omega^2} + (x_2 - x_{a2}^I) \right\} (1 - \cos\omega\Delta t) \\ \left\{ -\frac{\dot{R}_1}{\omega} + \omega(x_1 - x_{a1}^I) \right\} \sin\omega\Delta t \\ \left\{ -\frac{\dot{R}_2}{\omega} + \omega(x_2 - x_{a2}^I) \right\} \sin\omega\Delta t \\ \emptyset \\ \emptyset \end{bmatrix} \quad (35)$$

The noise term is $W_k \sim N(\emptyset, Q)$. The variances are estimated to be .01 NM for relative position, 1.0 (NM/Hr) for relative velocity, and .001 radians for inertial misalignments. As a result, the following constant diagonal matrix is used for

Q:

$$Q = \begin{bmatrix} .01 & & & & & \\ & .01 & & & & \\ & & 1.0 & & & \\ & & & 1.0 & & \\ & & & & .001 & \\ & & & & & .001 \end{bmatrix} \quad (36)$$

The same measurement information is available as before

in the larger system, namely interferometer bearings and doppler velocity and drift angle. These introduce non-linearities and must be modeled as in Equation (10).

$$Z_k = h(X_k) + V_k$$

A Taylor series expansion as in Equation (11) about the latest estimate of sonobuoy position provides a method of linearization. As a result

$$H = \left[\left. \frac{\partial z}{\partial \Delta x_1} \right|_{x=\hat{x}} \quad \left. \frac{\partial z}{\partial \Delta x_2} \right|_{x=\hat{x}} \quad \left. \frac{\partial z}{\partial \Delta v_1} \right|_{x=\hat{x}} \quad \left. \frac{\partial z}{\partial \Delta v_2} \right|_{x=\hat{x}} \quad \left. \frac{\partial z}{\partial \psi_1} \right|_{x=\hat{x}} \quad \left. \frac{\partial z}{\partial \psi_2} \right|_{x=\hat{x}} \right] \quad (37)$$

To determine z and its partial derivatives, recall that

$$z_1 = \cos \theta = \overrightarrow{\Delta X} \cdot \overrightarrow{RB} \quad (38)$$

where $\overrightarrow{\Delta X}$ is the unit vector representation of a line from the aircraft to the sonobuoy and \overrightarrow{RB} is the unit vector describing the base line between the antenna pairs of the interferometer.

$$\begin{aligned} \hat{z}_1 = \cos \theta \Big|_{x=\hat{x}} &= \frac{\Delta \hat{x}_1}{|\Delta \hat{x}|} RB_1 + \frac{\Delta \hat{x}_2}{|\Delta \hat{x}|} RB_2 + \frac{\Delta \hat{x}_3}{|\Delta \hat{x}|} RB_3 \\ \hat{z}_1 &= \frac{\Delta \hat{x}_1 RB_1 + \Delta \hat{x}_2 RB_2 + h RB_3}{(\Delta \hat{x}_1^2 + \Delta \hat{x}_2^2 + h^2)^{1/2}} \end{aligned} \quad (39)$$

where h is the aircraft altitude.

$$H = \begin{bmatrix} \frac{\partial z_1}{\partial \Delta x_1} \Big|_{x=\hat{x}} & \frac{\partial z_1}{\partial \Delta x_2} \Big|_{x=\hat{x}} & 0 & 0 & 0 & 0 \end{bmatrix} \quad (40)$$

where

$$\frac{\partial}{\partial \Delta x_1} (z_1) \Big|_{x=\hat{x}} = \frac{1}{(\Delta \hat{x}_1^2 + \Delta \hat{x}_2^2 + h^2)^{\frac{1}{2}}} \left[RB_1 - \frac{\Delta \hat{x}_1 (\Delta \hat{x}_1 RB_1 + \Delta \hat{x}_2 RB_2 + h RB_3)}{(\Delta \hat{x}_1^2 + \Delta \hat{x}_2^2 + h^2)} \right] \quad (41)$$

$$\frac{\partial}{\partial \Delta x_2} (z_1) \Big|_{x=\hat{x}} = \frac{1}{(\Delta \hat{x}_1^2 + \Delta \hat{x}_2^2 + h^2)^{\frac{1}{2}}} \left[RB_2 - \frac{\Delta \hat{x}_2 (\Delta \hat{x}_1 RB_1 + \Delta \hat{x}_2 RB_2 + h RB_3)}{(\Delta \hat{x}_1^2 + \Delta \hat{x}_2^2 + h^2)} \right] \quad (42)$$

The doppler velocity, V_d , is a measurement of aircraft speed relative to the ocean surface and doppler drift angle, β , is a measure of the angle between aircraft track and aircraft heading. These measurements can be related to the state vector by assuming the sonobuoys drift at the same velocity as the ocean surface. If this is true then

$$z_2 = V_d = (\Delta v_1^2 + \Delta v_2^2)^{\frac{1}{2}} \quad (43)$$

Expanding in a Taylor series yields

$$z_2 = (\Delta \hat{v}_1^2 + \Delta \hat{v}_2^2)^{\frac{1}{2}} \quad (44)$$

$$H_2 = \begin{bmatrix} 0 & 0 & \frac{\partial z_2}{\partial \Delta v_1} \Big|_{x=\hat{x}} & \frac{\partial z_2}{\partial \Delta v_2} \Big|_{x=\hat{x}} & 0 & 0 \end{bmatrix} \quad (45)$$

where

$$\frac{\partial z_2}{\partial \Delta v_1} \Big|_{x=\hat{x}} = \frac{\Delta \hat{v}_1}{(\Delta \hat{v}_1^2 + \Delta \hat{v}_2^2)^{\frac{1}{2}}} \quad (46)$$

$$\frac{\partial z_2}{\partial \Delta v_2} \Big|_{x=\hat{x}} = \frac{\Delta \hat{v}_2}{(\Delta \hat{v}_1^2 + \Delta \hat{v}_2^2)^{\frac{1}{2}}} \quad (47)$$

Similarly,

$$\begin{aligned} z_3' &= \beta = \text{Track} - \text{heading} \\ &= \tan^{-1}\left(\frac{\Delta v_2}{\Delta v_1}\right) - H_e \end{aligned} \quad (48)$$

or since the aircraft heading, H_e , is deterministic

$$z_3 = H_e + \beta = \tan^{-1}\left(\frac{\Delta v_2}{\Delta v_1}\right) \quad (49)$$

$$H_3 = \begin{bmatrix} 0 & 0 & \left. \frac{\partial z_3}{\partial \Delta v_1} \right|_{x=\hat{x}} & \left. \frac{\partial z_3}{\partial \Delta v_2} \right|_{x=\hat{x}} & 0 & 0 \end{bmatrix} \quad (50)$$

where

$$\left. \frac{\partial z_3}{\partial \Delta v_1} \right|_{x=\hat{x}} = \frac{-\Delta \hat{v}_2}{\Delta \hat{v}_1^2 + \Delta \hat{v}_2^2} \quad (51)$$

$$\left. \frac{\partial z_3}{\partial \Delta v_2} \right|_{x=\hat{x}} = \frac{\Delta \hat{v}_1}{\Delta \hat{v}_1^2 + \Delta \hat{v}_2^2} \quad (52)$$

Finally,

$$Z = \begin{bmatrix} \cos \theta \\ v_d \\ H_e - \beta \end{bmatrix} \quad (53)$$

$$H = \begin{bmatrix} \frac{\partial(\cos \theta)}{\partial x_1} & \frac{\partial(\cos \theta)}{\partial x_2} & 0 & 0 & 0 & 0 \\ 0 & 0 & \frac{\partial(v_d)}{\partial \Delta v_1} & \frac{\partial(v_d)}{\partial \Delta v_2} & 0 & 0 \\ 0 & 0 & \frac{\partial(H_e + \beta)}{\partial \Delta v_1} & \frac{\partial(H_e + \beta)}{\partial \Delta v_2} & 0 & 0 \end{bmatrix} \quad (54)$$

The measurement noise, V_d , is described by $N(0, R)$. It is assumed that the measurement noise R and the plant noise Q are white, gaussian, and uncorrelated. Based on information obtained from NADC, R was assigned the following values:

$$\begin{aligned} R_1 &= .0007 \text{ rad} && (\text{interferometer}) \\ R_2 &= 1.0 \text{ (NM/Hr)} && (\text{doppler velocity}) \\ R_3 &= .01 \text{ deg} && (\text{doppler drift angle}) \end{aligned} \quad (55)$$

It should be pointed out that the doppler measurements are not always available. The doppler system freezes the last value of groundspeed and drift angle anytime the doppler radar is not receiving good information. This happens whenever the aircraft is above 5000' altitude, or can happen when flying above a cloud cover or when the sea surface is too smooth. As a result, the doppler could be inaccurate during a significant portion of the flight.

The six-state system was programmed and tested for several conditions. Flow charts for significant portions of the program and the entire program listing are presented in Appendix A. The main program has two purposes: first, to control the simulation; and second, to read and prepare measurement data for the subroutine FILTER. This subroutine performs all the Kalman filter computations as specified in the above equations. The Carlson square root technique is used to ensure a positive definite covariance matrix. Also, in order to avoid inverting a matrix in the calculations for the Kalman gain, the three measurements are processed one at

a time. The results of the simulation are presented in section IV.B.

D. THE TWO-STATE SYSTEM

An attempt was made earlier on in this research to model sonobuoy motion as

$$X_{k+1} = X_k + U_k \Delta t \quad (56)$$

$$U_{k+1} = U_k$$

with a state vector made up of x_1 , x_2 , u_1 , and u_2 . This system proved to be unobservable although the simple approach was appealing. Since sonobuoy drift rates are generally slow, another attempt was made to model the system without velocity. The equations reduced to

$$X_{k+1} = X_k + W_k \quad (57)$$

With only x_1 and x_2 as states, this system was observable. By describing large statistical values of system noise there would hopefully be enough freedom in the "update" to compensate for any sonobuoy drifts. Unfortunately, this approach was not completely successful; however, it was observed that the general direction of sonobuoy drift was correct. As a result of these investigations a technique of cascading Kalman filters was used to solve the tracking problem. The intent was to use results from one filter as measurement for a second filter. Then, the result of the

second filter could be used as a deterministic control input to better propagate the first filter.

Two Kalman filters are used in this approach. Figure 5 shows how they are related (or cascaded). The first filter models sonobuoy position and is based on the discrete state equation

$$X_k = X_{k-1} + U_k \Delta t + W_k \quad (58)$$

The state vector consists of the sonobuoy positions, x_1 and x_2 . U_k is a deterministic input accounting for sonobuoy drift and W_k is system noise. The interferometer measurement, $\cos\theta$, is used to update this filter.

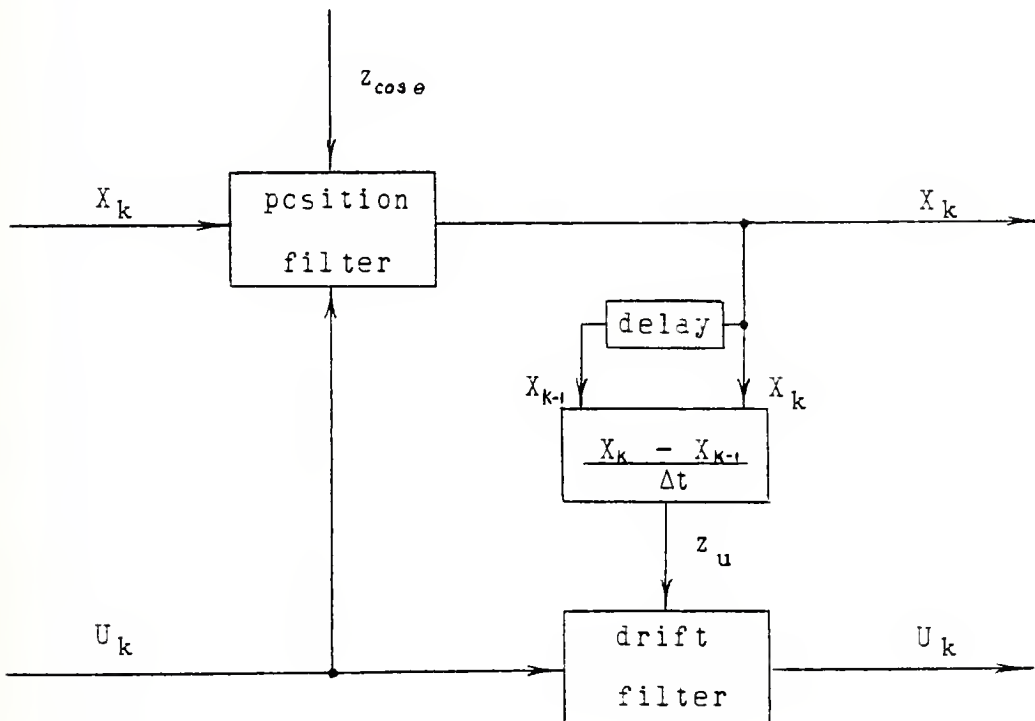


Figure 5. Cascaded Kalman filters.

The second filter models the sonobuoy drift with the state equation

$$\bar{U}_{k+1} = U_k \quad (59)$$

As the sonobuoy's position changes with each update of the position filter, the velocity required to move from X_k to X_{k+1} in the time interval Δt can be calculated. This value is used as a measurement for the drift filter. All sonobuoys contribute to this filter which produces one overall estimate of drift for the sonobuoy field. This value is then used as an input to the position filter when the next interferometer measurement occurs.

The technique is understandably sensitive to the output of the drift filter. If the estimated drift is too much in error, the estimated positions will be affected. Divergence could result. For this reason, a simplified Kalman filter is used to estimate the drift. It is of the form

$$\bar{U}_{k+1} = U_k + G_k (Z_k - U_k) \quad (60)$$

The gain is precomputed from $1/(n+1)$ where n is the total number of measurements and is limited to a value at least as great as $\Delta t/(84 \text{ min.})$. This limit is reached after the first 84 minutes of tracking time. From that point on the gain remains constant effectively averaging the drift over one period of the Schuler cycle. It must be understood that

the drift this filter estimates consists not only of sonobuoy drift but aircraft drift as well and is, in fact, the vector sum of these. An estimate which attempts to follow the changing velocities through the Schuler cycle tends to cause the position filters to diverge. This might be the case if larger values of gain are used, averaging only the last few measurements of drift. Therefore, many measurements of drift are averaged which provides an estimate for linear drift only. The lower limit of gain prevents new drift measurements from being ignored and also provides for flexibility in estimating the drift.

Unlike the six-state system, the interferometer measurement is the only measurement required by the position filter. The measurement equation is essentially the same as in the preceding section where z is determined as shown in Equation (39). Since there is only one term in z , the H matrix is a row vector consisting of

$$H = \left[\begin{array}{cc} \frac{\partial z}{\partial x_1} & \frac{\partial z}{\partial x_2} \end{array} \right] \quad (61)$$

where the terms are given in Equations (41) and (42). It is necessary to determine the aircraft-to-sonobuoy range for these values from

$$\Delta X = \hat{X} - X_a^I \quad (62)$$

where \hat{X} is the estimated sonobuoy position. X_a^I represents

the aircraft position and is considered deterministic. Undoubtedly, X_a^I is in error due to aircraft navigational drifts and therefore causes errors in the estimated geographical position of the sonobuoy. But, since the measurement of bearing is based on relative positions, the estimate is relatively correct.

An observability analysis on the 2-state position filter was performed again using

$$M_k = \sum_{k=1}^N \Phi_k^T H_k^T R^{-1} H_k \Phi_k \quad (63)$$

Substitution into this formula with $N=2$ yields

$$M = \begin{bmatrix} \left(\frac{\partial z}{\partial x_{1i}}\right)^2 & \left(\frac{\partial z}{\partial x_{1i}}\right)\left(\frac{\partial z}{\partial x_{2i}}\right) \\ \left(\frac{\partial z}{\partial x_{1i}}\right)\left(\frac{\partial z}{\partial x_{2i}}\right) & \left(\frac{\partial z}{\partial x_{2i}}\right)^2 \end{bmatrix} + \begin{bmatrix} \left(\frac{\partial z}{\partial x_{1i+1}}\right)^2 & \left(\frac{\partial z}{\partial x_{2i+1}}\right)\left(\frac{\partial z}{\partial x_{1i+1}}\right) \\ \left(\frac{\partial z}{\partial x_{1i+1}}\right)\left(\frac{\partial z}{\partial x_{2i+1}}\right) & \left(\frac{\partial z}{\partial x_{2i+1}}\right)^2 \end{bmatrix} \quad (64)$$

Expanding,

$$M = \begin{pmatrix} \left(\frac{\partial z}{\partial x_{1i+1}}\right)^2 & \left(\frac{\partial z}{\partial x_{2i}}\right)^2 \\ \left(\frac{\partial z}{\partial x_{1i+1}}\right)\left(\frac{\partial z}{\partial x_{2i+1}}\right) & \left(\frac{\partial z}{\partial x_{1i}}\right)\left(\frac{\partial z}{\partial x_{2i}}\right) \end{pmatrix} - \begin{pmatrix} \left(\frac{\partial z}{\partial x_{1i+1}}\right)\left(\frac{\partial z}{\partial x_{2i+1}}\right) & \left(\frac{\partial z}{\partial x_{1i}}\right)\left(\frac{\partial z}{\partial x_{2i}}\right) \\ \left(\frac{\partial z}{\partial x_{1i}}\right)\left(\frac{\partial z}{\partial x_{2i}}\right) & \left(\frac{\partial z}{\partial x_{1i+1}}\right)\left(\frac{\partial z}{\partial x_{2i+1}}\right) \end{pmatrix} + \begin{pmatrix} \left(\frac{\partial z}{\partial x_{1i}}\right)^2 & \left(\frac{\partial z}{\partial x_{2i+1}}\right)^2 \\ \left(\frac{\partial z}{\partial x_{1i}}\right)\left(\frac{\partial z}{\partial x_{2i+1}}\right) & \left(\frac{\partial z}{\partial x_{1i+1}}\right)\left(\frac{\partial z}{\partial x_{2i}}\right) \end{pmatrix} \quad (65)$$

This matrix is positive definite for all except the case when

$$\left(\frac{\partial z}{\partial x_{1i}}\right) = \left(\frac{\partial z}{\partial x_{1i+1}}\right) \quad \text{and} \quad \left(\frac{\partial z}{\partial x_{2i}}\right) = \left(\frac{\partial z}{\partial x_{2i+1}}\right)$$

This occurs whenever the relative bearing from the aircraft to the sonobuoy is not changing (i.e. when flying directly toward or away from the sonobuoy). This is intuitively correct since two or more bearings must cross in order to determine a position.

The two-state system was programmed and tested to determine the usefulness of this simplified filter. The majority of the program is the same as the one used for the six-state system. The significant differences occur in subroutine FILTER. The Carlson square root technique is used again but only one measurement instead of three is processed. The drift filter is programmed in this subroutine along with the position filter. A flow chart and program listing are presented in Appendix A.

IV. ANALYSIS

A. THE SIMULATION

Actual data from the Orion was not easily obtainable for this research. Consequently, a computer program had to be written to generate the information required by these algorithms. A flow chart in Appendix B describes the program. An aircraft track was created by alternating lines and curves of various lengths and then a determination of noise free measurements was made as the track was flown. (Measurement noise was added later during the simulations.) Sonobuoys were allowed to drift at a constant velocity, and the aircraft's navigational drift was modeled with a constant velocity and Schuler cycle variations as

$$X_a^I = X_a + K_x \Delta t + A_x \sin \omega t \quad (66)$$

where

X_a^I = aircraft inertial position

X_a = aircraft true position

ω = Schuler frequency $\sqrt{g/R}$

The constant drift rate, K_x , was found by NADC to have 0 mean and a standard deviation of 2.5 NM/HR. Likewise, the amplitude of the Schuler cycle, A_x , had 0 mean and a standard deviation of .5 NM. The effect of wind was also available in the program but was never included for analysis.

It was obvious that both algorithms were extremely sensitive to the aircraft flight path. Since there is no "typical" flight path for an Orion during its on-station period, several uniform patterns were selected which would provide meaningful information on each algorithm's performance. These base parameters were chosen:

airspeed	180 kts
altitude	3000 ft
range	15 NM aircraft-to-sonobuoy
frequency	20 sec between measurements on one sonobuoy

A circular pattern was flown around a sonobuoy at a range of about 15 NM. Initial sonobuoy placement was at $(1,1)^1$ with the aircraft flying clockwise starting at $(15,0)$. This is shown in Figure 6 which depicts a portion of the aircraft's true track. Sonobuoy drift was west at 1 NM/HR; aircraft navigational drift was south at 1 NM/HR and included a Schuler cycle (amplitude .5 NM) when specified. (This drift would be indicated in Figures 12 thru 30 by the following notation: DR=(a/c 180-1 + Schuler, b 270-1) .) The sonobuoy remained near the center of the pattern allowing the range to remain relatively constant. This was desirable since this basic flight path was used to test the response of the algorithms to variations in altitude and range. Similarly, a square pattern was flown counter-clockwise around a

¹ (x_1, x_2) measured in nautical miles from an arbitrary origin near the aircraft's starting point.

sonobuoy at a range of 15 NM. In this case the aircraft began on-top the initial position of the sonobuoy at (-3,-3) and proceeded to fly the track shown in Figure 7. The sonobuoy was allowed to drift to the east at 2 NM/HR and the aircraft's navigational system to the north at 2.5 NM/HR. This pattern was used eventually to analyze performance at different measuring frequencies. Figure 8 shows the output of the aircraft's navigational system when it has a northerly drift of 2.5 NM/HR while the aircraft is flying the square pattern. Figure 9 shows this same pattern when a Schuler cycle with an amplitude of .5 NM is also present.

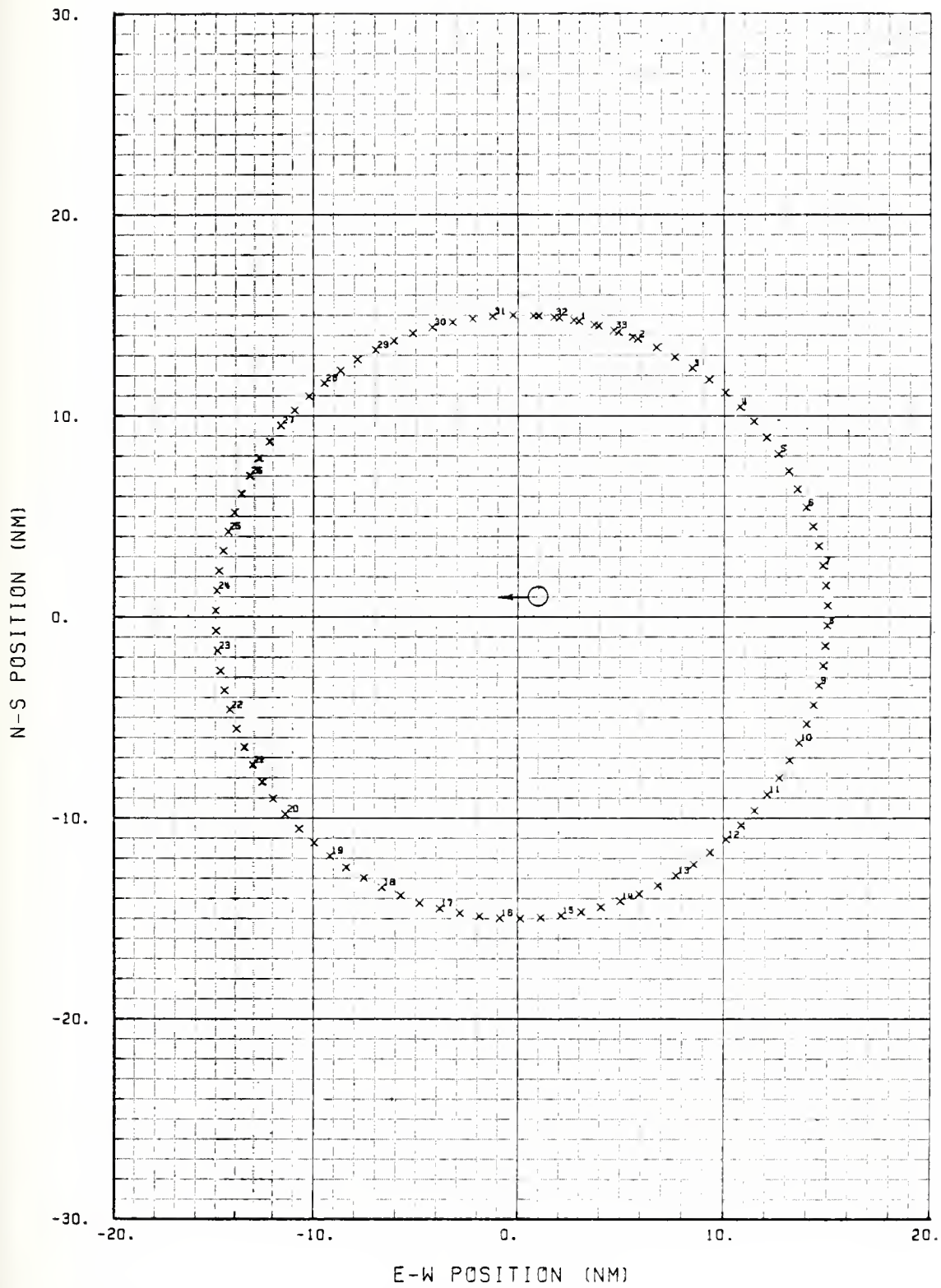


Figure 6. Aircraft track for the 15 NM circular pattern with initial sonobuoy location and direction of drift indicated.

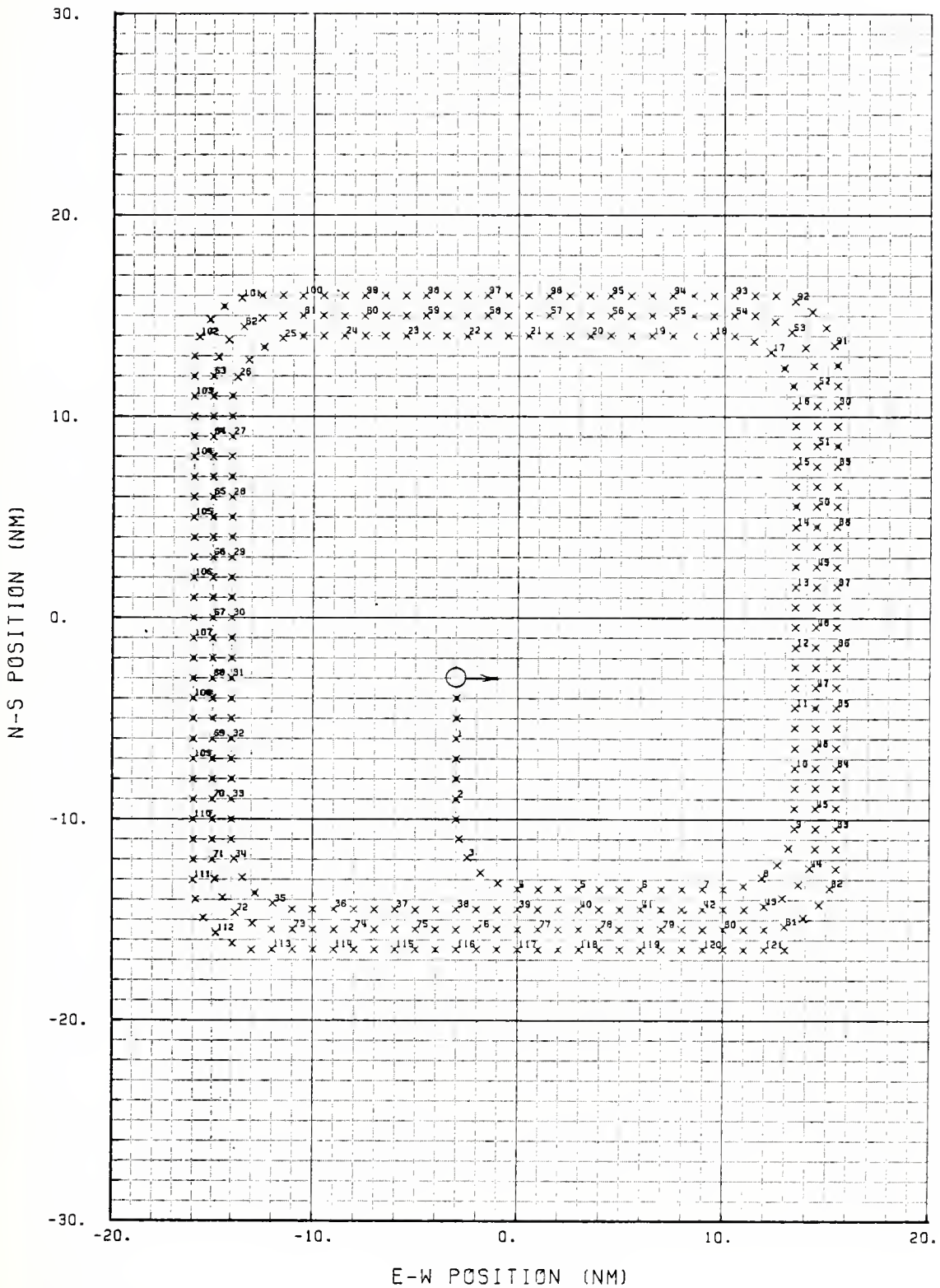


Figure 7. Aircraft track for the 15 NM square pattern with initial sonobuoy location and direction of drift indicated.

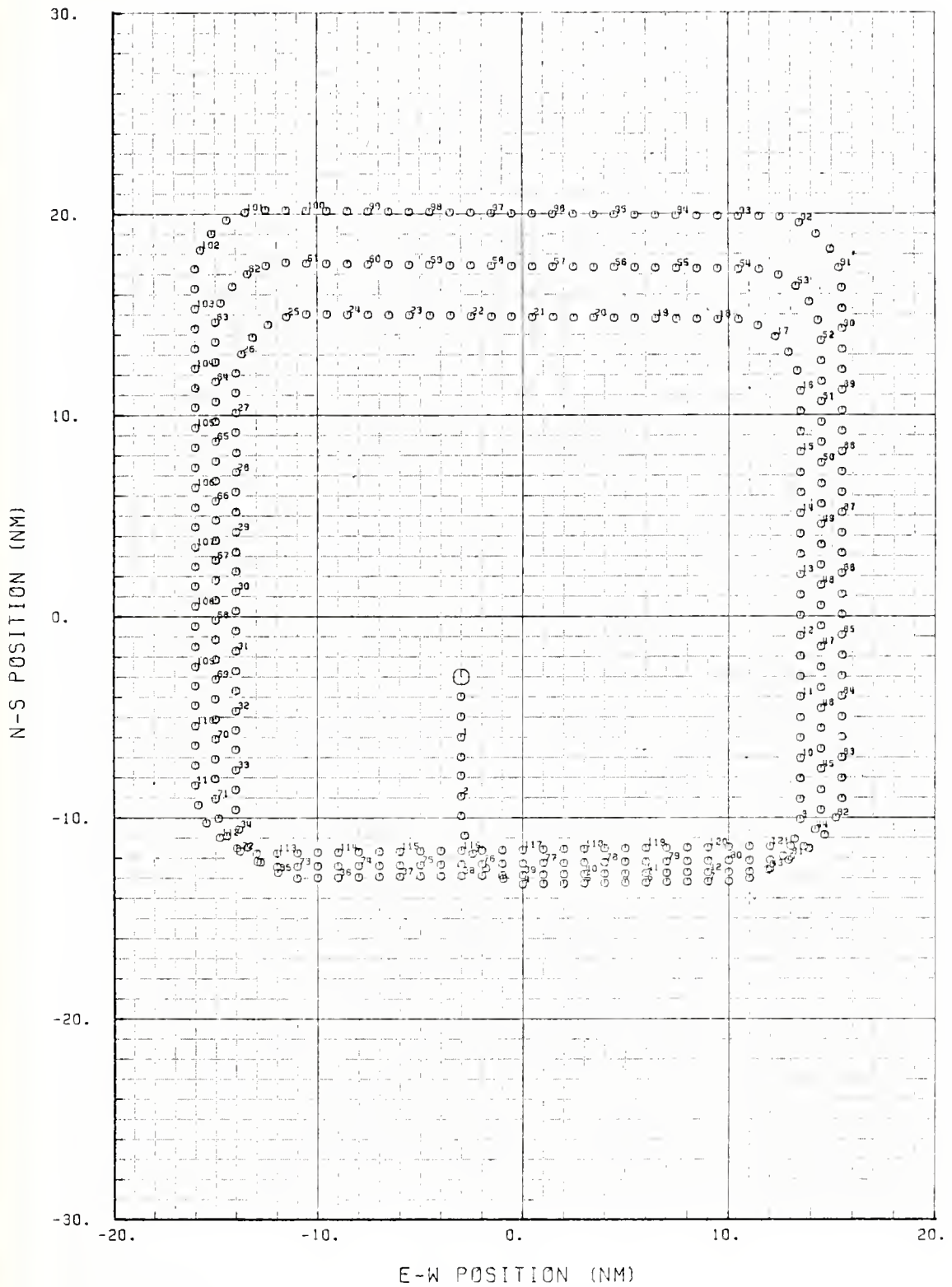


Figure 8. Aircraft's navigational output for the 15 NM square; navigational drift is 2.5 NM/Hr to the north.

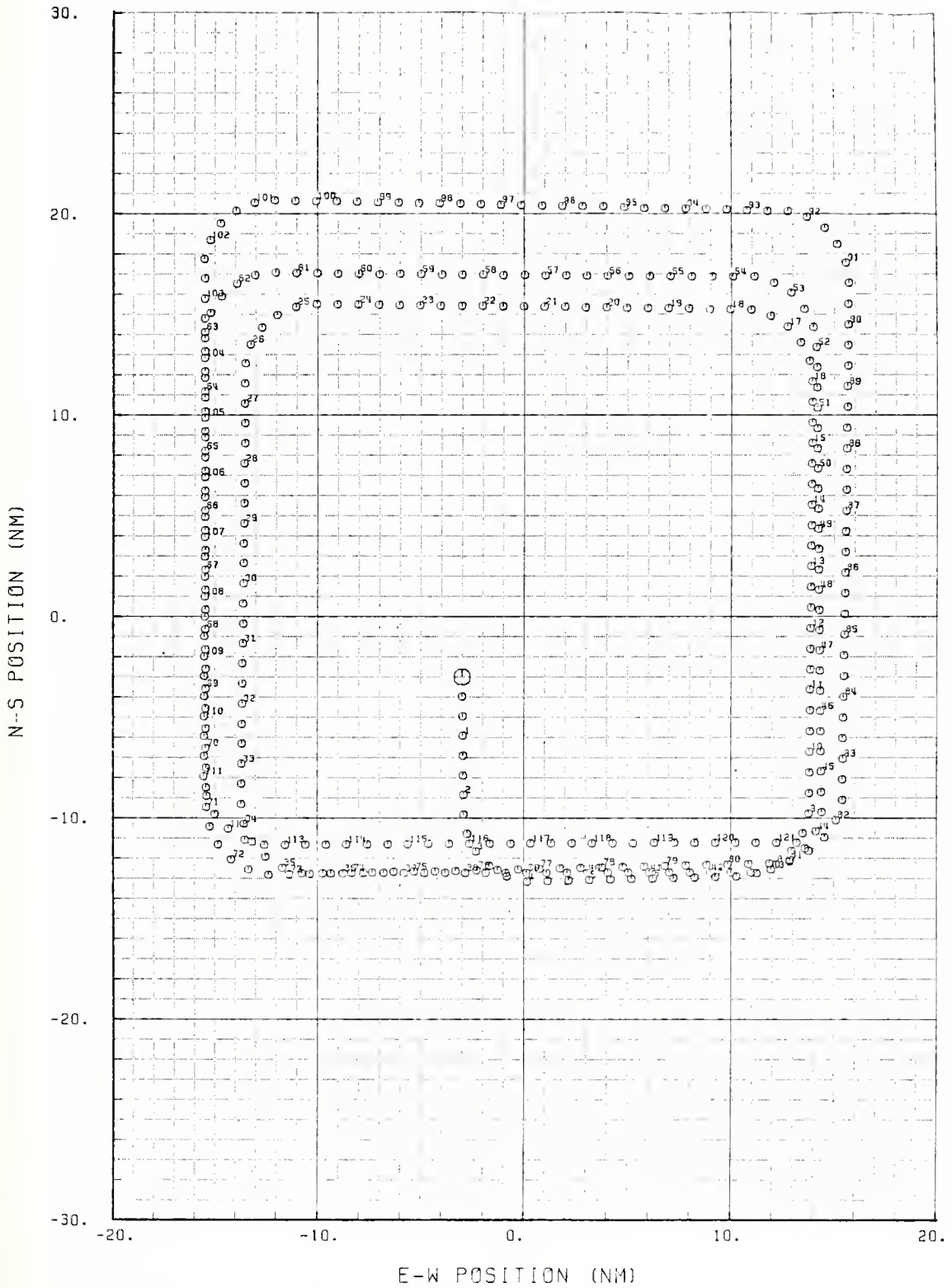


Figure 9. Aircraft's navigational output for the 15 NM square; navigational drift is 2.5 NM/Hr north with a Schuler cycle.

These patterns were used to generate the data which included sonobuoy number, time of measurement and measurement, aircraft latitude and longitude, altitude, heading, pitch angle, roll angle, N-S acceleration, E-W acceleration, and the antenna used for the measurement. Also determined, but used only for error analysis, were sonobuoy position and true aircraft position. This information was computed for the entire simulation period and stored in a file to be used when needed.

Initial estimates of the state and the square root of the covariance matrices were obtained as follows:

Six-state

$$X(\emptyset) = \begin{bmatrix} x_1(\emptyset) - x_{a_1}(\emptyset) \\ x_2(\emptyset) - x_{a_2}(\emptyset) + .5 \\ -V_a \cosh \\ -V_a \sinh \\ \emptyset \\ \emptyset \end{bmatrix} \quad S_D(\emptyset) = \begin{bmatrix} 5. \\ 5. \\ 5. \\ 5. \\ .0025 \\ .0025 \end{bmatrix} \quad (67)$$

Two-state

$$X(\emptyset) = \begin{bmatrix} x_1(\emptyset) \\ x_2(\emptyset) + .5 \end{bmatrix} \quad S_D(\emptyset) = \begin{bmatrix} \text{Alt} \\ \text{Alt} \end{bmatrix} \quad (68)$$

where $S_D(\emptyset)$ indicates the diagonal elements of $S(\emptyset)$.

For the circular pattern

$$x_1(0) = 1.$$

$$x_{a_1}(0) = 15.$$

$$x_2(0) = 1.$$

$$x_{a_2}(0) = 0.$$

and for the square pattern

$$x_1(0) = -3.$$

$$x_{a_1}(0) = -3.$$

$$x_2(0) = -3.$$

$$x_{a_2}(0) = -3.$$

The initial values of the covariance were chosen so as to describe the errors in the state associated with dropping a sonobuoy from an aircraft. The two-state system operated better with a lower initial variance than did the six-state system.

Simulations were run for a nominal period of two hours. Each unit of data was sequentially read into the simulation program from the storage file. Measurement noise was added with the following normal distributions:

cos θ $N(0, .0007)$ in radians

doppler velocity $N(0, 1.0)$ in NM/HR

doppler drift angle $N(0, .01)$ in degrees

These values agree with the ones chosen for R as described previously. A random number generator using an initial seed was used to create the noise from the proper distributions. After the estimate was made, errors were measured and manipulated in subroutine RESULT. This cycle was repeated

until the simulation was complete. (Refer again to Appendix A for a flow diagram of the simulation process.)

Information was gathered and is presented primarily in two ways. First, for both the square and circular patterns the results of the first run of the simulation are plotted. (Figure 13 is an example.) The top portion of the results shows the estimated positions of the sonobuoy on the aircraft's navigational plot. It should be noted that these are not true positions since inertial errors may be causing this plot to drift. The bottom portion shows the North-South and East-West errors in the estimated positions. These errors are the differences between the true and the estimated relative positions of the sonobuoy. They are depicted in Figure 10 and were computed from

$$\tilde{\Delta X}_k = \hat{\Delta X}_k - \Delta X_k \quad (69)$$

$$\tilde{\Delta X}_k = (\hat{X} - X_a^I)_k - (X - X_a)_k \quad (70)$$

where $\tilde{\Delta X}_k$ is the relative error at time k. The true aircraft

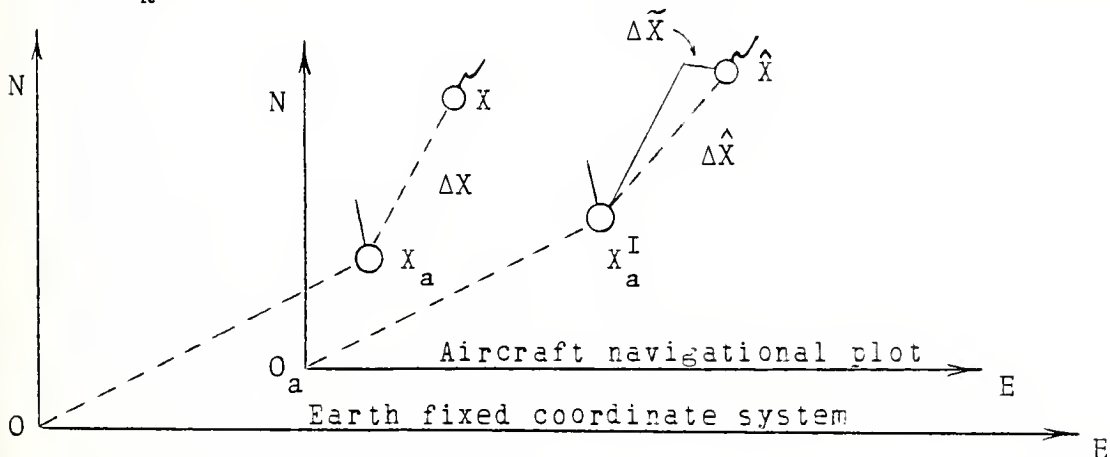


Figure 10. The effect of the aircraft navigational plot

position is denoted by X_a and the true geographical position of the sonobuoy is denoted by X . These values are known from the simulated data. \hat{X} is the filter's estimate of position and X_a^I is a deterministic input from the aircraft's navigational system. The errors indicated in these plots are different from those perceived in the upper plot whenever the aircraft's navigational picture is drifting. The positive and negative values of the square root of the covariance are also shown on these plots as solid lines. Specifically,

$$\begin{aligned} \text{N-S error} &= \pm \sqrt{P_{11}} \\ \text{E-W error} &= \pm \sqrt{P_{22}} \end{aligned}$$

(Only position errors are analyzed in this report.)

The second way in which the information was gathered consisted of a shortened Monte-Carlo simulation. For each scenario under study, 20 two-hour simulations were run, each with new values of measurement noise provided by the random number generator from their respective distributions. The objective was to compare the RMS errors predicted by the covariance matrix in the filters to the actual RMS errors observed in the simulations. Three RMS statistics were collected and plotted versus time as follows:

1. The square root of the covariance computed by the Kalman filter is represented by a solid line on the plots. It was computed from

$$\sigma_{f_k} = \sqrt{\frac{1}{n} \sum P_{11} + \frac{1}{n} \sum P_{22}}, \quad n=20, \quad k = 1, 2, 3, \dots \quad (71)$$

This standard deviation is the filter's estimate of its accuracy.

2. The mean and standard deviation of the error in the estimated sonobuoy position relative to the aircraft was determined by

$$\mu_k = \frac{1}{n} \sum_{i=1}^n \Delta \tilde{X}_{k,i}, \quad n = 20, k = 1, 2, 3, \dots \quad (72)$$

$$\sigma_{x_k}^2 = \frac{1}{n} \sum_{i=1}^n \Delta \tilde{X}_{k,i}^2 - \mu_k^2, \quad n = 20, k = 1, 2, 3, \dots \quad (73)$$

This standard deviation is represented by an 'X' on the plot and is a measure of the variability in the filter's estimated position.

3. The RMS value of the actual relative error was also determined. It was computed as

$$\sigma_{a_k}^2 = \frac{1}{n} \sum_{i=1}^n \Delta \tilde{X}_{k,i}^2, \quad n = 20, k = 1, 2, 3, \dots \quad (74)$$

and is represented by an 'O' on the plot. This value is a measure of the error which occurred between the actual relative position of the sonobuoy and the estimated one. (See Figure 11.)

These values are plotted over the two hour simulation period ($k = 1, 2, 3, \dots$) and provide a measure of the accuracy obtained by each of the algorithms.

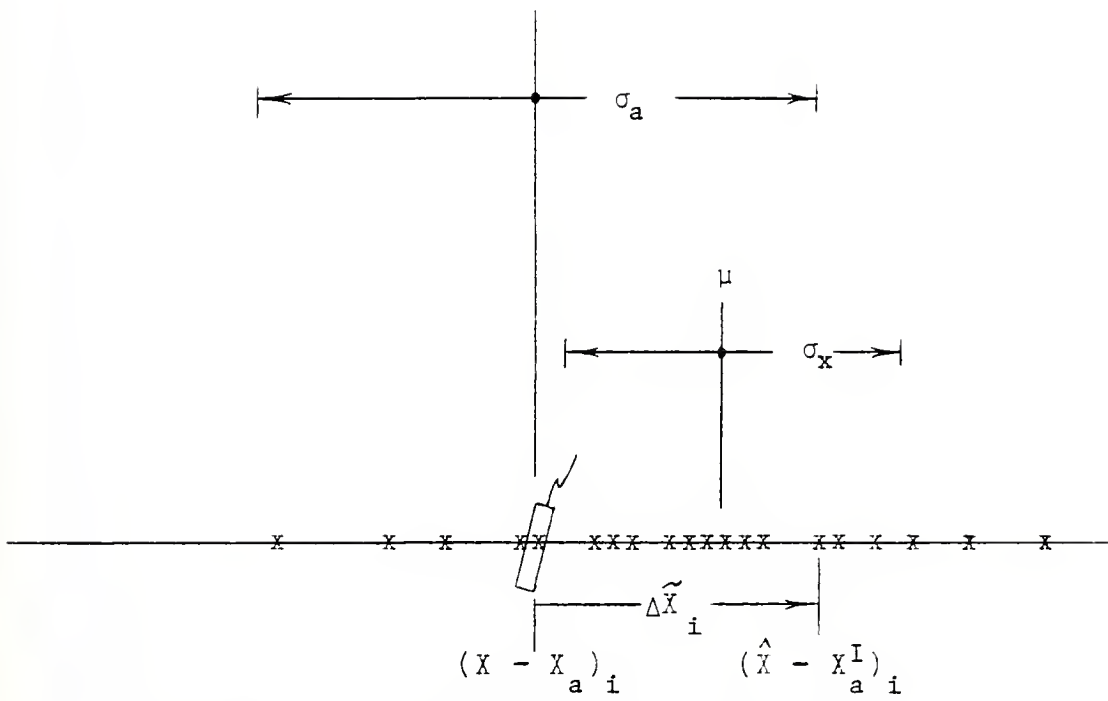


Figure 11. RMS statistics at time = k.

B. THE RESULTS

Orincon Corporation performed much of their analysis using the small circular pattern shown in Figure 12. The aircraft sped around this track at 388 knots taking a measurement every 20 seconds. Altitude was constant at 3000 feet. The initial position of the sonobuoy was at (2,2) and it drifted on a heading of 045 degrees at 5.5 NM/HR while the aircraft's navigational system drifted in the opposite direction at 5.2 NM/HR. A Schuler cycle was also superimposed on this drift.

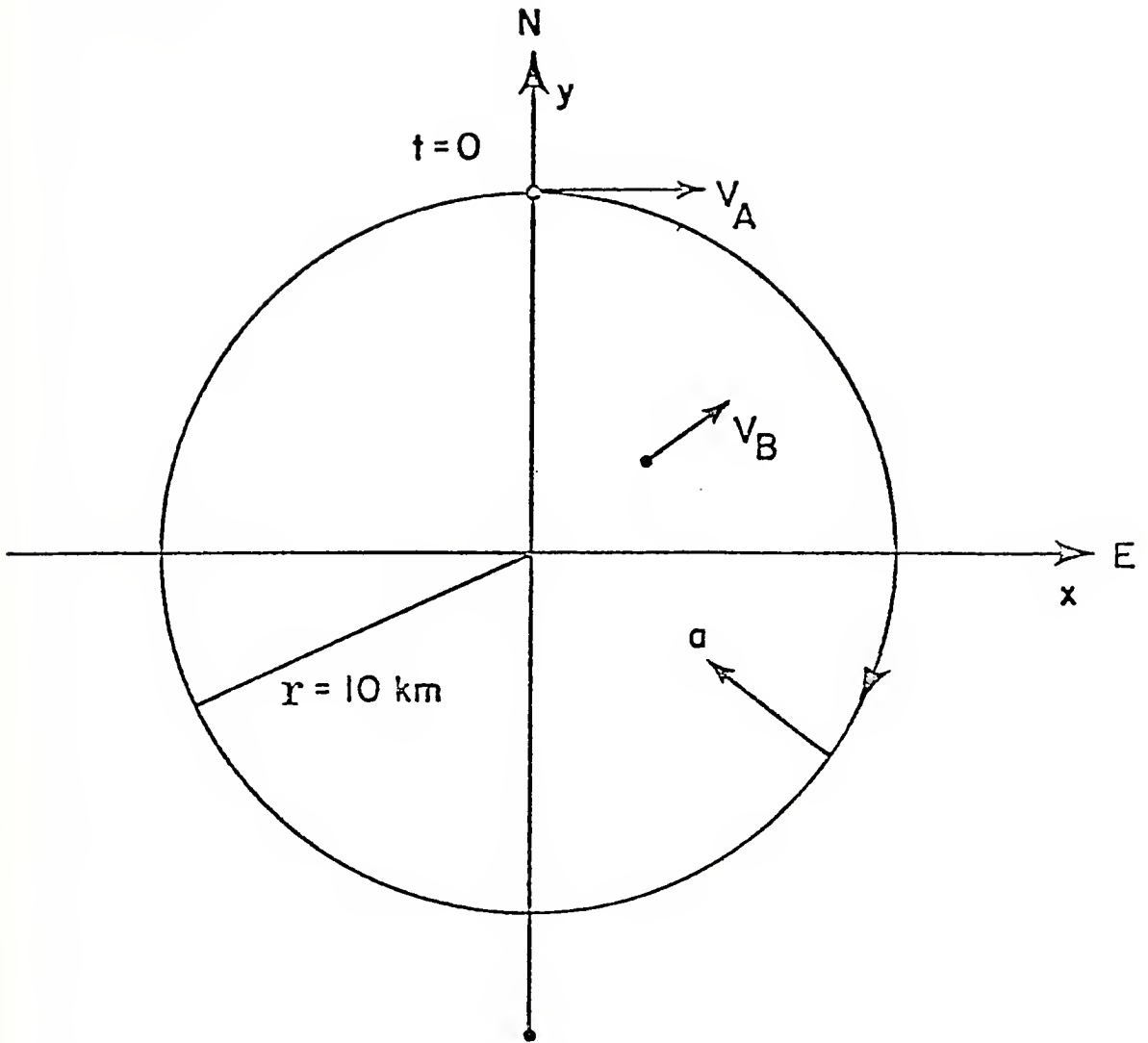
The initial estimates of sonobuoy position and variances used by the algorithms were different for this particular pattern in order to coincide with the Orincon simulation as much as possible. They were

Two-state

$$X(\delta) = \begin{bmatrix} \emptyset \\ \delta \end{bmatrix} \quad S_D(\emptyset) = \begin{bmatrix} 2. \\ 2. \end{bmatrix} \quad (74)$$

Six-state

$$X(\delta) = \begin{bmatrix} -5.4 \\ \delta \\ -V_a \cos H \\ -V_a \sin H \\ \emptyset \\ \emptyset \end{bmatrix} \quad S_D(\emptyset) = \begin{bmatrix} 2. \\ 2. \\ 5. \\ 5. \\ .0025 \\ .0025 \end{bmatrix} \quad (75)$$



CIRCLE

$$a = -4 \text{ M/S}^2 = -0.4 \text{ g}$$

$$v_A = 200 \text{ M/S}$$

$$v_B = 2.8 \text{ M/S}$$

Figure 12. Orincon's simulation flight path.

Initially, both the six-state and the two-state algorithms were tested using this flight path and comparisons were made with the results of Orincon's 13-state system. It was discovered that the six-state system's results did not change as a consequence of whether or not a Schuler cycle existed in the navigational system. Therefore, the six-state system was run only with the Schuler cycle active. The two-state system was run with and without a Schuler cycle.

The results of the first run of the simulation are shown in Figures 13, 14, and 15. The sawtooth shape of the covariance (solid lines) is the result of the circular pattern and is caused in two ways. Primarily, since the sonobuoy remains closer to one side of the circle, there is a minimum value of the variance each time the aircraft passes on this side. A second reason for a change in variance is the aircraft's location in the pattern. However, these modulations are not as apparent since the range variation dominates. RMS errors were obtained by repeating these runs 20 times and are shown in Figures 16 thru 18. The fluctuations generated by the flight path are apparent, more so in the six-state system than in the two-state system. Also, steady state values of the error gradually increase. This is true because the average range to the sonobuoy increases as the buoy moves farther away

from the center of the pattern. (It will be demonstrated later that the errors are range dependent.) The covariance of the six-state system increases from 400 yards at 25 minutes to 800 yards at the end of the simulation. The two-state system increases slowly from 250 yards until it is hampered by the Schuler cycle. It is worthy of note that without the navigational errors stemming from the Schuler cycle the RMS errors of the two-state system are considerably lower than those of the six-state system.

Table 1 compares the RMS errors of these two systems to the results obtained by Orincon for their 13-state system. (The values for the two-state and six-state systems are taken from the covariance at a point 35 minutes into the simulation.) The first line considers measurements of bearing, doppler velocity, and drift angle. Navigational errors are present including a Schuler cycle. As expected there is an increase in relative position error because of the reduction from 13 to 6 states. The next line considers the effect of the Global Positioning System (GPS), with very accurate aircraft positioning information, on the relative

	13-state	6-state	2-state
Schuler SRS+dv+DA	394	450	
No Schuler SRS+DV+DA+GPS		450	200

Table 1. Comparison of RMS results in yards.

position errors of the sonobuoy. In the 13-state system Orincon observed that the errors in the states pertaining to the aircraft inertials improved markedly; relative position errors most likely remained the same. This is exactly what was found in the analysis of the six-state system: that the relative position errors were unaffected by navigational errors. However, the two-state system is very much affected by navigational errors. Relative position errors were significantly less for the two-state system when accurate aircraft positions were known.

To obtain a more realistic analysis of their performance, each algorithm was tested using the circular and square flight patterns of Figures 6 and 7. The results of the first simulation run for the circular path at a range of 15 NM are shown in Figures 19 thru 21. In this case, the wavy nature of the covariance is due to the location of the aircraft in the pattern since the range to the sonobuoy remains relatively constant. For instance, as the aircraft passes directly north or south of the sonobuoy the ability to correct E-W errors is greatest. Therefore, the E-W variance reaches a minimum value at this time. The N-S variance is affected in a similar manner. The two-state filter is not as sensitive to this as the six-state filter. Also, the effect of the Schuler cycle on the two-state filter can be seen in Figure 20.

The RMS errors are shown in Figures 22 thru 24. The steady state RMS value of error predicted by the filter is

425 yards for the two-state and 750 yards for the six-state system. The actual RMS error in the relative position of the sonobuoy is 250 to 1200 yards for the two-state and 400 yards for the six-state system. Without Schuler cycle error the two-state system drops to a steady 250 yards, better than the six-state system. It is interesting to note that the measured errors are significantly less than those predicted by the filter. Both measured values of RMS error, σ_x and σ_a , are in close agreement; that is, the deviation of the filter's estimated position about its mean is generally the same as the deviation of the estimated position about the actual relative position of the sonobuoy. The closer these values are to one another, the more confidence can be placed in the analysis. The only exception to this is Figure 23 which shows the reaction of the two-state filter to the Schuler cycle. One complete cycle with a period of 84 minutes is obvious. The Kalman filter does not recognize this cycle since the modeling equations do not account for it. The dip in the center of the two peaks is once again the result of flight path geometry. The aircraft is in such a position relative to the sonobuoy that the measurements provide enough information to correct for Schuler cycle errors. However, it is not in this position long enough to influence the errors anymore than it does.

The same analysis was performed using the square pattern of Figure 7. This scenerio has more drift than the other and in a different direction providing the algorithms

with another motion to track. The outcome was generally the same as can be seen in Figures 25 thru 30. There is no measurable difference in the results from the two different flight paths. Flying a straight path does not adversely affect the results as was concluded by the Oricon Corporation for their 13-state system. The wavy nature of the covariance is again a result of the flight path. It is not as smooth as before because a square pattern was flown instead of a circular one. Another look at errors caused in the two-state system by the Schuler cycle can be seen in Figure 30. The algorithm does make some corrections to these errors but they are not as effective as before. In this case the time the aircraft was in a position to make the corrections did not coincide with the time the peak errors occurred. There appears to be no way to predict the optimum time and place for the aircraft to be without knowing when and how the Schuler cycle is occurring.

The distance the aircraft is from the sonobuoy is directly related to the accuracy the algorithms can achieve. Simulations were performed at ranges of 5, 15, 30, and 45 nautical miles using a circular flight path with the sonobuoy in the center. (The RMS plots can be found in Appendix C.) The steady state errors were observed and are plotted in Figure 31. Solid lines represent the RMS values of the covariance and dashed lines represent the actual errors. In all cases the errors increase with distance which is intuitively satisfying. Mathematically, the

covariance increases because the H matrix becomes smaller with an increase in range. Consequently, the updated value of the covariance, $P(+)$, is larger from Equation (19). For the six-state system there is an increase in actual error from 240 yards at 5 NM to 750 yards at 45 NM. And for the two-state system, actual errors increase from 130 yards at 5 NM to 500 yards at 45 NM. (Note that for the two-state system, Schuler cycle errors, indicated by circles, peak approximately 1000 yards above these plotted values; the lower values, indicated by x's, were used since they were more reliable for comparison between ranges.) There is a slight decrease in the slopes of all the error curves as distance increases. However, this decrease is small and the curves might well have been interpreted as linear within the limits of the analysis.

The frequency at which measurements are made also affects the accuracy of the estimate. Each algorithm was tested with measurement intervals of 4, 10, 20, and 30 seconds on one sonobuoy. The outcomes of the steady state RMS errors are plotted in Figure 32. (Once again the two-state system's errors do not show the effect of the Schuler cycle.) The actual errors in the six-state system increase steadily as the measurement interval increases. However, the covariance decreases rapidly at first to a minimum value somewhere around 10 seconds and then increases with increasing interval. An abbreviated run with a two second measurement interval confirmed these results.

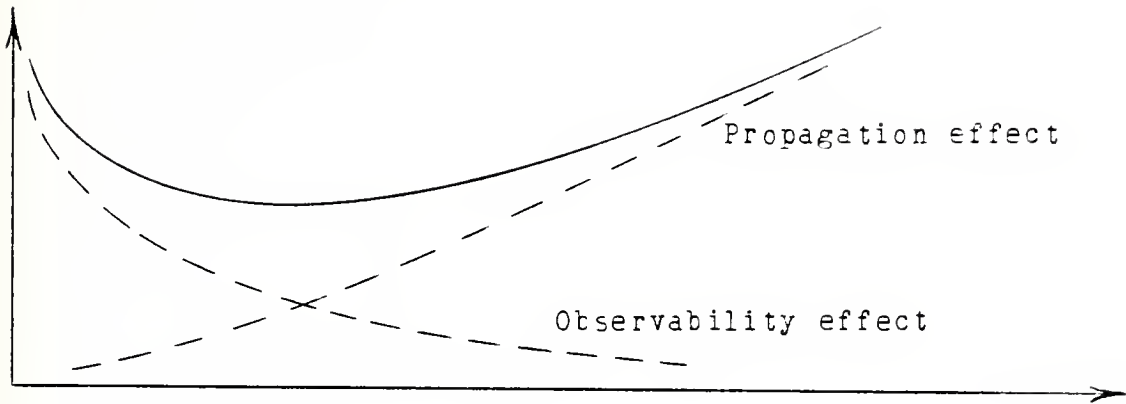


Figure 33. Factors which influence the covariance.

Figure 33 helps to explain this outcome. There are two conditions which affect the covariance. The most obvious is the increase in covariance due to an increase in the propagation interval. This occurs because the plant matrix, which is a function of time, affects the covariance in Equation (16). The second condition is a consequence of the model's observability. If the relative bearing between the aircraft and the sonobuoy does not change then the state is not observable. In other words, two successive bearings must intersect to determine an estimated position. By allowing the interval between measurements to become too small, the aircraft is unable to make a significant change relative to the sonobuoy. The covariance increases as the conditions approach those which make the problem unobservable. There appears to be an optimum frequency with which to make measurements on one buoy, namely 10 seconds for this range of 15 NM and speed of 180 knots.

The two-state system exhibited similar characteristics in Figure 32. In this case the covariance never does increase in the range of intervals studied. The actual errors remain constant. Since the plant matrix for this system is equal to the identity matrix and the Q matrix is prescribed to be constant, the propagation interval, Δt , does not effect the covariance. However, the effects of the observability conditions do cause the covariance to increase when Δt becomes too small. It is believed that as Δt becomes smaller the actual errors would begin to increase also.

The statistical plots for the range tests found in Appendix B show that the Schuler cycle causes larger peaks in the actual error as the range from the sonobuoy increases. However, the peaks are decreasing with time. Further simulation revealed that the peak errors decrease to a steady value about 1000 yards greater than non-Schuler cycle errors. This coincides with the amplitude of the Schuler cycle as it was programmed for this particular flight path. Therefore, in the steady state a Schuler cycle may cause additional estimation errors approximately equal to its amplitude.

Altitude was also tested for any effect it might have on these algorithms. Using the circular pattern at a range of 15 NM, altitudes of 300, 3000, 10,000, and 20,000 feet were tested. Neither the six-state nor the two-state system showed any effect for these changes in altitude. It is

believed that at very small ranges (less than two nautical miles) altitude might hamper good position estimation. However, for the majority of the time altitude is of no concern.

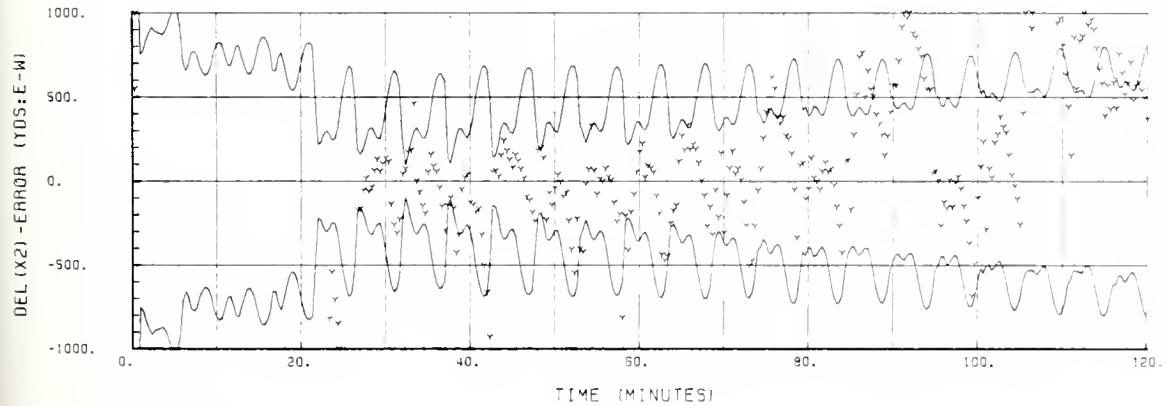
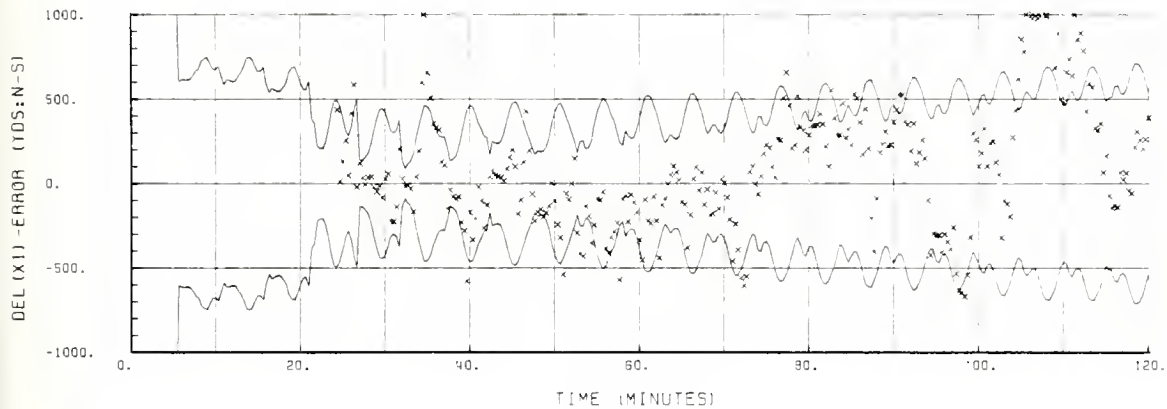
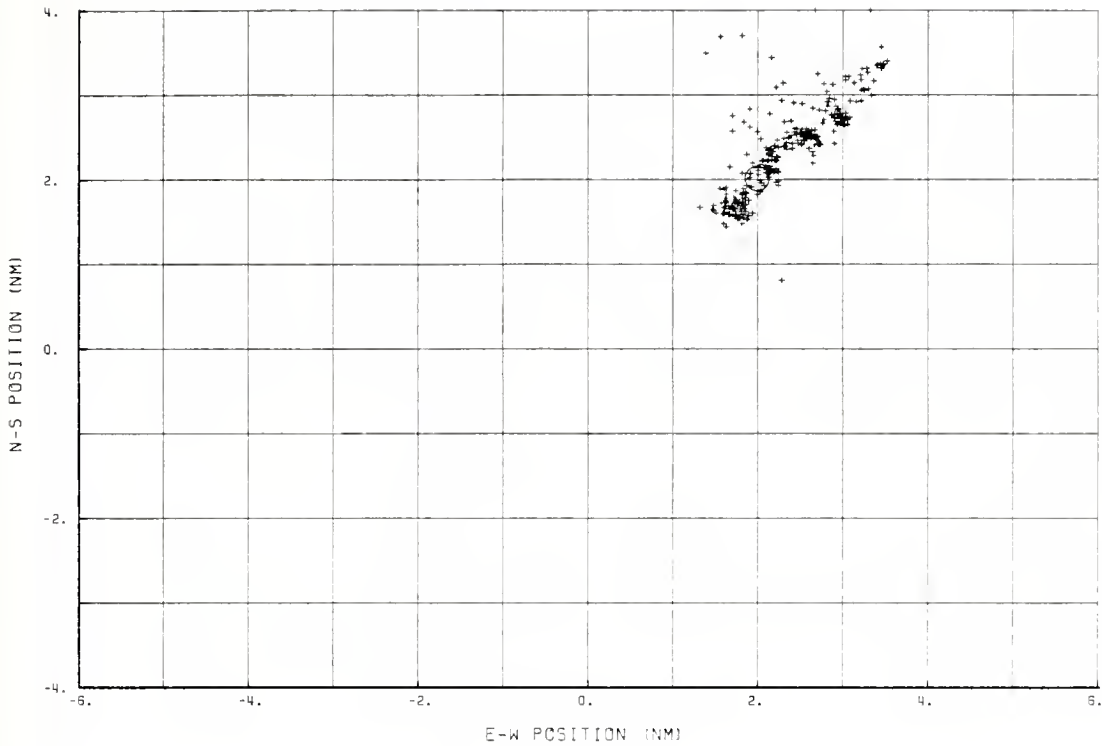


Figure 13. Est. position and relative errors for the six-state system using Orincon's pattern. $DR=(a/c\ 225-5.2 + \text{Schuler}, b\ 045-5.5)$, $\Delta t=20s$, $Alt=3000'$.

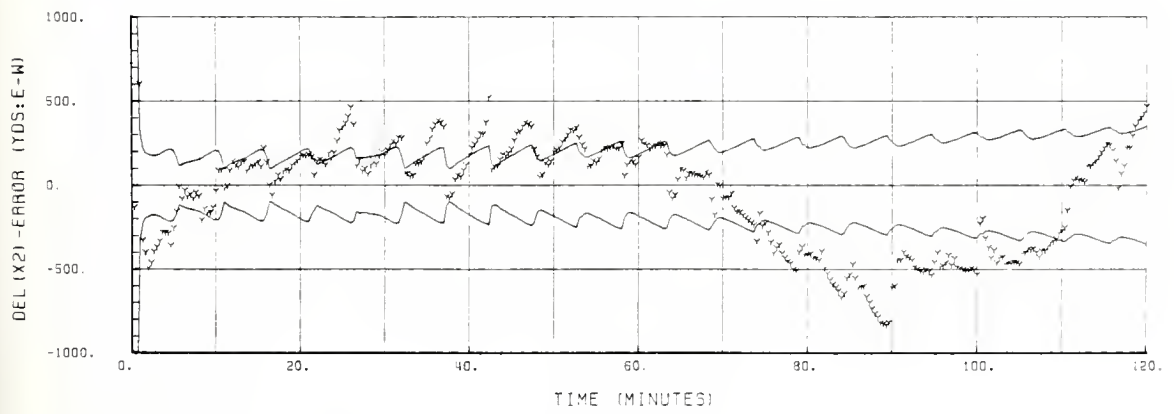
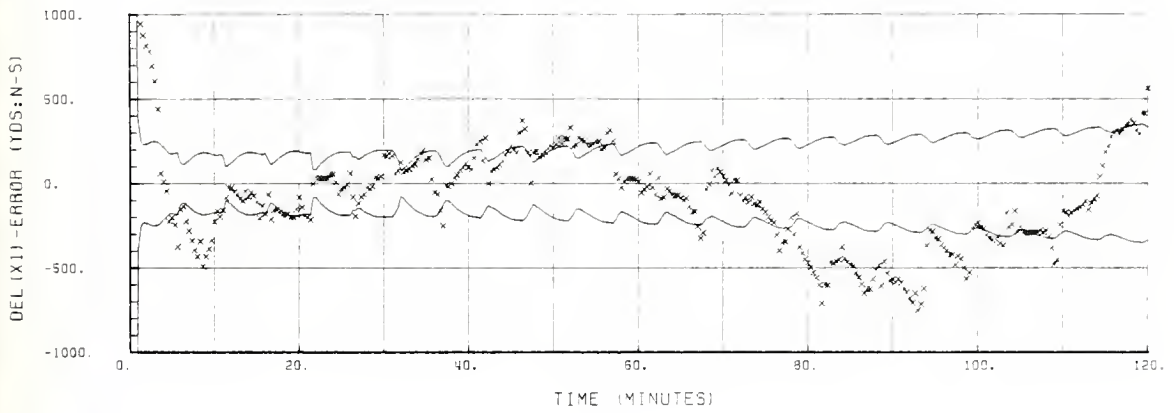
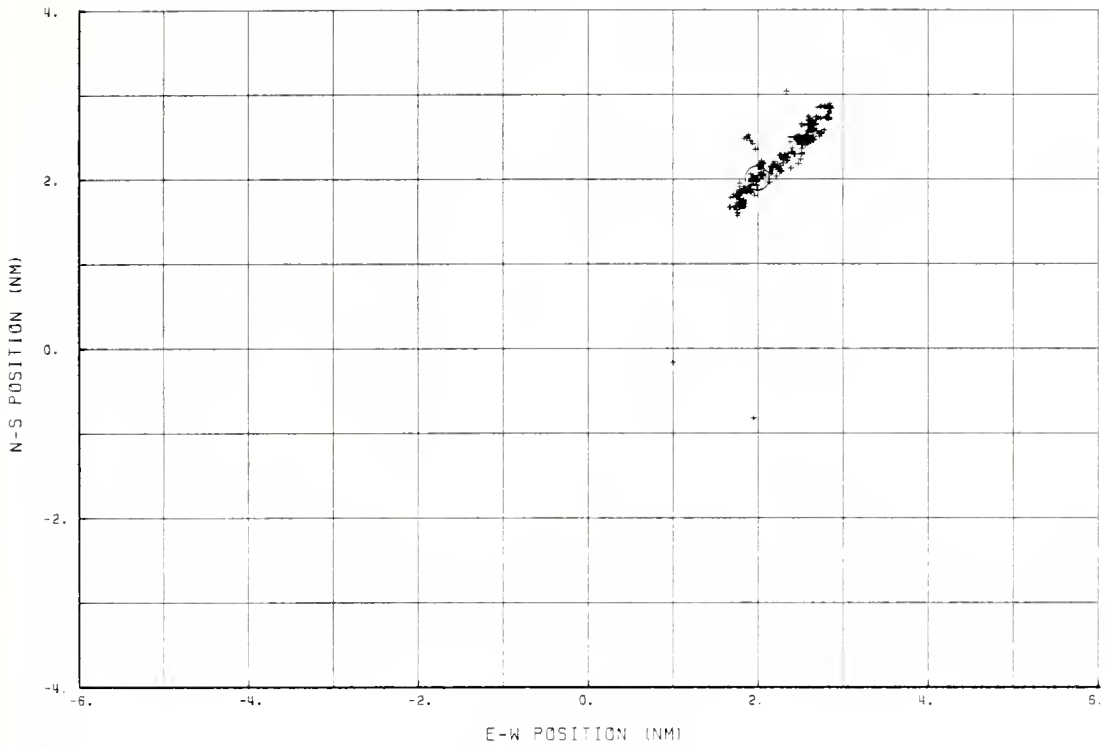


Figure 14. Est. position and relative errors for the two-state system using Orincon's pattern. $DR=(a/c\ 225-5.2 + \text{Schuler}, b\ 045-5.5)$, $\Delta t=20s$, $Alt=3000'$.

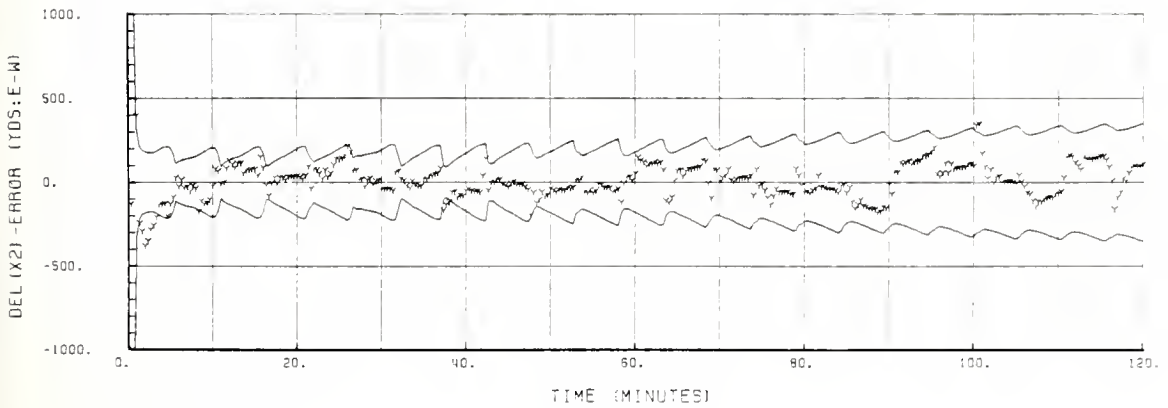
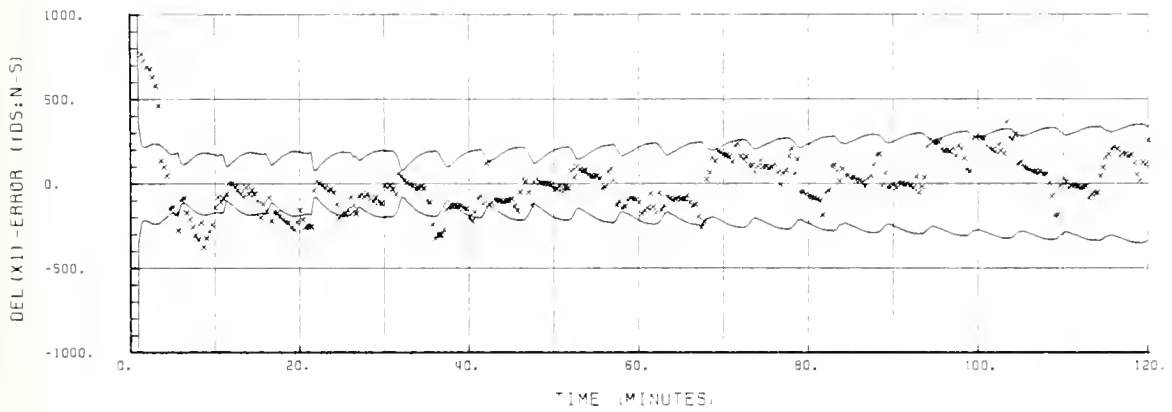
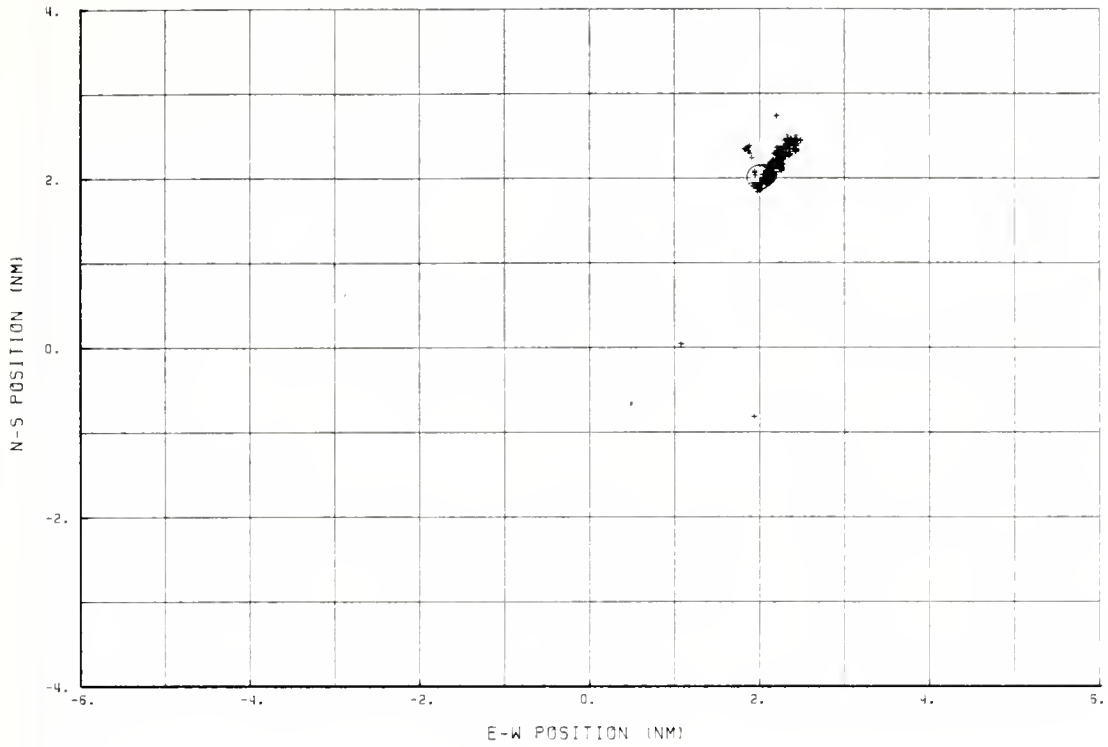


Figure 15. Est. position and relative errors for the two-state system using Orincon's pattern. $DR=(a/c\ 225-5.2 + No\ Sch.,\ b\ 045-5.5)$, $\Delta t=20s$, $Alt=3000'$.

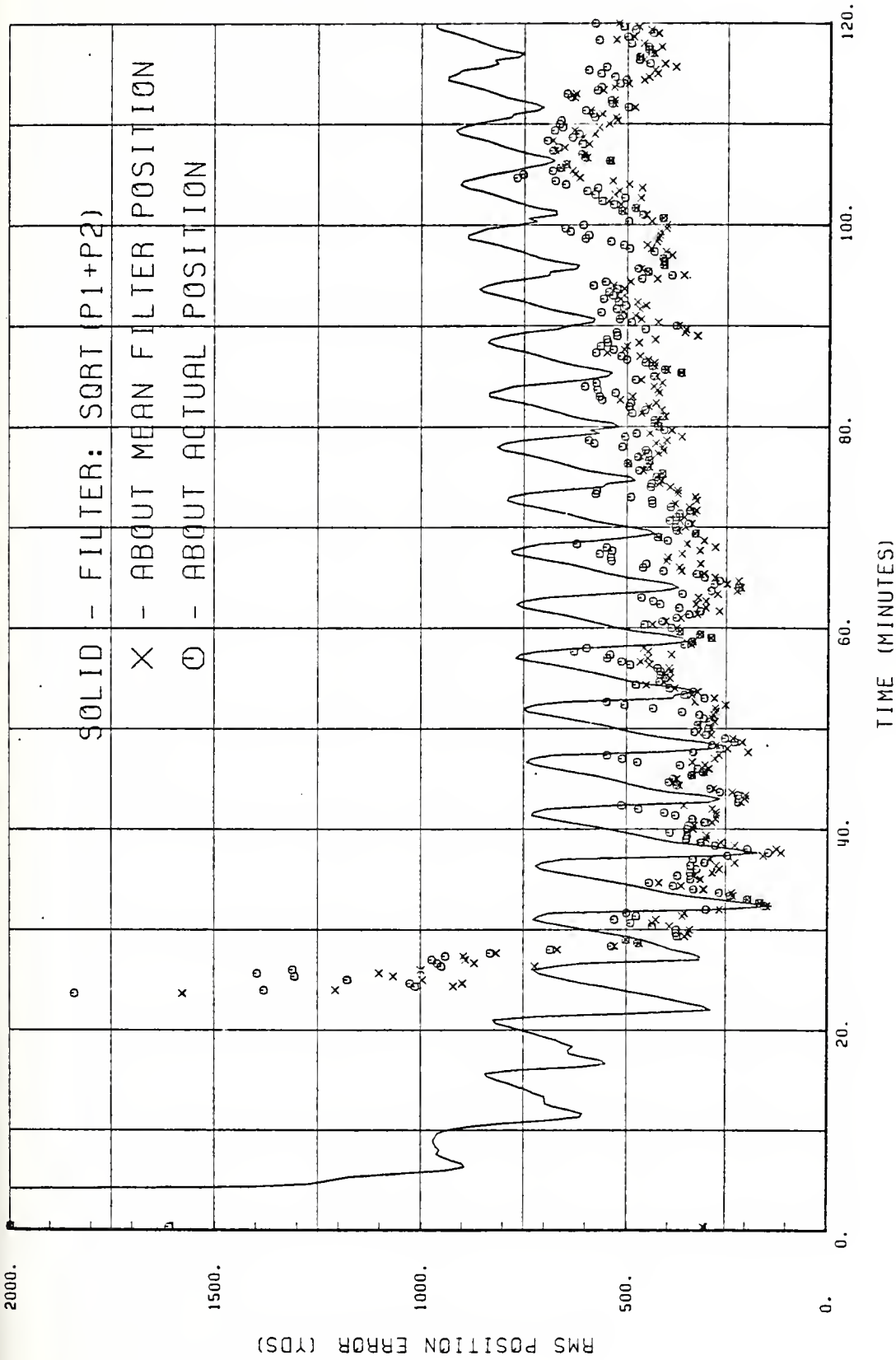


Figure 16.- RMS position errors for the six-state system while flying the circular pattern developed by Orincon Corp. DR=(a/c 225-5.2 + Schuler, b 045-5.5), $\Delta t=20s$, Alt=3000'.

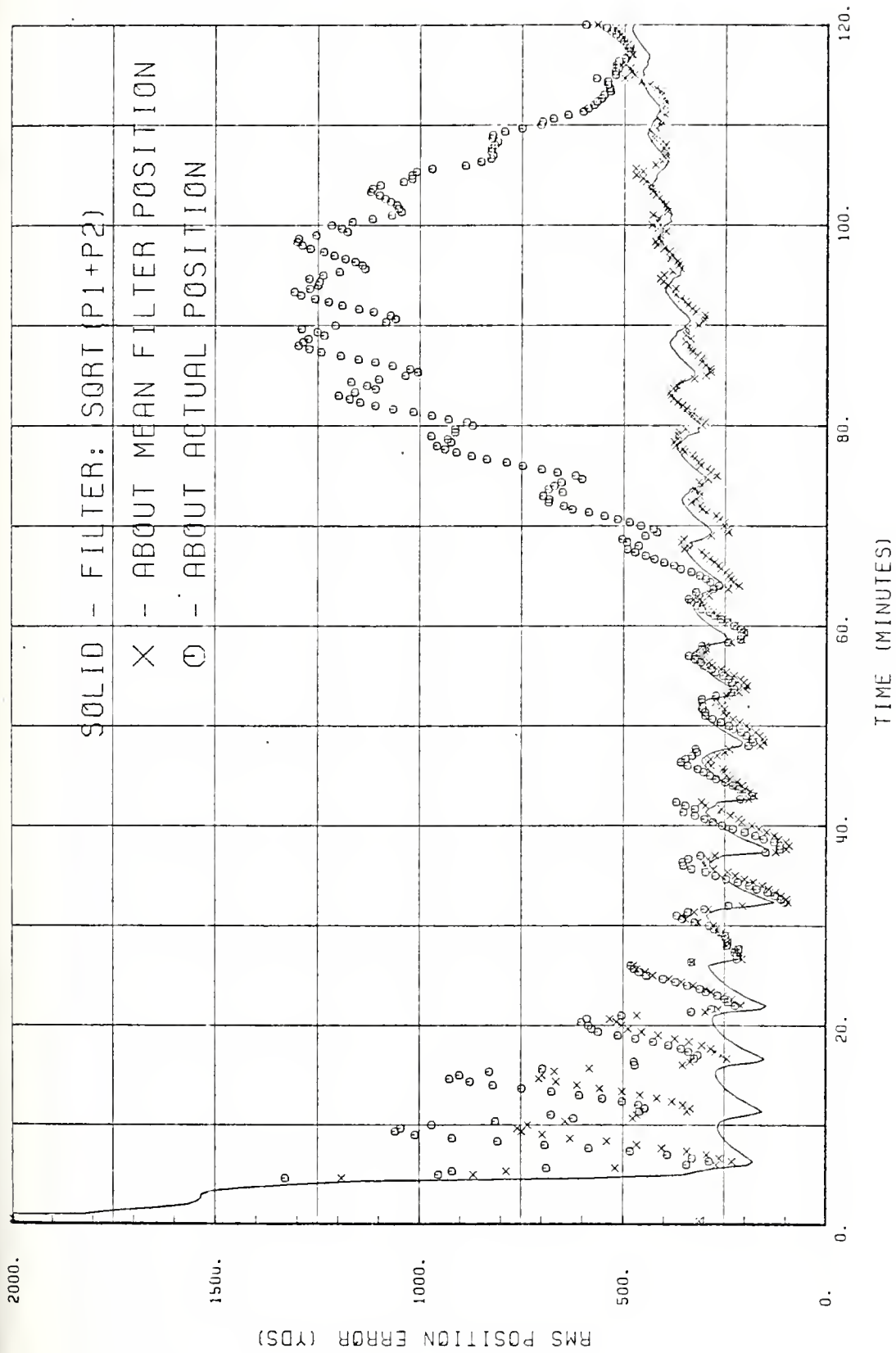


Figure 17. RMS position errors for the two-state system while flying the circular pattern developed by Orincon Corp. DR=(a/c 225-5.2 + Schuler, b 045-5.5), $\Delta t=20s$, Alt=3000'.

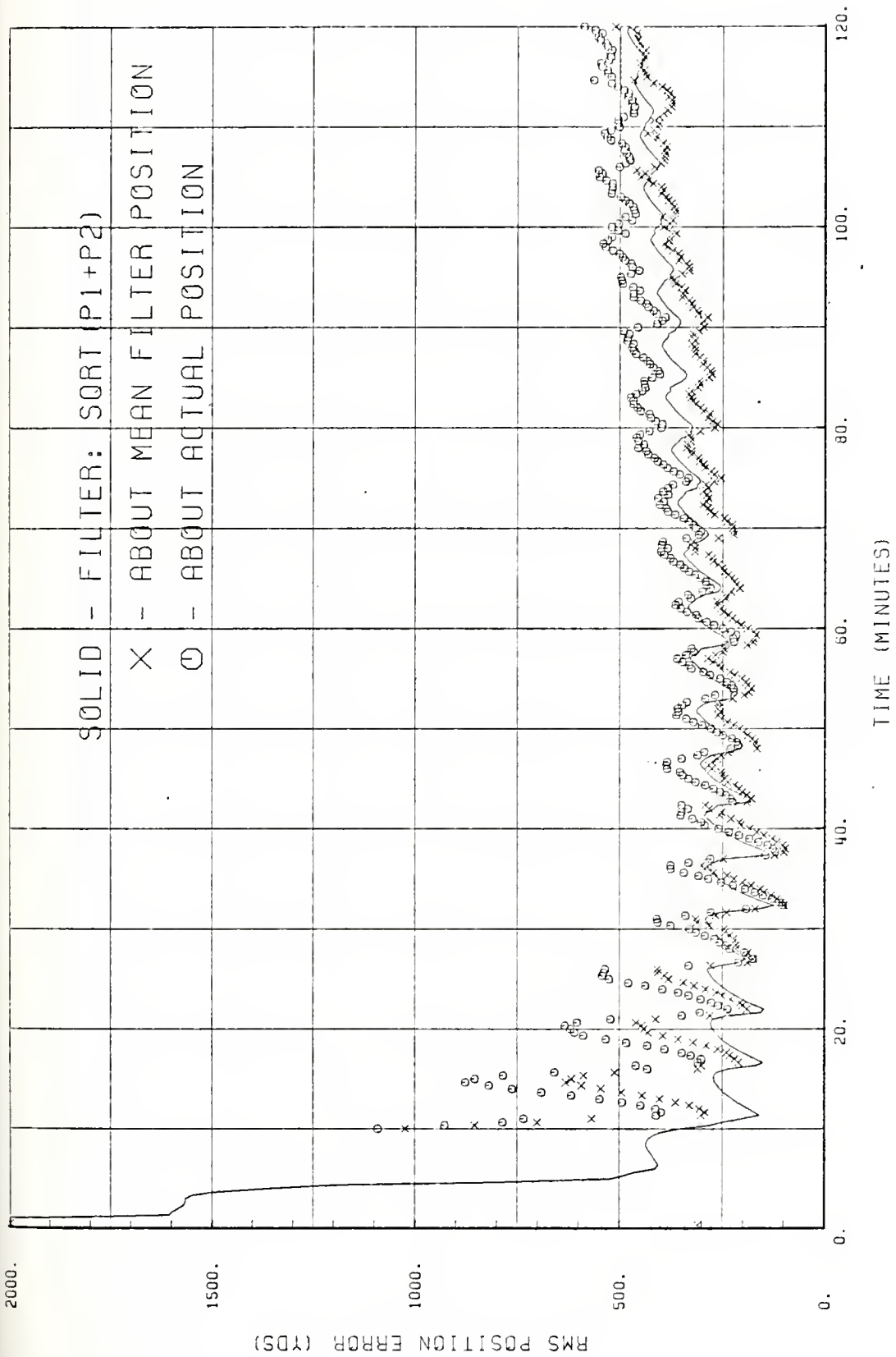


Figure 18. RMS position errors for thr two-state system while flying the circular pattern developed by Orincon Corp. DR=(a/c 225-5.2 No Sch., b 045-5.5), At=20s, Alt=3000'.

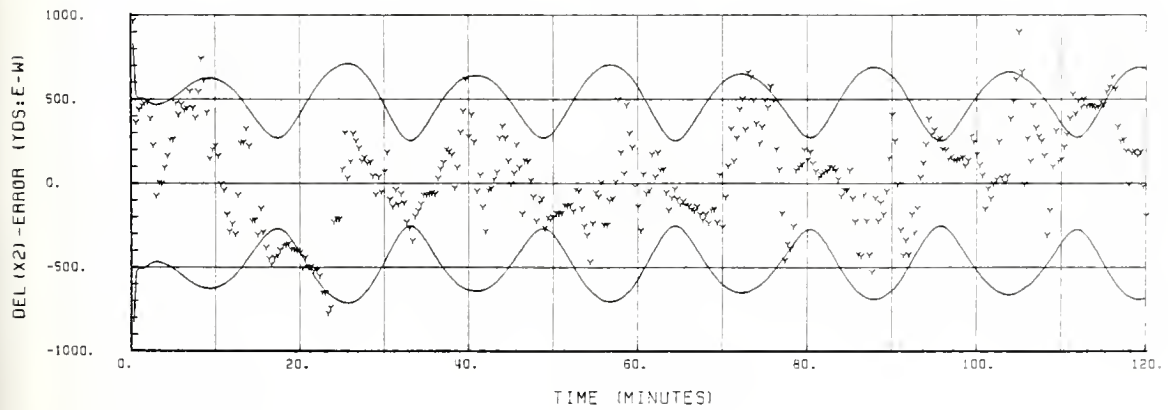
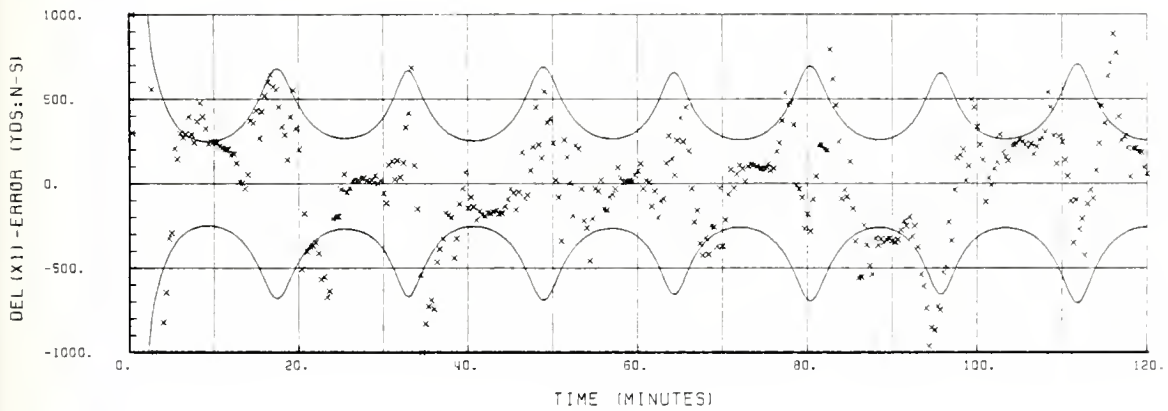
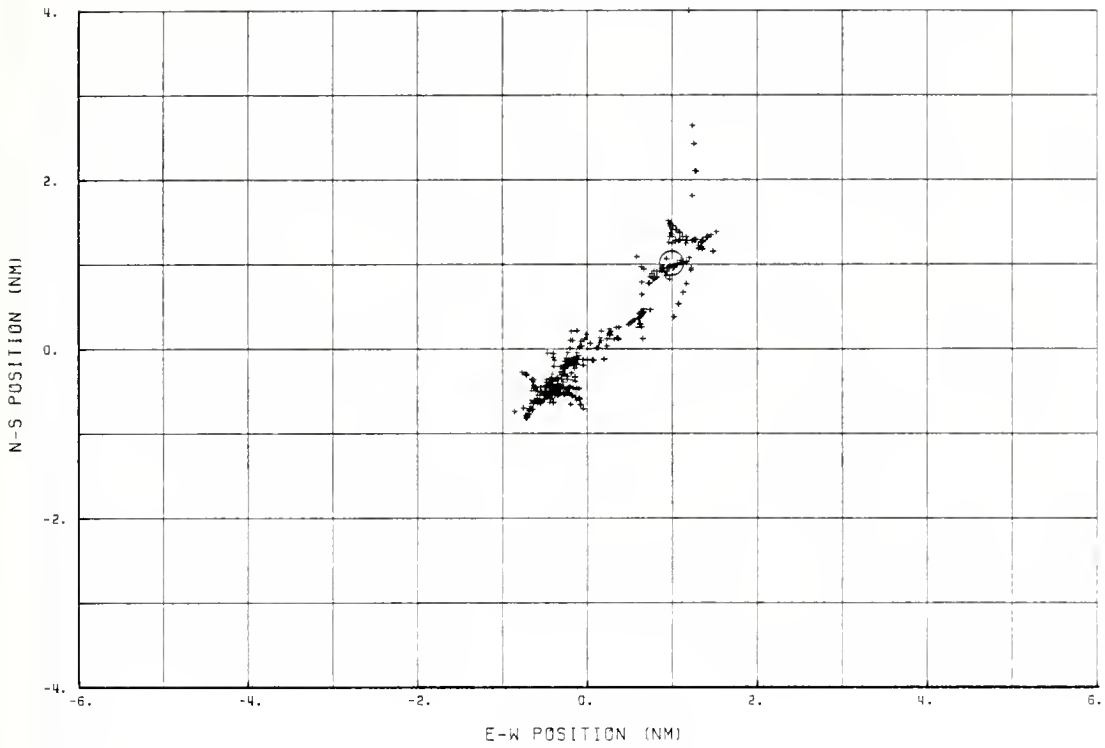


Figure 19. Est. position and relative errors for the six-state system using circular pattern at 15NM. $DR=(a/c\ 180-1 + \text{Schuler}, b\ 270-1)$, $\Delta t=20s$, $Alt=3000'$

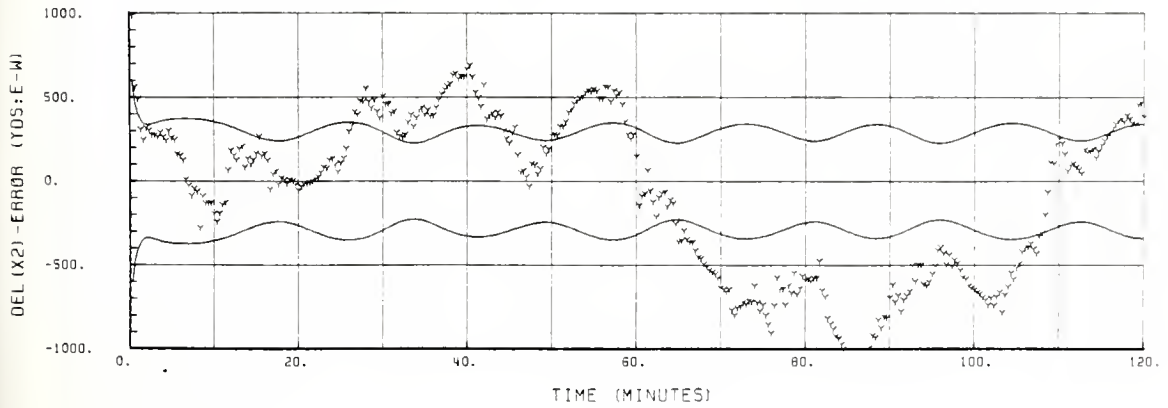
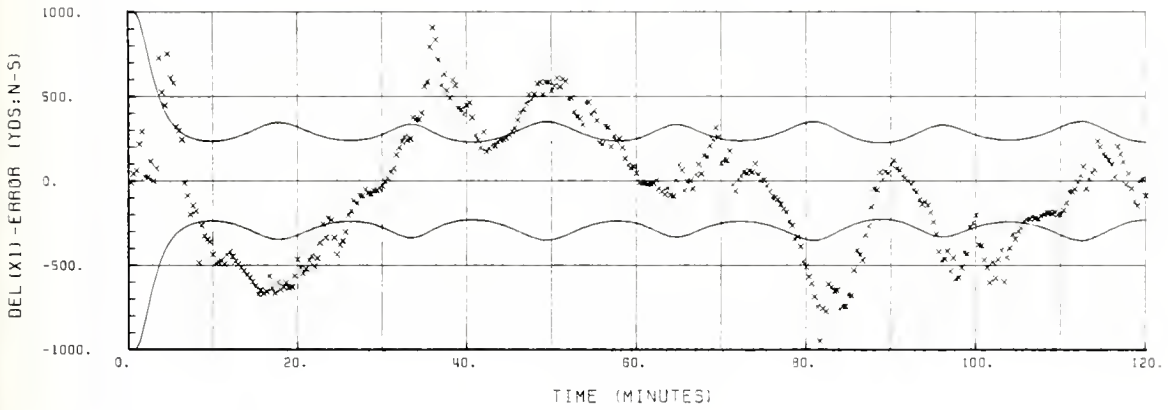
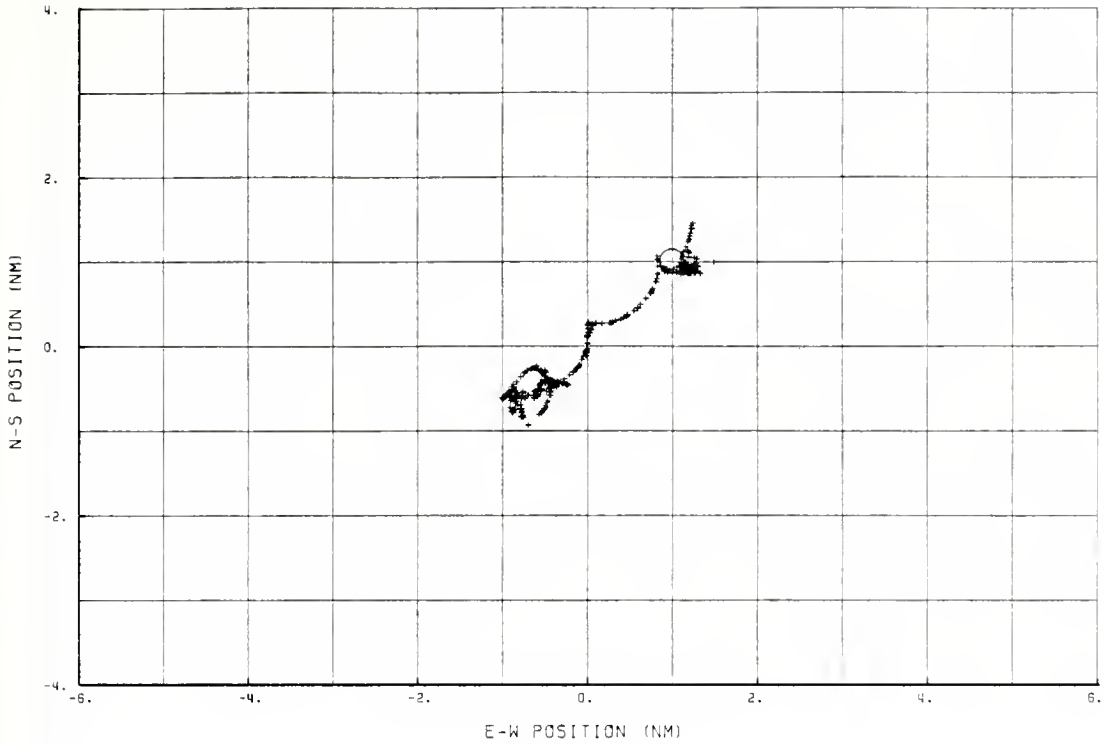


Figure 20. Est. position and relative errors for the two-state system using circular pattern at 15NM. DR=(a/c 180-1 + Schuler, b 270-1), $\Delta t=20s$, Alt=3000'

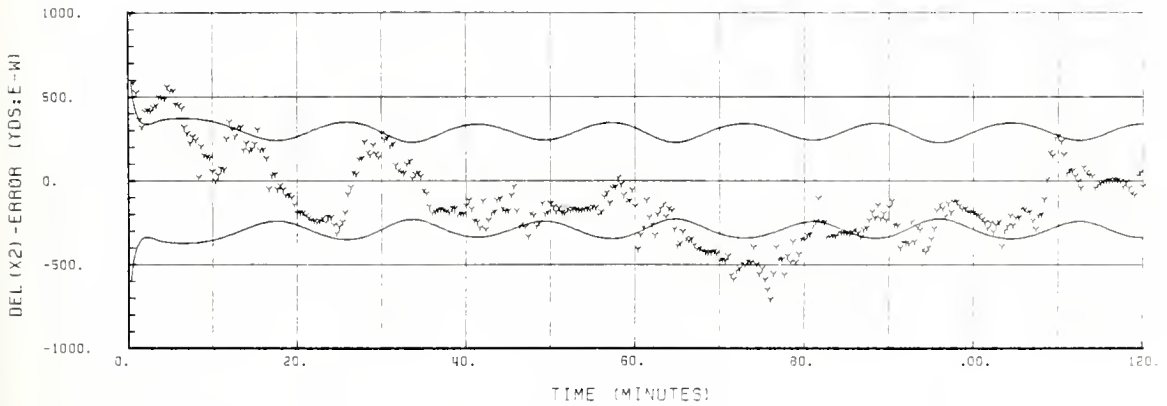
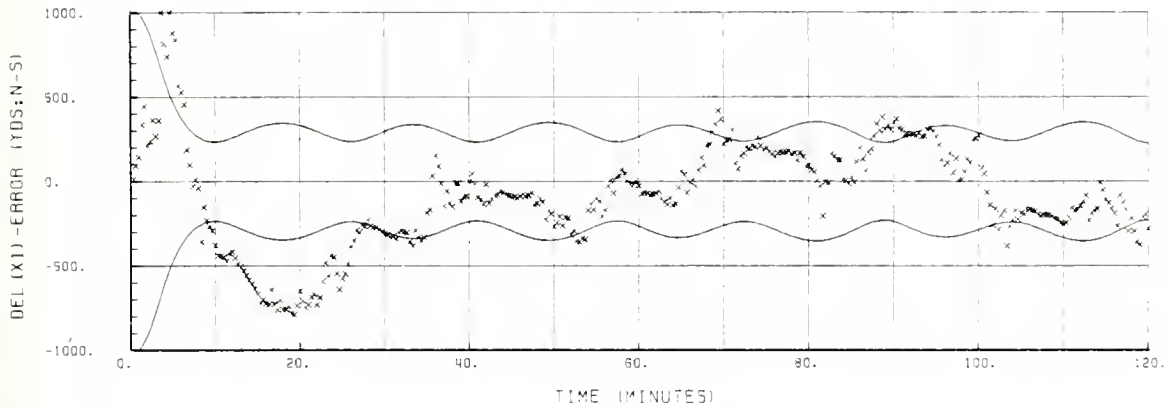
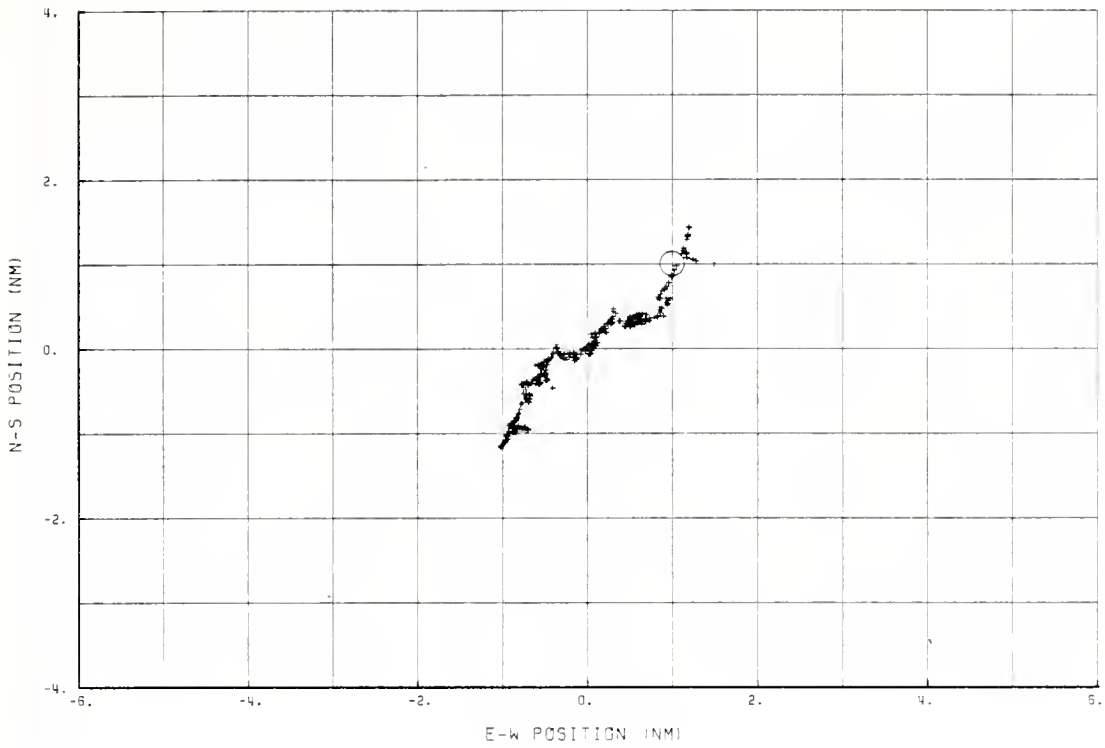


Figure 21. Est. position and relative errors for the two-state system using circular pattern at 15NM. DR=(a/c 180-1 + No Sch., b 270-1), $\Delta t=20s$, Alt=3000'

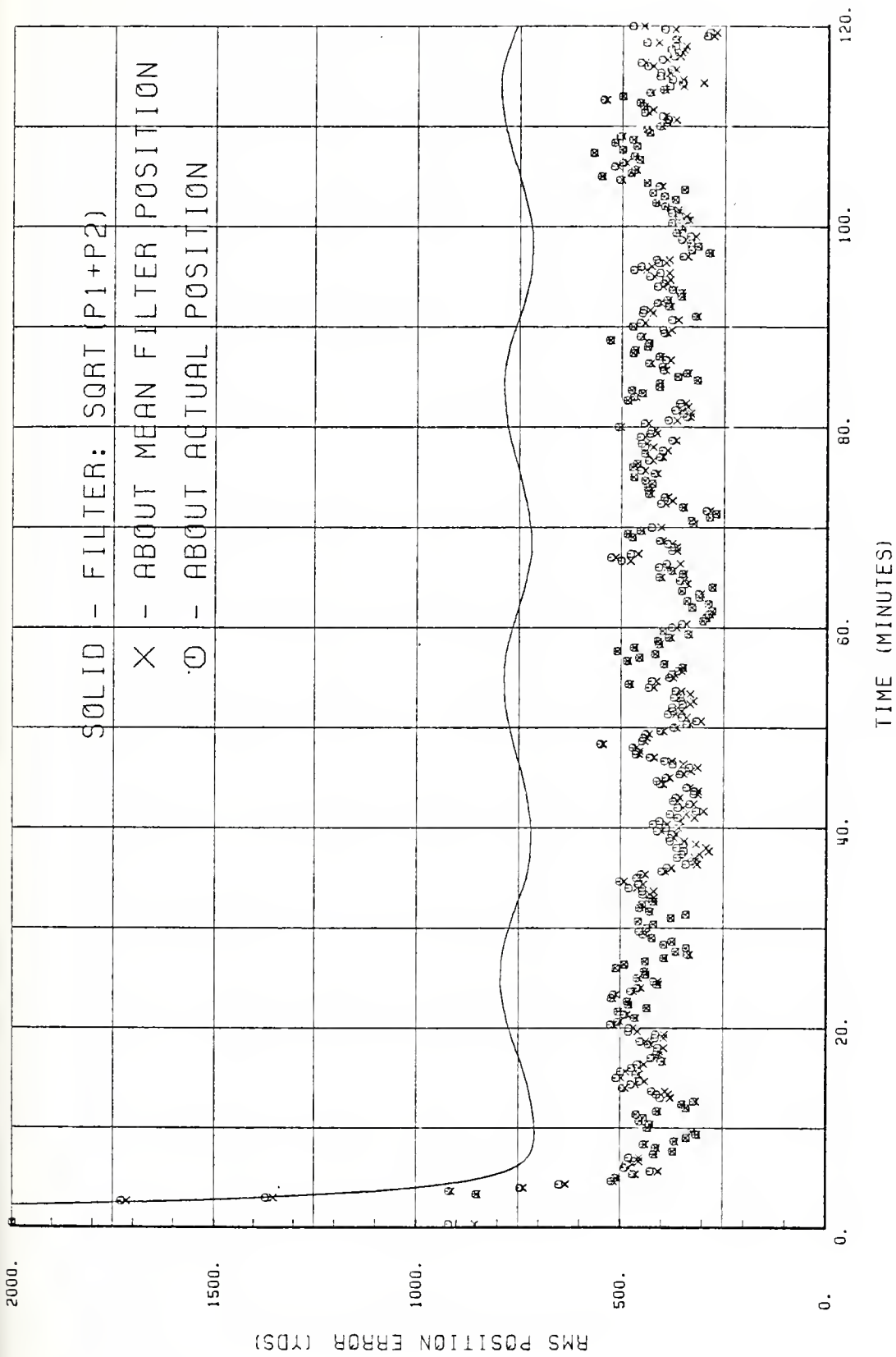


Figure 22. RMS position errors for the six-state system while flying a 15 NM circular pattern around the sonobuoy. DR=a/c 180-1 + Schuler, b 270-1), $\Delta t=20s$, Alt=3000'.

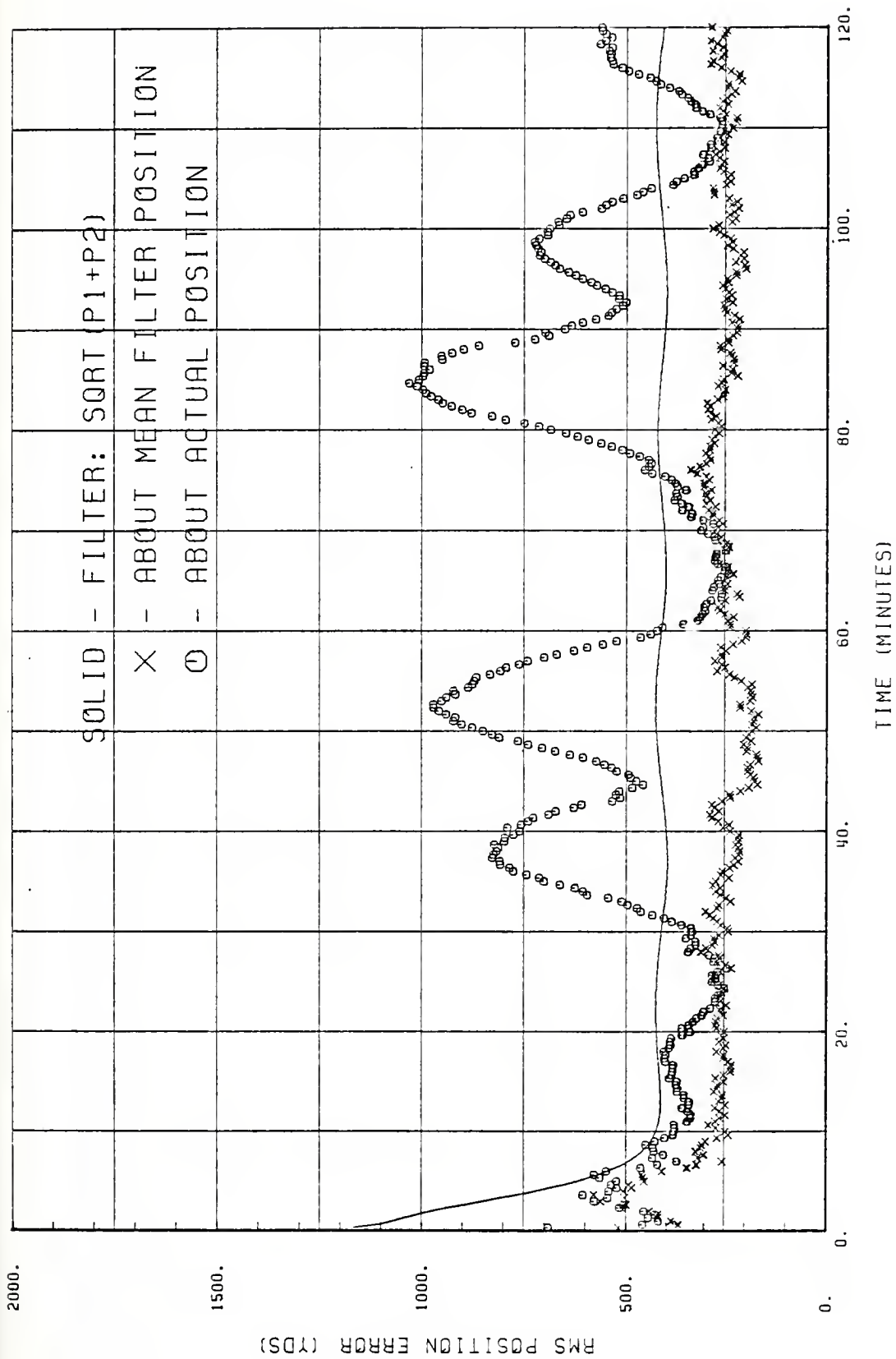


Figure 23. RMS position errors for the two-state system while flying a 15 NM circular pattern around the sonobuoy. $\Delta R = (a/c \ 180-1 + \text{Schuler}, b \ 270-1)$, $\Delta t = 20s$, $\text{Alt} = 3000'$.

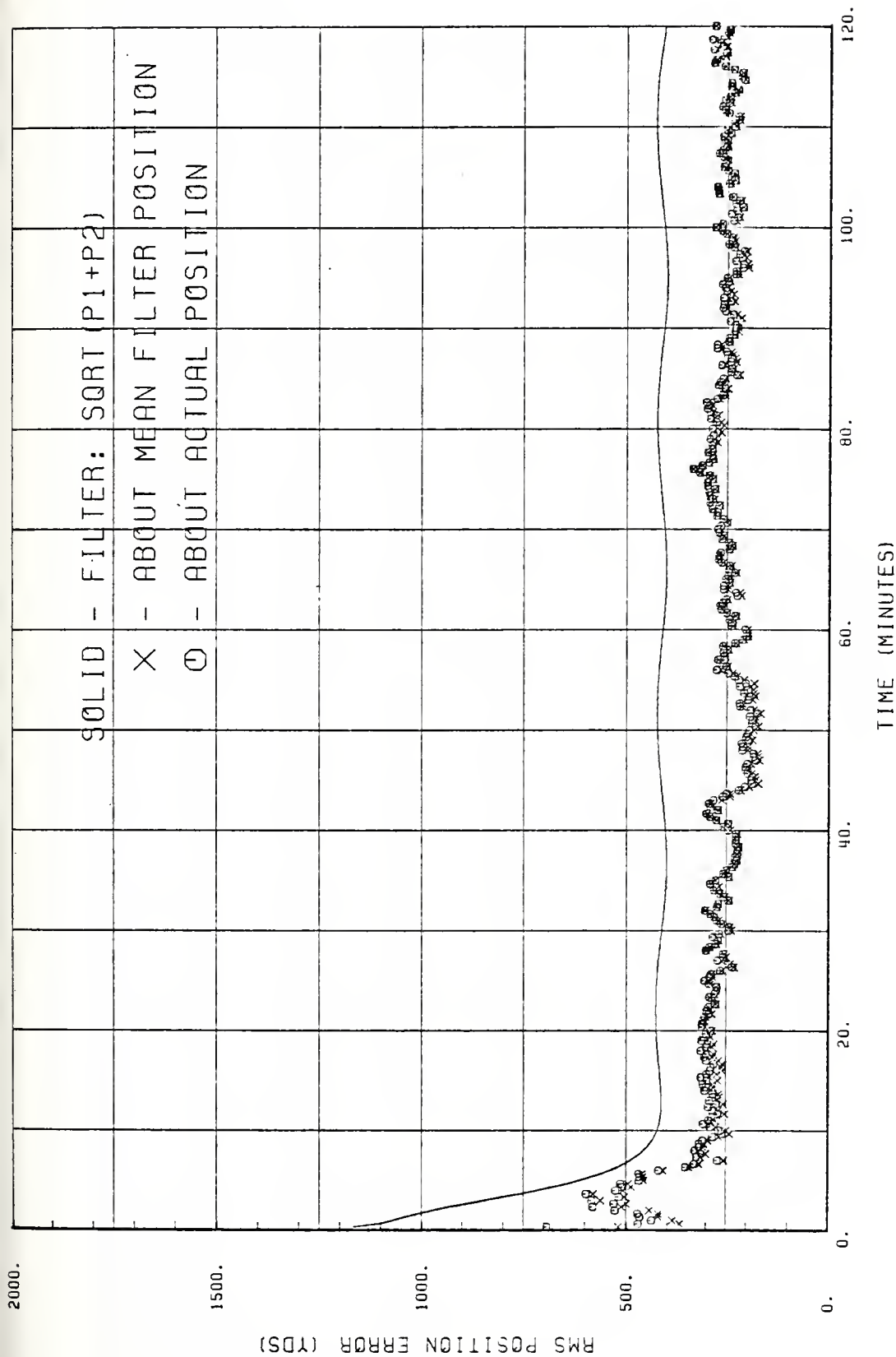


Figure 24. RMS position errors for the two-state system while flying a 15 NM circular pattern around the sonobuoy. DR=(a/c 180-1 + No Sch., b 270-1), t=20s, Alt=3000'.

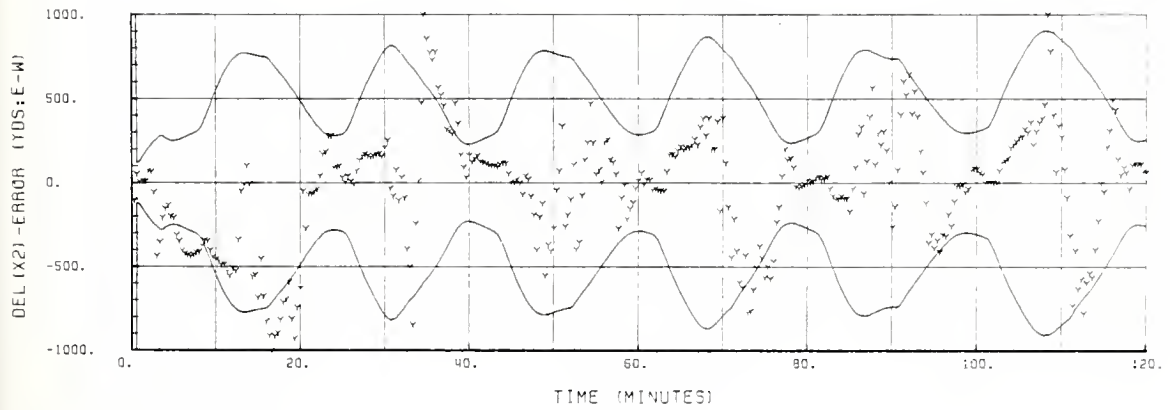
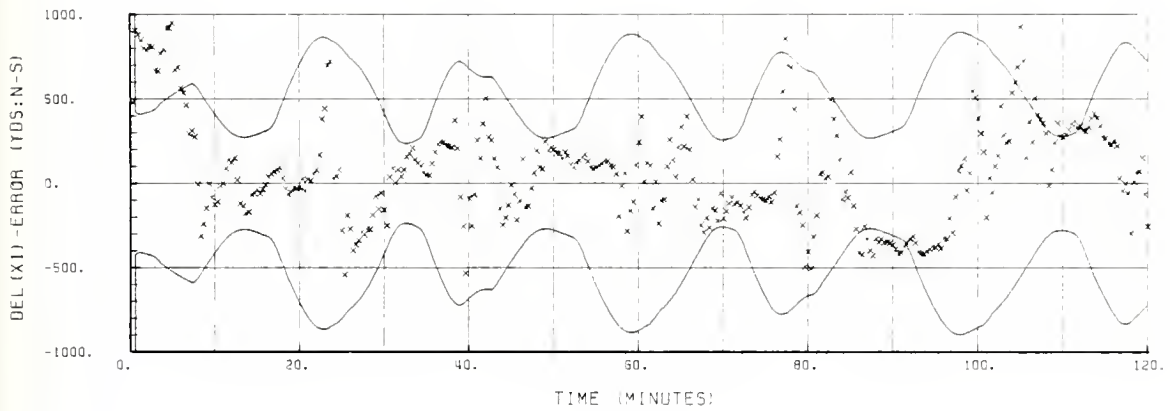
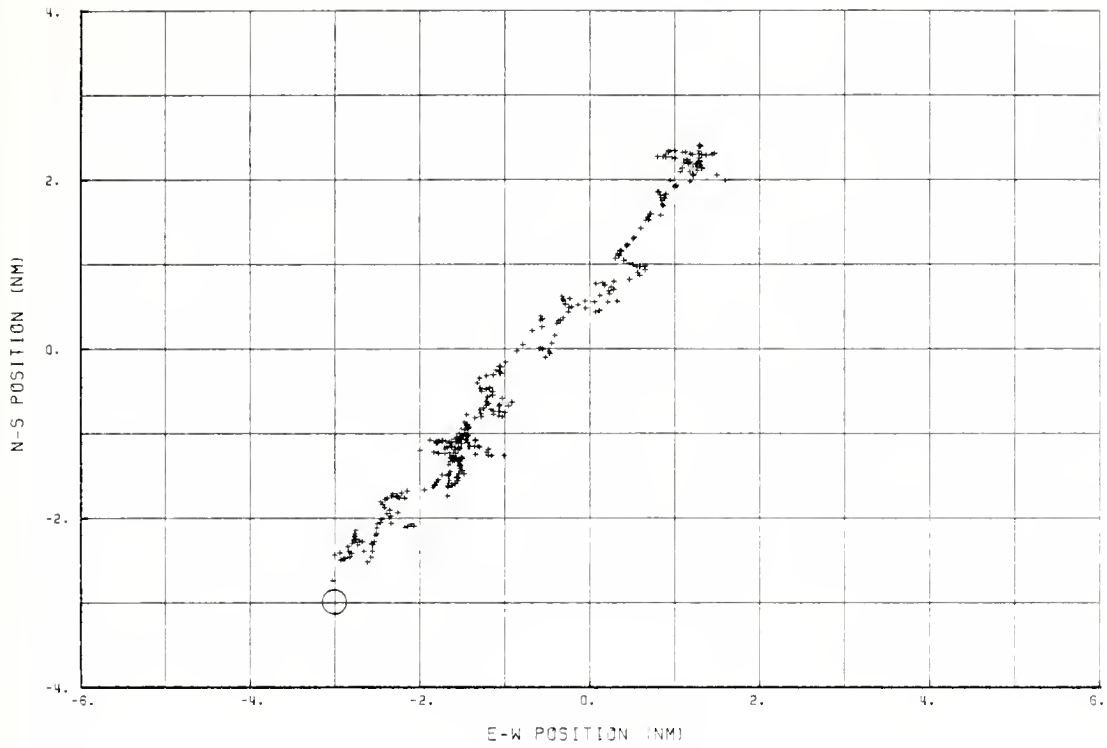


Figure 25. Est. position and relative errors for the six-state system using square pattern at 15NM. DR=(a/c 000-2.5 + Schuler, b 090-2), $\Delta t=20s$, Alt=3000'

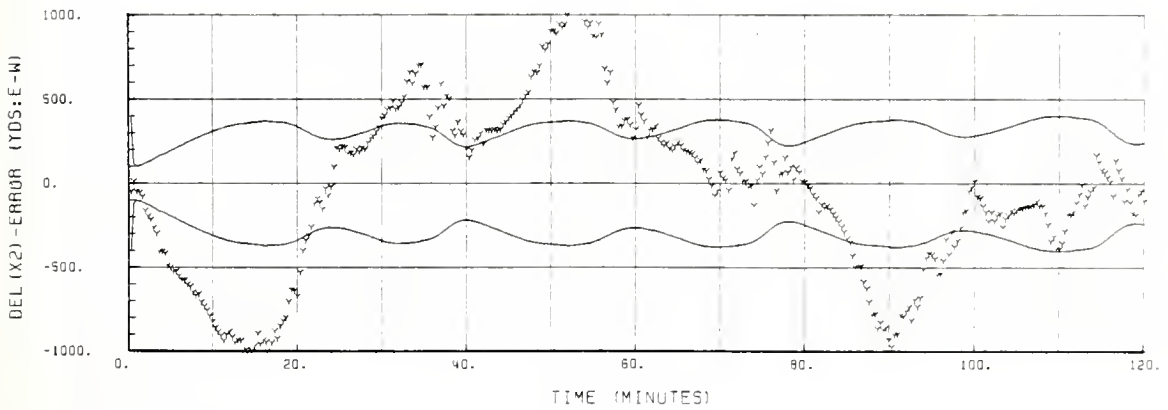
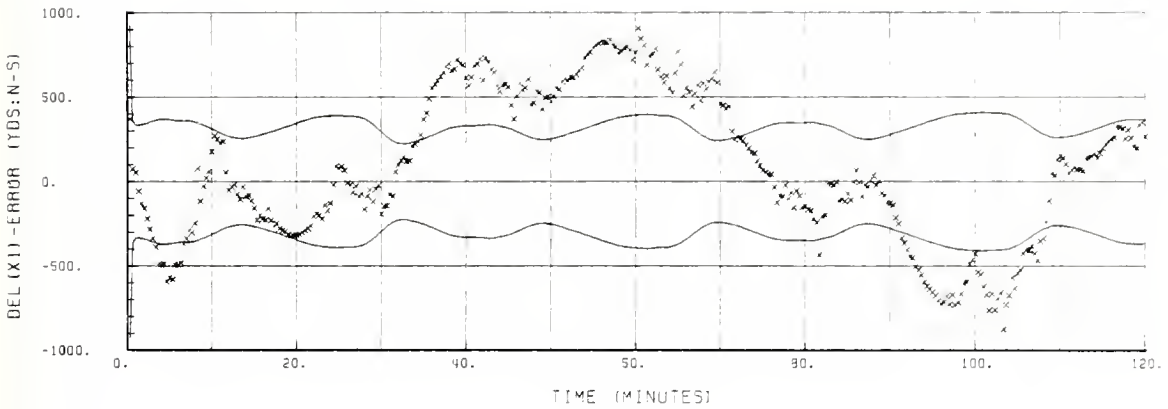
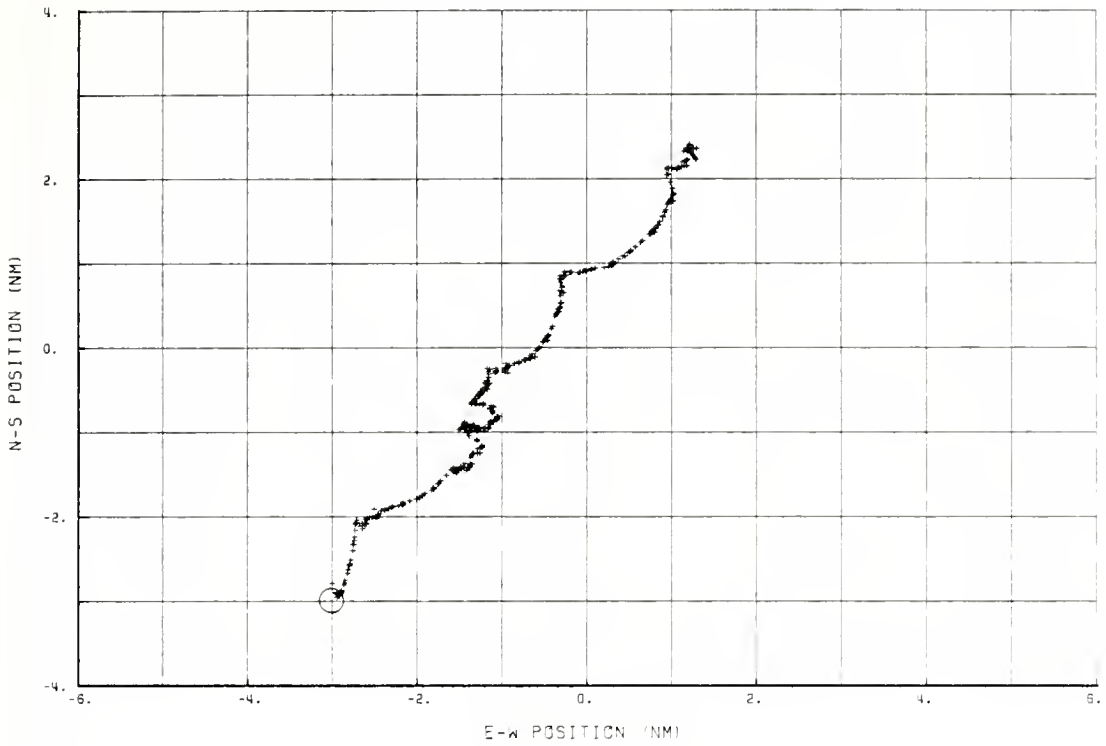


Figure 26. Est. position and relative errors for the two-state system using square pattern at 15NM. DR=(a/c 000-2.5 + Schuler, b 090-2), $\Delta t=20s$, Alt=3000'

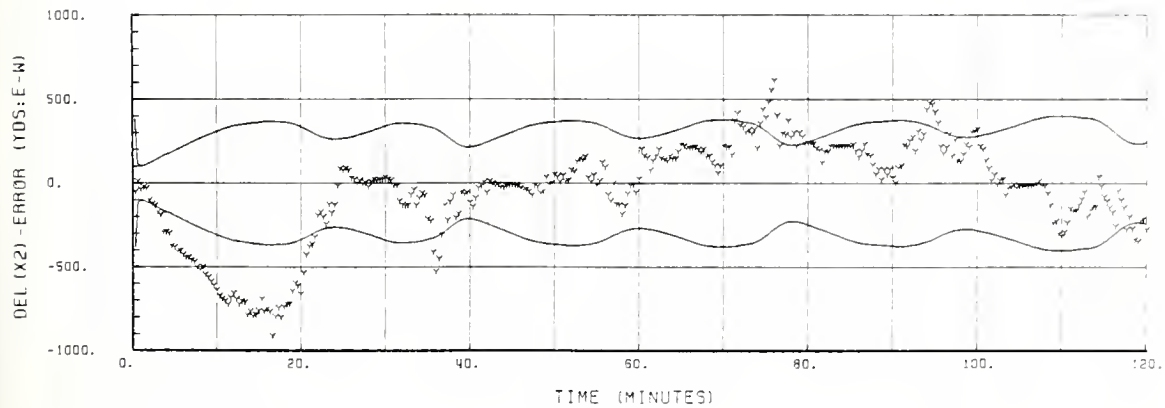
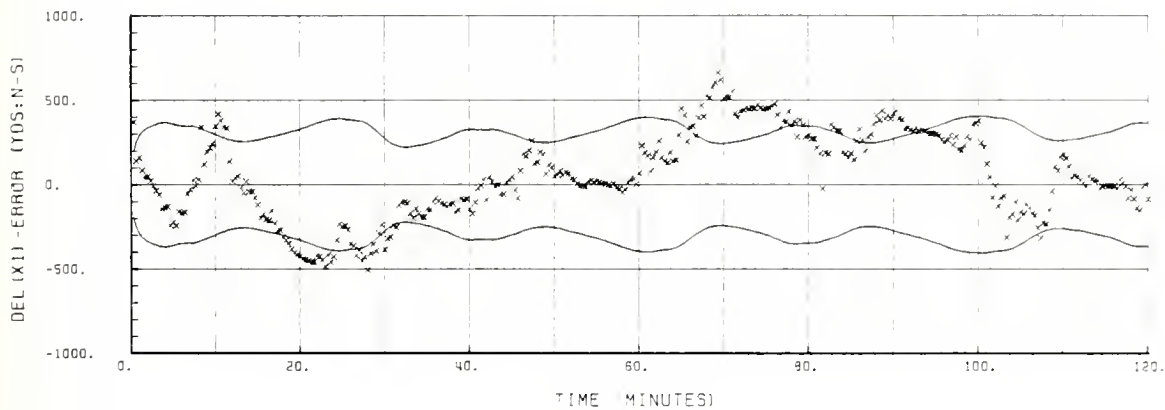
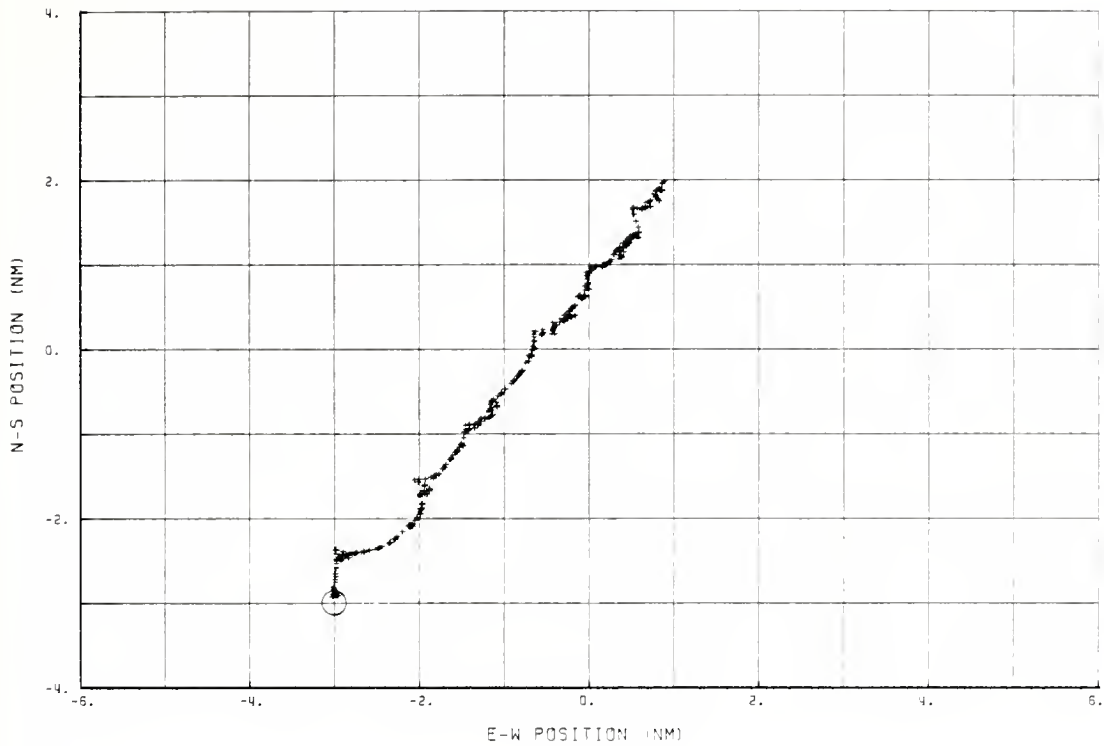


Figure 27. Est. position and relative errors for the two-state system using square pattern at 15NM. DR=(a/c 000-2.5 + No Sch., b 090-2), $\Delta t=20s$, Alt=3000'

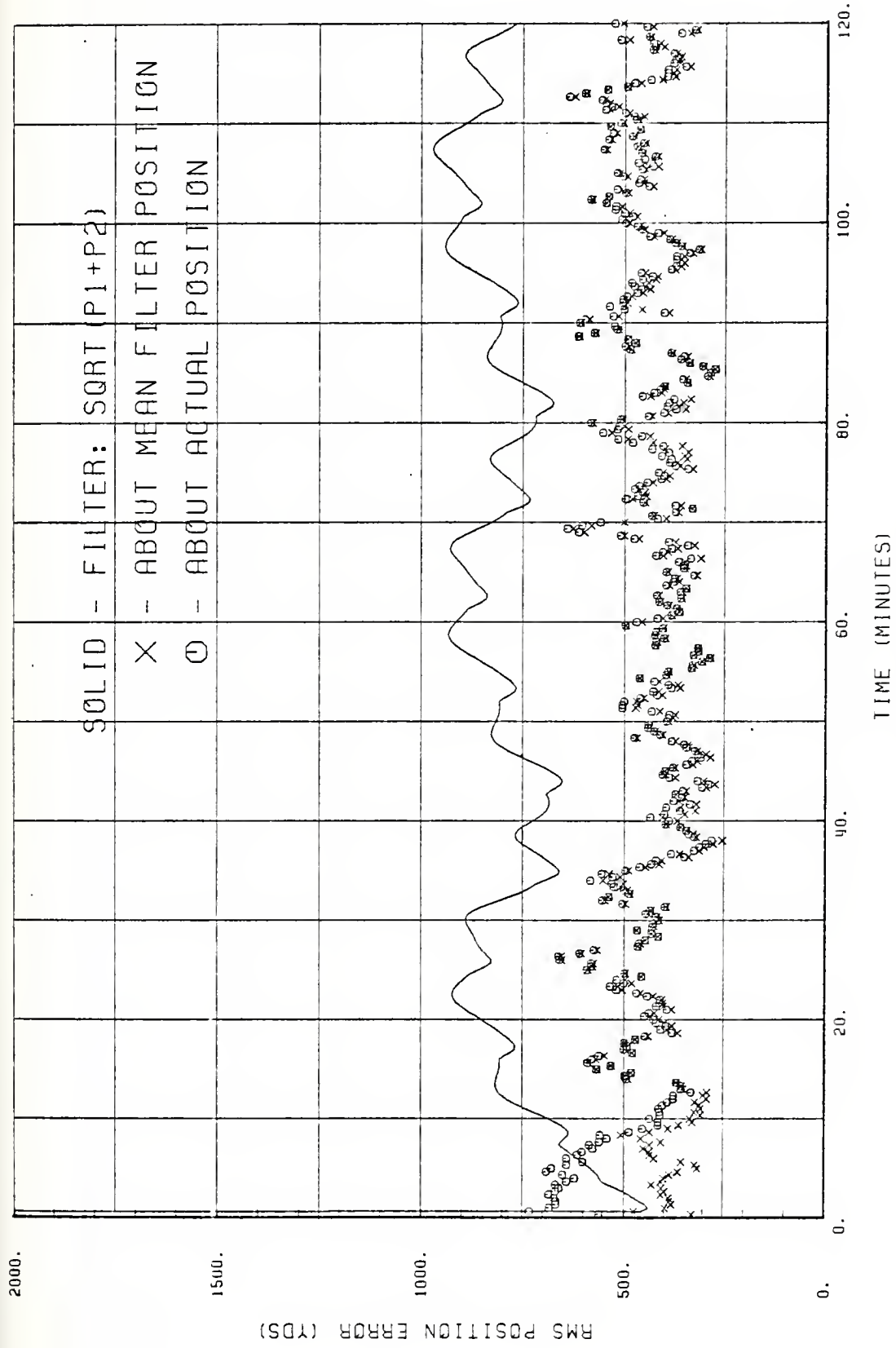


Figure 28. RMS position errors for the six-state system while flying a 15 NM square pattern around the sonobuoy. DR=(a/c 000-2.5 + Schuler, b 090-2), t=20s, Alt=3000'.

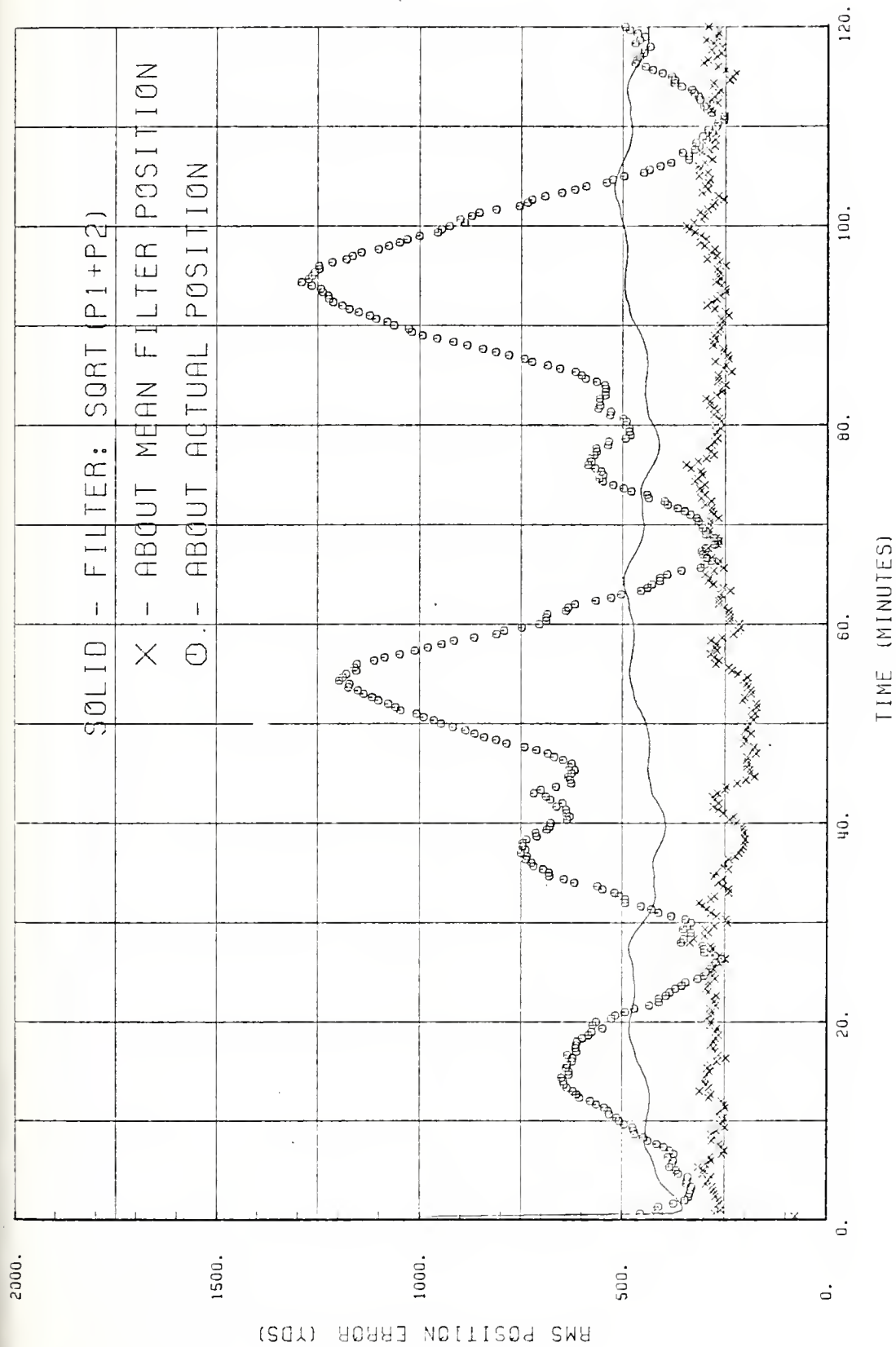


Figure 29. RMS position errors for the two-state system while flying a 15 NM square pattern around the sonobuoy. DR=(a/c 00-2.5 + Schuler, b 090-2), $\Delta t=20s$, Alt=3000'.

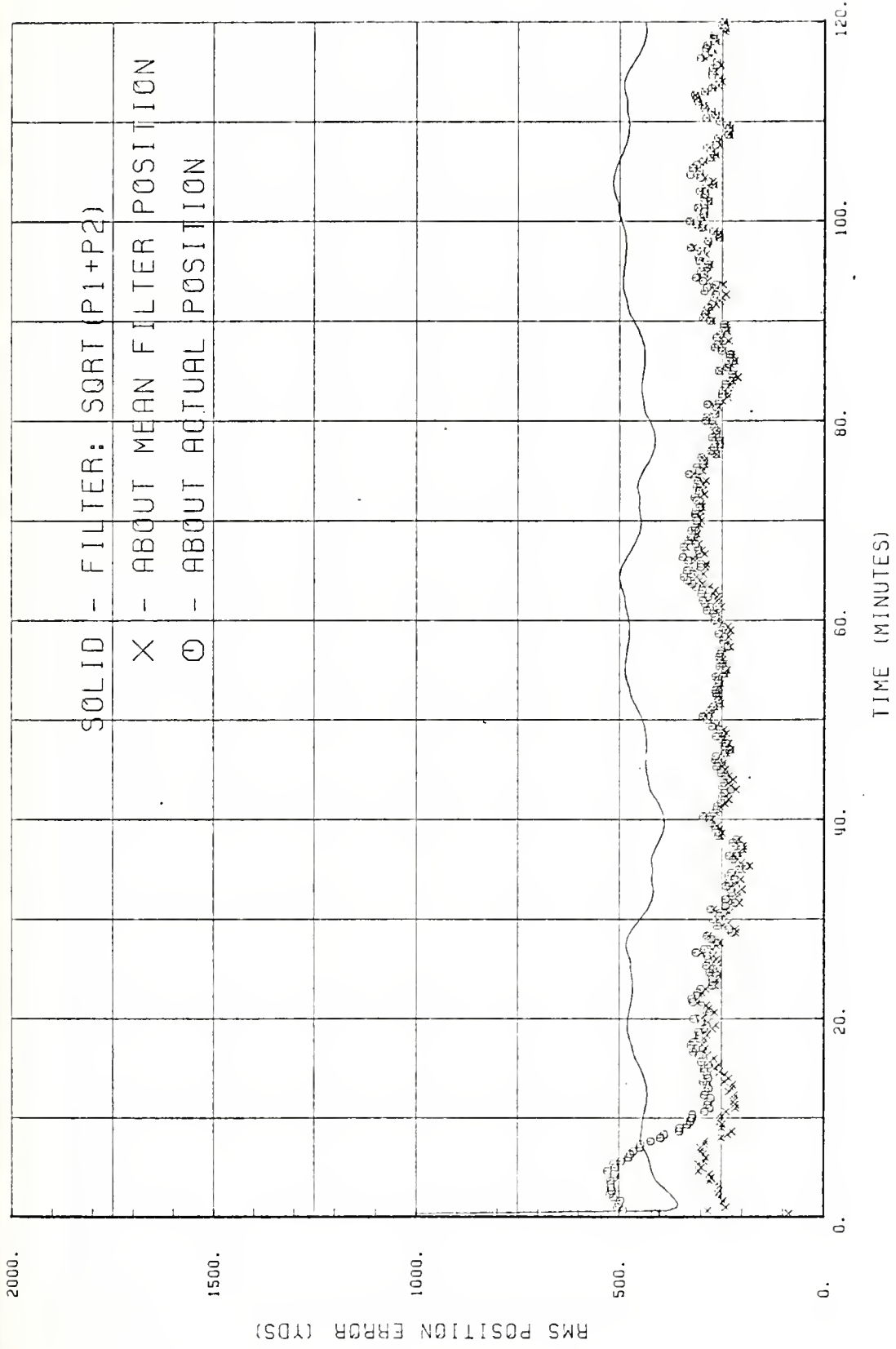


Figure 30. RMS position errors for the two-state system while flying a 15 NM square pattern around the sonobuoy. DR(a/c 000-2.5 + No Sch., b 090-2), $\Delta t=20s$, Alt=3000'.

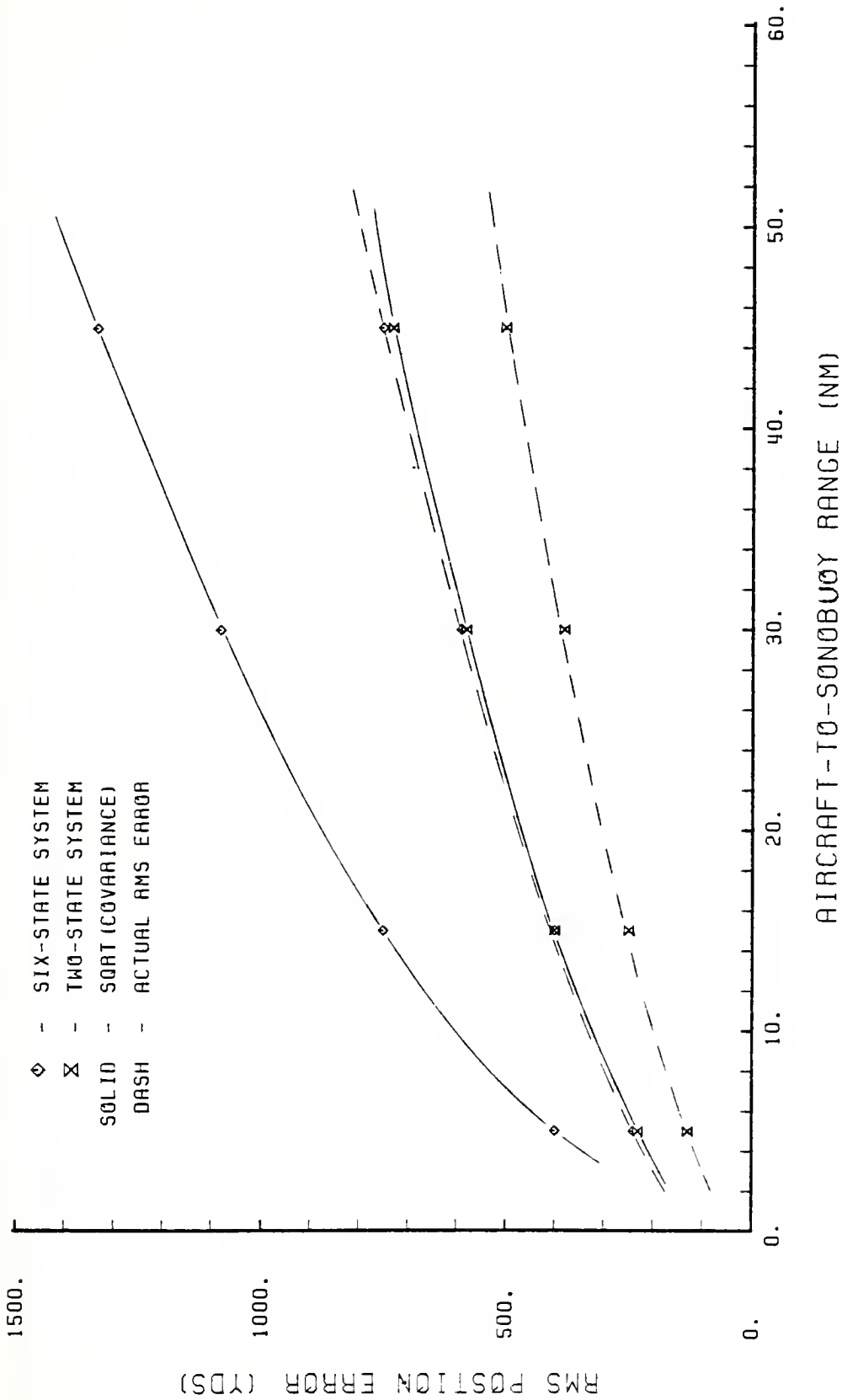
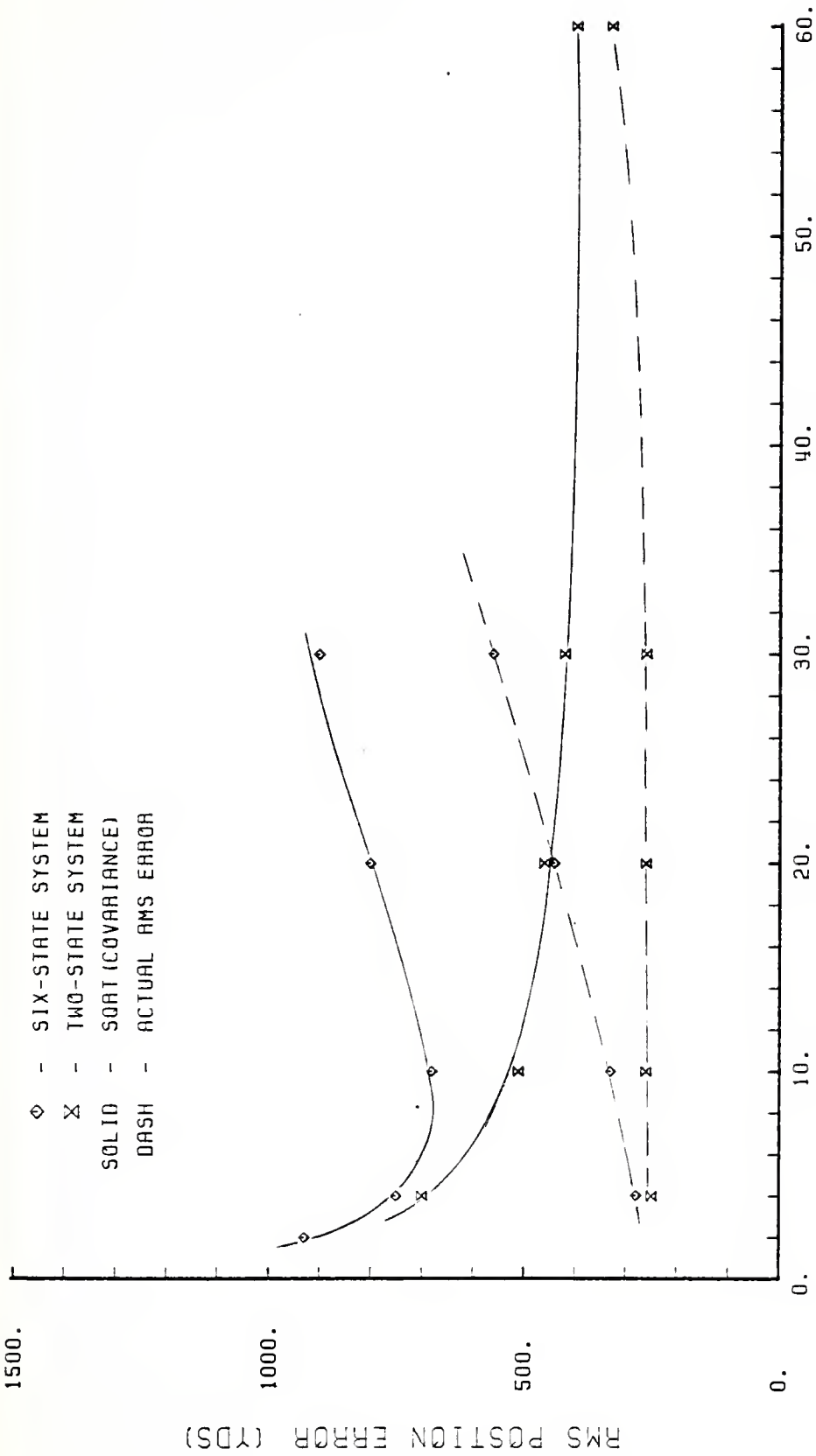


Figure 31. RMS position error as a function of aircraft-to-sonobuoy range, Δx , for the six-state and two-state systems.



MEASUREMENT INTERVAL - ONE SONOBUOY (SEC)

Figure 32. RMS position error as a function of measurement interval, Δt , for the six-state and two-state systems.

V. CONCLUSION

The following are the conclusions reached at the end of this research:

1. The six-state algorithm developed in this report produced estimates of relative sonobuoy position with a standard deviation in the error of 500 yards at a range of 20 NM. Aircraft drift, which included the Schuler cycle, had no effect on this system since the states were defined relative to the aircraft.
2. The two-state algorithm developed in this report produced estimates of relative sonobuoy position with a standard deviation of 300 yards plus an amount equal to the amplitude of the Schuler cycle error at a range of 20 NM. When no Schuler cycle navigational errors were present, the two-state system out-performed the six-state system.
3. Both algorithms showed an increase in steady state RMS error with an increase in range.
4. The six-state system showed an increase in actual steady state RMS error for an increase in the time interval between measurements; however, the covariance of this system indicated minimum error occurred with a 10 second interval on one sonobuoy at a range of 15 NM and an aircraft speed of 180 kts. (This translates to a $1\frac{1}{2}$ degree change in relative bearing.) The two-state

system showed no change in the actual steady state RMS error for intervals between 4 and 30 seconds and only a slight increase in these errors as a 60 second interval was approached. The covariance of the system actually decreased with increasing interval.

5. Neither system showed any dependence on altitudes within the operational limits at a range of 15 NM.
6. No adverse effect was observed while flying straight tracks as opposed to curved ones.
7. Steady state RMS error was affected by two conditions as measurement intervals changed. The longer the interval the more the error tended to increase, especially for the six-state algorithm, as a result of system propagation. The shorter the interval the more the error tended to increase as the systems encroached upon their non-observability condition. An optimum measurement interval existed for each system which was a function of range.

VI. SUMMARY

Both the six-state and the two-state algorithms were able to successfully track the sonobuoy. However, the six-state system was the best choice given the navigational system in use by the Orion. It was capable of providing estimated sonobuoy positions at a range of 20 NM such that the errors had a standard deviation of 500 yards. The computer time required to process one measurement was on the order of 200 milliseconds. On the other hand, the much simpler two-state system required only 28 milliseconds or one seventh ($\frac{1}{7}$) the amount of computer time. However, its estimate of sonobuoy position was degraded by Schuler cycle errors in the navigational system. Without these, this system was subject to errors having a standard deviation of 300 yards at a range of 20 NM. The Schuler cycle periodically increased these errors by an amount equal to its amplitude.

The algorithms were very much affected by the aircraft's flight path including the relative location of the sonobuoy, the range to the sonobuoy, and the amount of angular change in the bearing to the sonobuoy as measurements were taken. Since the sonobuoy position was to be estimated in two-dimensions, the aircraft was required to maneuver in such a way so as to provide information in both dimensions. For example, as the aircraft crossed north or south of the

sonobuoy the E-W errors decreased while the N-S errors increased. The trend reversed when the aircraft flew east or west of the sonobuoy. It was also observed that steady state RMS errors grew with range at a slightly decreasing rate. They were twice as large at 45 NM as they were at 15 NM. Finally, the sonobuoy position was not observable if the relative bearing to the sonobuoy did not change implying that two lines of bearing must cross in order to obtain an estimated position. If the amount of angular change between each measurement was too small it began to affect the errors because this condition was being approached. Anytime the aircraft flew in such a way as to reduce the rate of bearing change, or the frequency at which measurements were made was too high, this condition was prevalent. It was observed that at least $1\frac{1}{2}$ degrees of change was required to avoid this problem.

The six-state system showed no tendency toward divergence as long as initial conditions were reasonable. The two-state system, on the other hand, did have a tendency to diverge when the gains on the drift filter were not adjusted correctly. For example, if the gain was too high the estimated drift was heavily dependent on the last few measurements and was too quickly affected by changes in the position filter. But, it was also necessary for the drift filter to have non-zero gains in the steady state in order to provide some insurance against an initially wrong estimate of sonobuoy drift. With these modifications made

the algorithm operated correctly during all tests and, in fact, had less error in some cases than did the six-state system.

It is the opinion of the author that either one of these algorithms is an improvement on the historical method of "marking-on-top" the sonobuoy. Further, it adds a great deal more uncertainty as to exactly how much accuracy could be obtained in the old way. Non-linear navigational effects were not even considered and the number of measurements made to determine sonobuoy position was on the order of 10 or less for any one sonobuoy pattern. Nevertheless, in an operational sense the accuracies achieved here would need to be improved. Without the non-linear navigational errors the accuracies could have been much better. However, the results of this research do provide another perspective for the problem at hand.

APPENDIX A
THE COMPUTER PROGRAMS

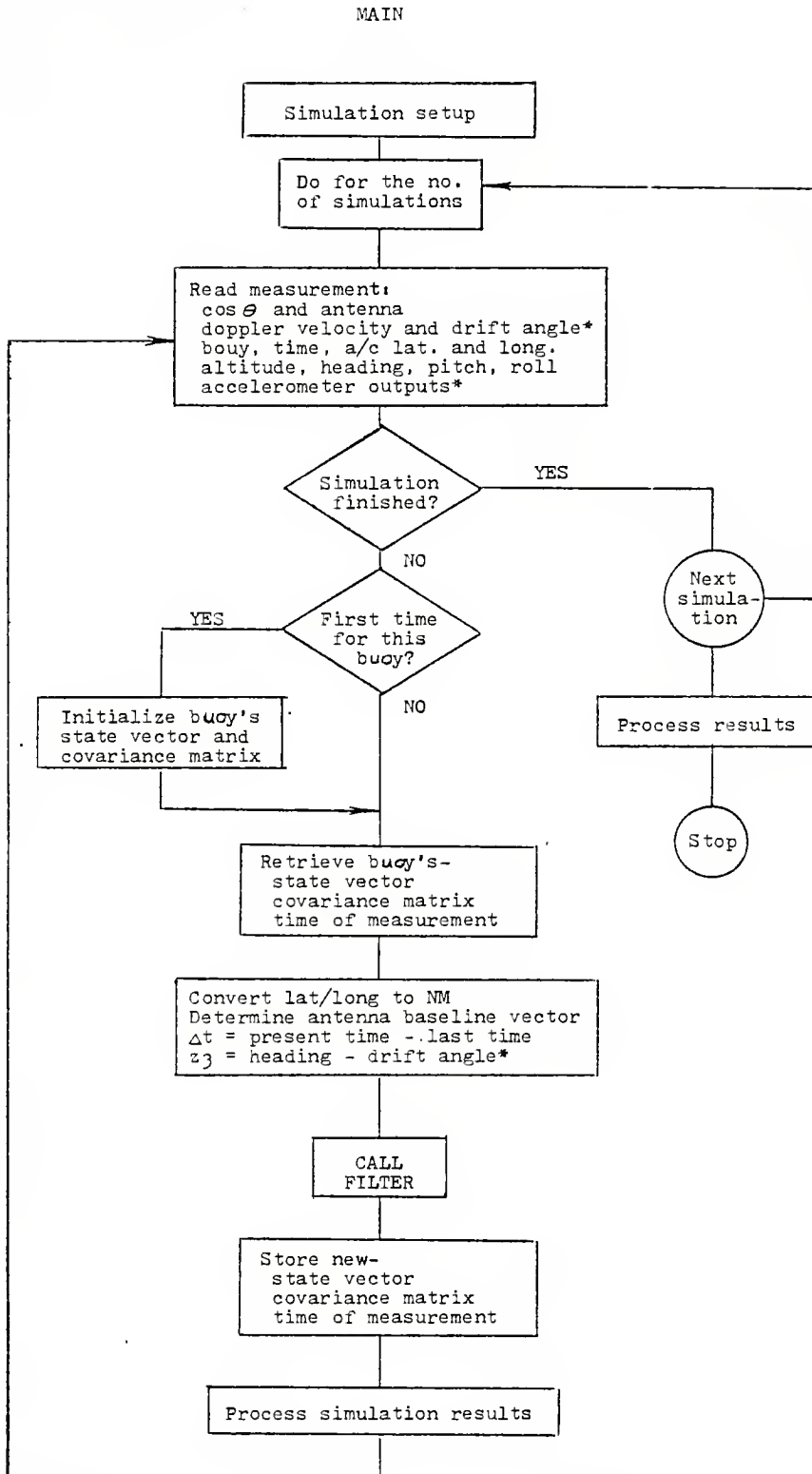


Figure 34. Flow chart:
main program

* Required for six-state system only.

SUBROUTINE FILTER
SIX-STATE

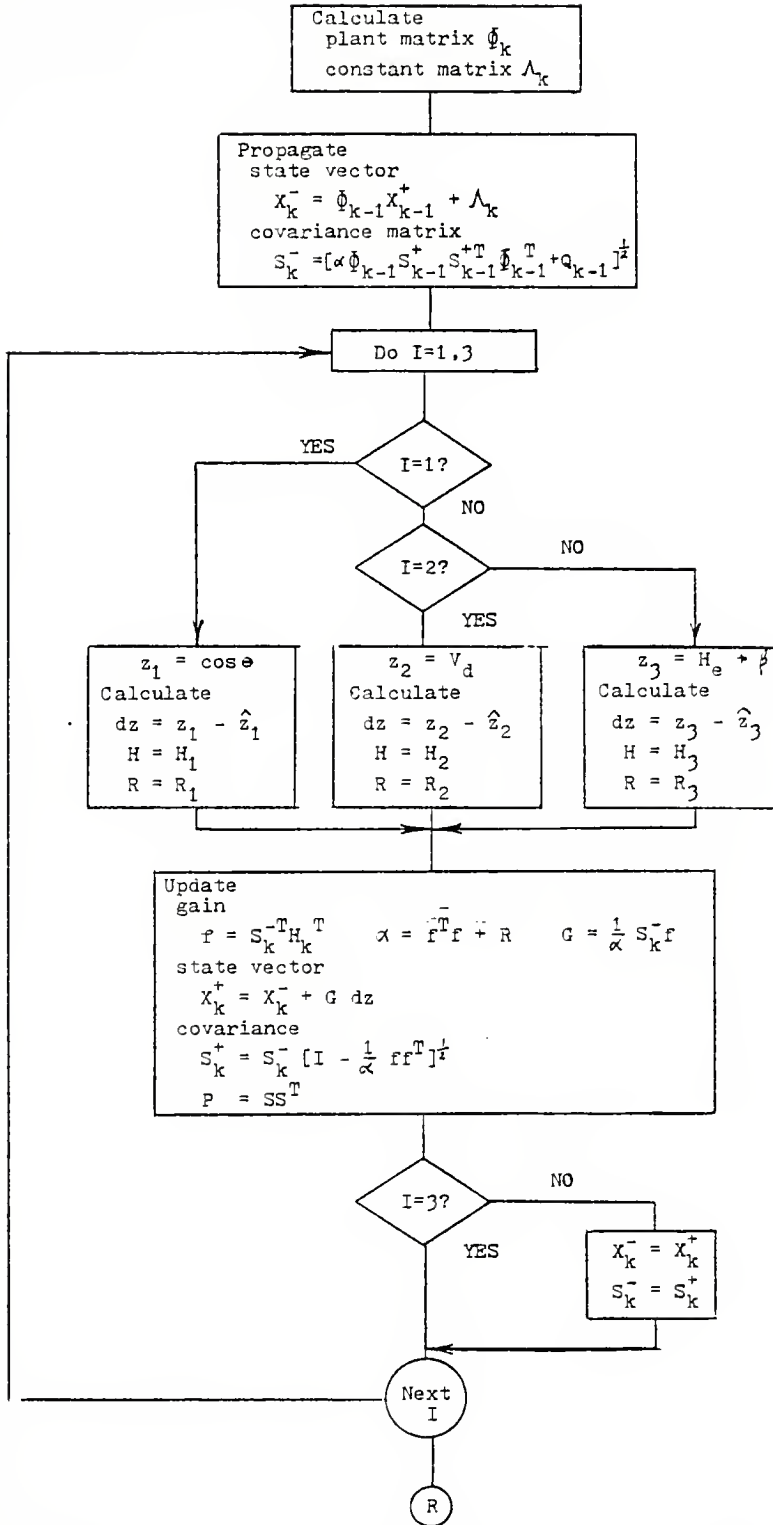


Figure 35. Flow chart: Subroutine FILTER six-state

SUBROUTINE FILTER
TWO-STATE

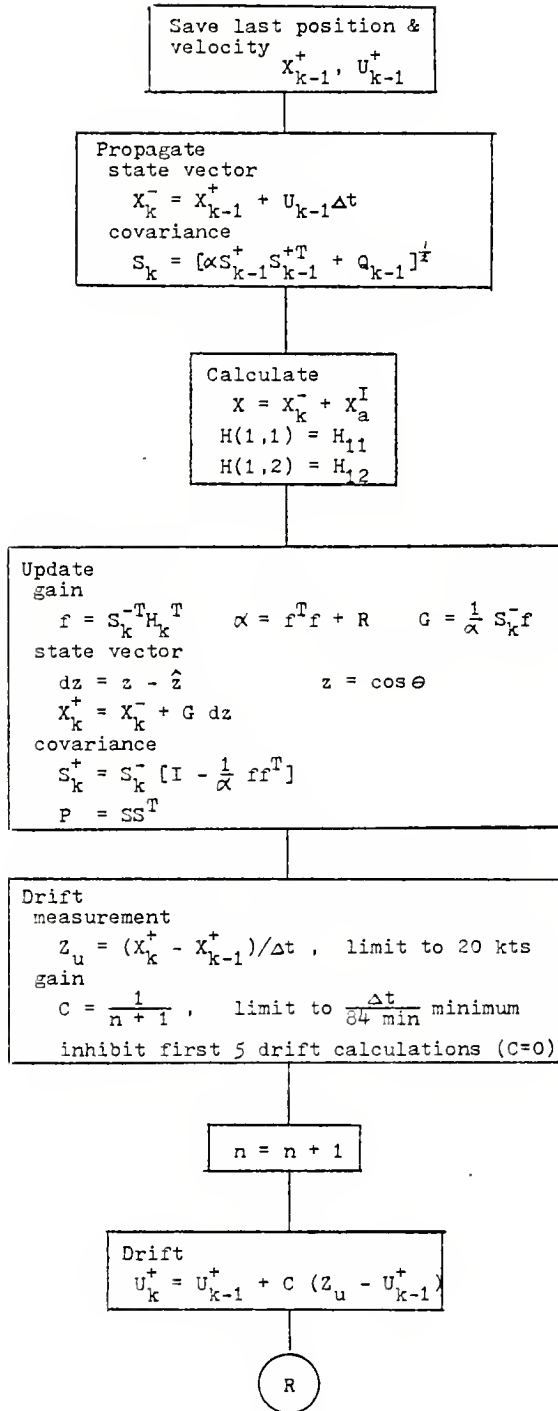


Figure 36. Flow chart: Subroutine FILTER two-state

GLOSSARY OF COMPUTER VARIABLES
SIMULATION PROGRAM

A	Vector of aircraft accelerations
ALPHA I	Result of $\frac{1}{f^T f + R}$ or $\frac{1}{\alpha}$
ALT	Altitude
ANGLE	Direction of sonobuoy drift from North
ANT	Antenna
AVEL	Initial aircraft velocity
AS	Matrix result of $I - \frac{ff^T}{\alpha}$
B	Matrix result of $\{eSS^T + Q\}^{1/2}$
BOUY	Sonobuoy RF channel or number
C	Gain of drift filter
CA	Result of $\Delta t / (84 \text{ min.})$
CK	Constant matrix in six-state system's equations
CKL	Rate of change of nautical miles for a change in degrees of longitude
D	Array which holds all items requiring storage from one measurement to the next
DELTA	Interval between measurements, Δt
DELX1	Relative position, Δx_1
DELX2	Relative position, Δx_2
DELX3	Relative position, Δx_3
DRIFT	Magnitude of sonobuoy drift in yards
DSEED	Seed for the random number generator
DTIME	Array of initial drop times for the sonobuoy
DZ	Residual, dz
EDELX1	Error in the est. relative position of sonobuoy, Δx_1

EDELX2 Error in the est. relative position of sonobuoy, Δx_2
 EOSSO Matrix result of $\epsilon \mathbb{Q}^T S^T S \mathbb{Q}$
 EPSLN Age weighting factor,
 ESST Matrix result of $\epsilon S S^T$
 EX1 Error in est. geographical position of sonobuoy, Δx_1
 EX2 Error in est. geographical position of sonobúcy, Δx_2
 F f vector from Carlson square root technique
 FFT Matrix result of ff^T
 FFTA Matrix result of $\frac{ff^T}{\alpha}$
 FT Transpose of f
 G Gain matrix
 GAMMA Aircraft pitch angle, γ
 GDZ Vector result of $G dz$
 GR Gamma in radians
 H Aircraft heading
 H The H matrix when used in subroutine FILTER
 HOUR Time in hours
 HR Heading in radians
 HT Transpose of the H matrix
 I Index
 I Identity matrix when used in subroutine FILTER
 IEND Indicator of EOF
 IFFTA Matrix result of $I - \frac{ff^T}{\alpha}$
 IN File from which data is read
 INRES File from which true sonobuoy positions are read
 IOUT Device on which print is made
 IOUPT File in which results are written

IOUTZ File in which random vectors are inspected
 IRUN Index for run number
 IZ Index for measurement, $z = 1,2,3$
 K Incremental measure of time
 LAT Latitude
 LATI The latitude of the origin of the local earth fixed coordinate system
 LONG Longitude
 LONGI The longitude of the origin of the local earth fixed coordinate system
 MARK Indicates whether information is to be stored or retrieved
 MEAN1 Mean estimated sonobuoy position, μ_1
 MEAN2 Mean estimated sonobuoy position, μ_2
 MIN Time in minutes
 N Total number of measurements made on all sonobuoys
 N Index when used in subroutines INITIAL and DATA
 NRUNS Integer equivalent of RUNS
 O Plant matrix, Φ
 OS Matrix result of ΦS
 OST Transpose of ΦS^T
 OSSO Matrix result of $\Phi^T S^T S \Phi$
 OX Matrix result of ΦX
 P Covariance matrix
 PHI Aircraft roll angle, ϕ
 PI π
 PR Phi in radians
 Q Variance of plant noise from $N(0, Q)$
 R Variance of measurement noise from $N(0, R)$

RAD $\pi / 180$
 RANGE Range to sonobuoy from aircraft
 RANGE2 Squared value of range
 RB1 Unit vector component of antenna baseline
 RB2 Unit vector component of antenna baseline
 RB3 Unit vector component of antenna baseline
 RBX Result of $(RB_1 \Delta x_1 + RB_2 \Delta x_2 + RB_3 \Delta x_3)$
 RNO Normally distributed random number from $N(0,1)$
 RUNS Number of simulation runs to be made
 S Array in Carlson's square root technique which represents square root of covariance matrix
 S1 Square root of variance, $\sqrt{P_{11}}$
 S2 Square root of variance, $\sqrt{P_{22}}$
 SEC Time in seconds
 SF Matrix result of $S f$
 SIGMA RMS error in the estimate about the actual location
 SIGMAF RMS value from the Kalman filter, $\sqrt{P_{11} + P_{22}}$
 SIGMAX RMS error in the estimate about the mean estimate
 SKL Rate of change of nautical miles for a change in degrees of latitude
 SNEXT Propagated matrix of S
 SST Matrix result of $S S^T$
 ST Transpose of S matrix
 SUMP1 Array for the sum of $P(1,1)$ over NRUNS
 SUMP2 Array for the sum of $P(2,2)$ over NRUNS
 SUMSQ1 Array for sum of $\tilde{\Delta x}_1^2$ over NRUNS
 SUMSQ2 Array for sum of $\tilde{\Delta x}_2^2$ over NRUNS
 SUMX1 Array for sum of $\tilde{\Delta x}_1$ over NRUNS

SUMX2 Array for sum of Δx_2 over N#UNS

T Last time in seconds the sonobuoy was processed by the filter

TIME Time from aircraft clock in seconds

U Sonobuoy drift vector

U1 Old value of U(1)

U2 Old value of U(2)

VAR1 Variance of the estimated sonobuoy position about the actual location σ_f^2

VAR2 Variance of the estimated sonobuoy position about the actual location σ_f^2

VARX1 Variance of the estimated sonobuoy position about the mean estimated position, σ_{x1}^2

VARX2 Variance of the estimated sonobuoy position about the mean estimated position, σ_{x2}^2

VELCT Relative velocity, ΔV

VELCT2 Squared value of relative veclocity

X State vector

XAI Aircraft inertial position, X_a^I

XAT Aircraft true position, X_a

X1 Old value of X(1)

X2 Old value of X(2)

XB Vector including XB1, XB2, velocity of sonobuoy, and two zeros used in the six-state system

XB1 True geographical location of sonobuoy, x_1

XB2 True geographical location of sonobuoy, x_2

XB1I Array of initial sonobuoy positions

XB2I Array of initial sonobuoy positions

XNEXT Propagated value of X

Z Measurement vector

ZHAT Estimate of z
ZN Normally distributed random number from $N(z,R)$
ZU Vector of velocity measurement for drift filter

CAT00040
 CAT00050
 CAT00060
 CAT00070
 CAT00080
 CAT00090
 CAT00100
 CAT00110
 CAT00120
 CAT00130
 CAT00140
 CAT00150
 CAT00160
 CAT00170
 CAT00180
 CAT00190
 CAT00200
 CAT00210
 CAT00220
 CAT00230
 CAT00240
 CAT00250
 CAT00260
 CAT00270
 CAT00280
 CAT00290
 CAT00300
 CAT00310
 CAT00320
 CAT00330
 CAT00340
 CAT00350
 CAT00360
 CAT00370
 CAT00380
 CAT00390
 CAT00400
 CAT00410
 CAT00420
 CAT00430
 CAT00440
 CAT00450
 CAT00460
 CAT00470
 CAT00480
 CAT00490
 CAT00500
 CAT00510
 CAT00520
 CAT00530
 CAT00540
 CAT00550
 CAT00560
 CAT00570
 CAT00580
 CAT00590
 CAT00600

1 MAIN PROGRAM
 2
 3
 4
 5
 6
 7
 8
 9
 10
 11
 12
 13
 14
 15
 16
 17
 18
 19
 20
 21
 22
 23
 24
 25
 26
 27
 28
 29
 30
 31
 32
 33
 34
 35
 36
 37
 38
 39
 40
 41
 42
 43
 44
 45
 46
 47
 48
 49
 50
 51
 52
 53
 54
 55
 56
 57
 58
 59
 60
 61
 62
 63
 64
 65
 66
 67
 68
 69
 70
 71
 72
 73
 74
 75
 76
 77
 78
 79
 80
 81
 82
 83
 84
 85
 86
 87
 88
 89
 90
 91
 92
 93
 94
 95
 96
 97
 98
 99
 100

```

CALL P(B)
DIMENSION S(0,0), P(0,0), X(0), XEL(Z), X0(0), Z(3), MARK(0), A(?)
REAL IAT, LCAC
IAT=6, IY=100, HRP, MIN, SEC, TIME, T, AUT
DOUBLE PRECISION DEFED
DATA MARK, P/0, 3.1415926/

```

```

      DIMENSION S(0,0)
      DIMENSION S(0,0), P(0,0), X(0), XEL(Z), X0(0), Z(3), MARK(0), A(?)
      REAL IAT, LCAC
      IAT=6, IY=100, HRP, MIN, SEC, TIME, T, AUT
      DOUBLE PRECISION DEFED
      DATA MARK, P/0, 3.1415926/

```

```

      DIMENSION S(0,0)
      DIMENSION S(0,0), P(0,0), X(0), XEL(Z), X0(0), Z(3), MARK(0), A(?)
      REAL IAT, LCAC
      IAT=6, IY=100, HRP, MIN, SEC, TIME, T, AUT
      DOUBLE PRECISION DEFED
      DATA MARK, P/0, 3.1415926/

```

```

      DIMENSION S(0,0)
      DIMENSION S(0,0), P(0,0), X(0), XEL(Z), X0(0), Z(3), MARK(0), A(?)
      REAL IAT, LCAC
      IAT=6, IY=100, HRP, MIN, SEC, TIME, T, AUT
      DOUBLE PRECISION DEFED
      DATA MARK, P/0, 3.1415926/

```

```

      DIMENSION S(0,0)
      DIMENSION S(0,0), P(0,0), X(0), XEL(Z), X0(0), Z(3), MARK(0), A(?)
      REAL IAT, LCAC
      IAT=6, IY=100, HRP, MIN, SEC, TIME, T, AUT
      DOUBLE PRECISION DEFED
      DATA MARK, P/0, 3.1415926/

```

```

      DIMENSION S(0,0)
      DIMENSION S(0,0), P(0,0), X(0), XEL(Z), X0(0), Z(3), MARK(0), A(?)
      REAL IAT, LCAC
      IAT=6, IY=100, HRP, MIN, SEC, TIME, T, AUT
      DOUBLE PRECISION DEFED
      DATA MARK, P/0, 3.1415926/

```

```

      DIMENSION S(0,0)
      DIMENSION S(0,0), P(0,0), X(0), XEL(Z), X0(0), Z(3), MARK(0), A(?)
      REAL IAT, LCAC
      IAT=6, IY=100, HRP, MIN, SEC, TIME, T, AUT
      DOUBLE PRECISION DEFED
      DATA MARK, P/0, 3.1415926/

```

```

      DIMENSION S(0,0)
      DIMENSION S(0,0), P(0,0), X(0), XEL(Z), X0(0), Z(3), MARK(0), A(?)
      REAL IAT, LCAC
      IAT=6, IY=100, HRP, MIN, SEC, TIME, T, AUT
      DOUBLE PRECISION DEFED
      DATA MARK, P/0, 3.1415926/

```

```

      DIMENSION S(0,0)
      DIMENSION S(0,0), P(0,0), X(0), XEL(Z), X0(0), Z(3), MARK(0), A(?)
      REAL IAT, LCAC
      IAT=6, IY=100, HRP, MIN, SEC, TIME, T, AUT
      DOUBLE PRECISION DEFED
      DATA MARK, P/0, 3.1415926/

```



```

50 CALL GETA(BODY, S, X, XP, T, K, AVEK(BODY))
C     FLUPAIR FOR FLITER
CALL LATION(LAT, LONG, XAL)
CALL ACISE(OCES, Z(1), .026)
CALL FEISE(OFIF, Z(2), .2)
CALL ACISE(OCES, Z(3), .008)
CALL O=SE(ART, H, CMMVA, PHI, K=1, F=2, K=3)
TIME=SECC(PHUR+O)M*IN+SFC
CALL=FI(CAT(TIME-T)/3600.
Z(3)=H+(.3)
C     GET FLITER AND STOPS NEW DATA
C     GET (DELTA, 900?) BODY, K, F=0, M, M, SFC
CALL FLITER(S, T, X, XP, Z, DELT, XFI, LAT, ALT, K=1, R=2, R=3, V, BODY, K)
CALL DATA(PHXY, S, X, XP, TIME, K, MARK(BODY))
CALL RESCUT(BODY, K, X, XP, P, IN, OUF)
WRITE(UNIT, 9004) TIME
C     CONTINUE SUBROUTINE
C
60 RT=IND IN
70 RE=IND IMPES
9701 CALL RESCUT(S, X, XP, P, IN, PUMS)
WRITE(UNIT, 9004) TIME
C
9992 F=STAT(///)
9991 F=VAL(I, 3, 12, 17, 3, F6.1, F5.5, F6.0, F6.1, F4.1, F5.1,
Z(7.2, 12)
WRITE(UNIT)
9991 F=VAL(I, 3, 12, 17, 3, F6.1, F5.1, F4.5, F6.0, F6.4, F4.3, F5.1,
Z(7.2, 12)
9992 F=VAL(I, 3, 12, 17, 3, K=1, 14, 13, 2(1, 1, 1))
9993 F=STAT( K=1, 12)
9994 F=STAT(18)
9995 F=VAL(I, 3, 12, 17, 3, O=STAT: RUM 3/00, TT, TT, 5000F1, F0=25, /
, C=STAT: 15 F=CF=CT, DR (V/C 18)-1 ADO SCHULER, R 2(0-1))
9996 F=VAL(I, 3, 12, 17, 3, F6.2)
9997 F=STAT(I, 3, 12, 17, 3, XP, K=1, 14, 13, 2(1, 1, 1),
, V, E=VAL(I, 3, 12, 17, 3, LX, 16, MA, 1, 3, 1, 5(CMA, 2))
C
9998
9999
1000 F=

```

```

PAT00520
PAT00550
PAT00540
PAT00550
PAT00560
PAT00570
PAT00580
PAT00590
PAT00600
PAT00610
PAT00620
PAT00630
PAT00640
PAT00650
PAT00660
PAT00670
PAT00680
PAT00690
PAT00700
PAT00710
PAT00720
PAT00730
PAT00740
PAT00750
PAT00760
PAT00770
PAT00780
PAT00790
PAT00800
PAT00810
PAT00820
PAT00830
PAT00840
PAT00850
PAT00860
PAT00870
PAT00880
PAT00890
PAT00900
PAT00910
PAT00920
PAT00930
PAT00940
PAT00950
PAT00960
PAT00970
PAT00980

```


() 1. 2. 3. 4. 5. 6. 7. 8. 9. 10. 11. 12. 13. 14. 15. 16. 17. 18. 19. 20. 21. 22. 23. 24. 25. 26. 27. 28. 29. 30. 31. 32. 33. 34. 35. 36. 37. 38. 39. 40. 41. 42. 43. 44. 45. 46. 47. 48. 49. 50. 51. 52. 53. 54. 55. 56. 57. 58. 59. 60. 61. 62. 63. 64. 65. 66. 67. 68. 69. 70. 71. 72. 73. 74. 75. 76. 77. 78. 79. 80. 81. 82. 83. 84. 85. 86. 87. 88. 89. 90. 91. 92. 93. 94. 95. 96. 97. 98. 99. 100.

```

SUMCUTLINE LATE M(LAT,LUNG,XAI)
  SET L=1, LUNC=LAT, LUGI
  DUFFRILN XAI(2)
  DATA P1,A1,A2,A3,A4/3.1415926,2.9035546E-04,5.75320E8E-07,
    1.0067682,0.7581702E-13/
  LUGI=30.
  LUGI=L.
  LUGI=L.
  KP=L./((A1-A2)*(SIN(LAT))*P2)
  RPL= P/(A2-A4*(SIN(LAT))*P2)
  SKL=PP*P1/I30.
  CKL=PP*P1/I30.
  XAI(1)=(LAT-LAT1)*SKL
  XAI(2)=(LUG-LUGI)*CKI
  SET L=L+1
  ENDD
  
```

DAT01010
 DAT01020
 DAT01030
 DAT01040
 DAT01050
 DAT01060
 DAT01070
 DAT01080
 DAT01090
 DAT01100
 DAT01110
 DAT01120
 DAT01130
 DAT01140
 DAT01150
 DAT01160
 DAT01170
 DAT01180
 DAT01190
 DAT01200
 DAT01210
 DAT01220
 DAT01230
 DAT01240
 DAT01250
 DAT01260
 DAT01270
 DAT01280
 DAT01290
 DAT01300
 DAT01310
 DAT01320
 DAT01330
 DAT01340
 DAT01350
 DAT01360
 DAT01370
 DAT01380
 DAT01390
 DAT01400
 DAT01410
 DAT01420
 DAT01430
 DAT01440
 DAT01450
 DAT01460
 DAT01470
 DAT01480

```

SUBROUTINE R/ST(AUT,F,CAMPA,DH1,ER1,ER2,ER3)
  
```

```

  U(L)GUG=ALT
  PAE=3.1415926/I30.
  DE=CAMPA*EKAD
  P=C*PHI*EAD
  H=H0*EAD
  FE(L)AT=C*E.3) 60 TO 1
  GDI=COS(PD)*SIN(H)
  K2=COS(PD)*COS(H)
  BK=STK(PR)
  GO TO 5
  AL=COS(GD)*COS(H)
  K2=COS(GD)*SIN(H)
  K3=5IN(CR)
  L=I+1
  ENDD
  
```


DAT01490
 DAT01500
 DAT01510
 DAT01520
 DAT01530
 DAT01540
 DAT01550
 DAT01560
 DAT01570
 DAT01580
 DAT01590
 DAT01600
 DAT01610
 DAT01620
 DAT01630
 DAT01640
 DAT01650
 DAT01660
 DAT01670
 DAT01680
 DAT01690
 DAT01700
 DAT01710
 DAT01720
 DAT01730
 DAT01740
 DAT01750
 DAT01760
 DAT01770
 DAT01780
 DAT01790
 DAT01800
 DAT01810
 DAT01820
 DAT01830
 DAT01840
 DAT01850
 DAT01860
 DAT01870
 DAT01880
 DAT01890
 DAT01900
 DAT01910
 DAT01920
 DAT01930
 DAT01940
 DAT01950
 DAT01960

```

SUBROUTINE INITIAL(BUCY,ALT,H,AVCL)
  COMMON/DC(5,00)
  STEINSEIGN AR11(6),X821(6),DTI P(6)
  TIME GAE RUCY
  DATA PI/3.1415926/
  K=34*8BUCY-47
  ** INITIAL BUCY DATA **
  DATA X811/-5.,-5.,-10.,-15.,-24.,0./
  DATA X811/-3.5,-5.5,-10.5,-15.5,0.,0./
  DATA DTI P/0.,1.0.,1.280.,1.420.,1.340.,0./
  ** INITIAL VELOCITIES **
  U(6)=ALT/60/6.115
  D(6+1)=ALT/60/6.115
  D(6)=5.
  D(N+1)=5.
  D(6+14)=5.
  D(N+21)=5.
  D(6+28)=0.025
  D(6+32)=0.025
  ** INITIAL PUL. POSITION **
  L(6+36)=0.
  D(6+37)=.5
  ** INITIAL REF. VELOCITY **
  D(6+36)=-AVCL*5(H*PI/180.)
  D(6+39)=-AVCL*PI*(H*PI/180.)
  ** INITIAL BODY POSITIF **
  L(6+43)=X811(300Y)
  L(6+45)=X821(400Y)
  ** INITIAL BUCY VELOCITY **
  D(6+49)=0.
  D(6+45)=0.
  ** INITIAL TIME **
  L(6+65)=PI*(H*PI)

```


B_TURN
END

SUBROUTINE DATA(PLOY,S,X,XP,T,b,PARK)

COMMON D(500)
DIMENSION S(2,b), X(b), XB(b)
LIT, G, R, PLOY, T
N=84
POLY=97
IT(PARK.CE.2) GO TO 9

PAR FTRIEVE * *

1 DO 10 I=1,b
21 20 J=1,b
5(I,J)=D(N)

26
10 CONTINUE

X(1)=D(N)
X(2)=D(N+1)
X(3)=D(N+2)
X(4)=D(N+3)
X(5)=D(N+4)
X(6)=D(N+5)
XP(1)=D(N+6)
XP(2)=D(N+7)
XP(3)=D(N+8)
XP(4)=D(N+9)
XP(5)=C.
XB(6)=C.
T=111X(C(N+10))
P=111X(L(N+11)) + 1
PARK=Z

1010 GO TO 90

PAR FTRIEVE * *

1 DO 10 I=1,b
21 20 J=1,b
5(I,J)=S(I,J)
N=N+1
CONTINUE
P(1)=A(1)
P(2)=A(2)
P(3)=X(1)

CAT01970
CAT01980
CAT01990
CAT02000
CAT02010
CAT02020
CAT02030
CAT02040
CAT02050
CAT02060
CAT02070
CAT02080
CAT02090
CAT02100
CAT02110
CAT02120
CAT02130
CAT02140
CAT02150
CAT02160
CAT02170
CAT02180
CAT02190
CAT02200
CAT02210
CAT02220
CAT02230
CAT02240
CAT02250
CAT02260
CAT02270
CAT02280
CAT02290
CAT02300
CAT02310
CAT02320
CAT02330
CAT02340
CAT02350
CAT02360
CAT02370
CAT02380
CAT02390
CAT02400
CAT02410
CAT02420
CAT02430
CAT02440


```

D(N+3)=X(4)
D(N+4)=X(5)
D(N+5)=X(6)
D(N+6)=X(1)
D(N+7)=X(2)
D(N+8)=X(3)
D(N+9)=X(4)
D(N+10)=FLOAT(T)
D(N+11)=FLOAT(R)
MARK=1
CONTINUE
R=TURN
END

```

70

```

SUBROUTINE FILTER(S,P,X,X3,Z,BUILT,XAI,LAT,ALT,FB1,PEO,C,B3,A,NOBY,KLAT)
DIMENSION P(6,6),G(6),X(6),HT(6),XUEXT(6),GDZ(6),SYEVT(6,6),
F(1,6),FI(1,6),FFI(6,6),P(6,6),FFTA(6,6),IFFTA(6,6),AS(6,6),
SI(6,6),SST(6,6),SF(6),J(6,6),OX(6),CK(6),DS(6,6),
J(1,6),J(6,6),XR(6),XAT(2),A(2),FDSCT(6,6)
FB1=1,IFFTA=1,PAC=1,AM
DATA O,3,NOBY
DATA O/36*0./
DATA I/36*0./
DATA C/36*0./
DATA CR/6*0./
DATA PI,FPSEM/3.1415926,1./
END

```

```

1 X31=X(1)
X32=X(2)
X33=X(3)
X34=X(4)
G=Z/3600.*2/60/6.114
LX=FLOAT*PI/180.
WF=DC154*3600.
W31F=.72924-0.435600.
AT=Z/6.114
S31F=AC*AF+SI*(LX)
S32F=BC*P*AS*(LX)*P*AT
DF=(S31F*Y4(LX)*X31+S32F*Y4(LX)*X32)-9.56
C(LX)=.001

```


PAT03090
 PAT03091
 PAT03092
 PAT03093
 PAT03094
 PAT03095
 PAT03096
 PAT03097
 PAT03098
 PAT03099
 PAT03100
 PAT03101
 PAT03102
 PAT03103
 PAT03104
 PAT03105
 PAT03106
 PAT03107
 PAT03108
 PAT03109
 PAT03110
 PAT03111
 PAT03112
 PAT03113
 PAT03114
 PAT03115
 PAT03116
 PAT03117
 PAT03118
 PAT03119
 PAT03120
 PAT03121
 PAT03122
 PAT03123
 PAT03124
 PAT03125
 PAT03126
 PAT03127
 PAT03128
 PAT03129
 PAT03130
 PAT03131
 PAT03132
 PAT03133
 PAT03134
 PAT03135
 PAT03136
 PAT03137
 PAT03138
 PAT03139
 PAT03140

G(1,1)=.001
 G(2,1)=.25
 G(3,1)=.25
 G(4,1)=.001
 G(5,1)=.001
 G(6,1)=.001
 H(1,1)=1.0

PL/INT MATRIX

P(1,1)=COS(WT)
 P(1,2)=SIN(WT)/W
 P(1,3)=-GR*(SML/W)*SIN(WT)-SIN(SMLT)/DEN
 P(1,4)=-6P*(COS(WT)-COS(SMLT))/DEN
 P(2,1)=C(1,1)
 P(2,2)=-C(1,6)
 P(2,3)=C(1,5)
 P(2,4)=-W*SIN(WT)
 P(3,1)=SML*X(1,6)
 P(3,2)=GR*(W)*SIN(WT)-SML*SIN(SMLT)/DEN
 P(4,1)=C(3,1)
 P(4,2)=-C(3,6)
 P(4,3)=C(3,5)
 P(4,4)=COS(SMLT)
 P(5,1)=-SIN(SMLT)
 P(5,2)=-P(5,6)
 P(5,3)=C(5,5)

R2=WT
 X(1,1)=A(1)
 X(1,2)=A(2)
 CK(1)=(-R2*IT1/W**2+XB(1)-XAI(1))* (1-COS(WT))
 CK(2)=(-R2*IT1/W**2+XB(2)-XAI(2))* (1-COS(WT))
 CK(3)=(-R2*IT1/W+M*(XB(1)-XAI(1)))*SIN(WT)
 CK(4)=(-R2*IT1/W+M*(XB(2)-XAI(2)))*SIN(WT)

P=X(2,6)IF
 X=N(K/R-1)**4

1) CALL VPRG(0,X,CK,6,6,1)
 CALL VADD(CX,K,XNEXT,6,1)

* S(K/K-1)**4

2) CALL MPK(0,5,15,0,0,6,6)
 CALL MTRG(05,15,6,6)
 CALL GMPK(05,05,15SC,0,0,6,6)
 CALL WSPW(155,15SLN,1055,6,6)

PAT03410
 PAT03420
 PAT03430
 PAT03440
 PAT03450
 PAT03460
 PAT03470
 PAT03480
 PAT03490
 PAT03500
 PAT03510
 PAT03520
 PAT03530
 PAT03540
 PAT03550
 PAT03560
 PAT03570
 PAT03580
 PAT03590
 PAT03600
 PAT03610
 PAT03620
 PAT03630
 PAT03640
 PAT03650
 PAT03660
 PAT03670
 PAT03680
 PAT03690
 PAT03700
 PAT03710
 PAT03720
 PAT03730
 PAT03740
 PAT03750
 PAT03760
 PAT03770
 PAT03780
 PAT03790
 PAT03800
 PAT03810
 PAT03820
 PAT03830
 PAT03840
 PAT03850
 PAT03860
 PAT03870
 PAT03880

```

CALL GGADE(ROSSH,0,B,6,6)
CALL CMSRT(R,S,XI,6)
30  D1=79  IZ=1,3
    RANGE2=XNFXT(1)*3+XNFXT(2)*2+(ALT/6076.115)*2
    RANGE=SCRT(RANGE2)
    REX=X(1)*XNFXT(1)+P16.2*XNFXT(2)+P13.3*(ALT/6076.115)
    VV2=(XNFXT(3)*2+XNFXT(4)*2)
    VV=SQRT(VV2)
    X(1)=X(1)+XAI(1)
    X(2)=X(2)+XAI(2)
    B=MATRIX AND 7
40  D1=1  I=1,0
41  F(1,L)=C.
    F(1Z,KF,1) GO TO 42
    DZ=Z(1)-PEX/PAGE
    H(1,1)=(R1-XNFXT(1))*PEX/RANGE2/PAGE
    H(1,2)=(R2-XNFXT(2))*PEX/RANGE2/PAGE
    R=VOCG/
    GO TO 50
42  I(1Z,KL,2) GO TO 43
    DZ=Z(2)-VV
    H(1,3)=XNFXT(3)/VV
    H(1,4)=XNFXT(4)/VV
    R=1.0
    GO TO 50
43  IF (XNFXT(4).NE.0.) GO TO 44
    ZHAT=0.
    I(XNFXT(3).LT.0.) ZHAT=PI
    GO TO 45
    ZHAT=ATAN(XNFXT(3)/XNFXT(4))
    I(XNFXT(4).LE.0.) ZHAT=PI/P
    I(XNFXT(4).GT.0.) ZHAT=3.14159-ZHAT
    IZ=Z(3)*PI/180.-ZHAT
    F(1Z,GT,PI) DZ=2*PI-FZ
    I(1Z,LT,-PI) IZ=2*PI+FZ
    F(1,2)=-XNFXT(4)/VV2
    H(1,4)=XNFXT(3)/VV2
    R=C1
  
```



```

(  UPB(1)
(  X(K) ) *
50  CALL GMPFC(H,HT,1,6)
     CALL GMPFC(SMEXT,ST,6,6)
     CALL GMPFC(ST,HT,F,6,6,1)
     CALL GMPFC(SMEXT,F,SE,6,6,1)
     CALL GMPFC(FT,6,1)
     CALL GMPFC(FT,F,FT,F,1,6,1)
     ALPHA=1/(P+FTF)
     CALL GMSPR(SF,ALPHA1,C,6,1)
(  X(K) ) *
66  CALL GMPFC(G,J,6DZ,6,1,1)
     CALL GMPFC(XMXT,6DZ,X,6,1)
( 9814 WHITE(I,UCT,9C1) ) /
( 9815 WHITE(I,UCT,941) ) * X(1,J),J=1,6),G(L),H(L),L=1,6)
(  X(K) ) *
70  CALL GMPFC(F,FT,FET,6,1,6)
     CALL GMSFC(FET,LDPHY,FEFS,6,6)
     CALL GMSLE(I,FTA,IFTA,6,6)
     CALL GMSKT(IFA,AS,6)
     CALL GMPFC(SMEXT,S,5,6,5,6)
     CALL GMPFC(S,ST,6,6)
     CALL GMPFC(S,ST,6,6,6,6)
     IF(L=FO,9) GO TO 74
     DO 72 L=1,6
     DO 71 J=1,6
     S(1,J)=S(L,J)
     X(L)=X(L)
     CONTINUE
( 9804 WHITE(I,UCT,907)
( 9805 WHITE(I,OUT,942) ) * X(1),J=1,6),L=1,6)
(  COMPUTATION DE POUY POSITION
60  AB(1)=X(1)+XΔ(1)
     AB(2)=X(2)+XΔ(2)
66  AB(1)=C(5X,10),2,10X,6,10,5,10X,F10,5,10X,F10,5,1) * P(1)
     AB(2)=C(5X,10),2,10X,6,10,5,10X,F10,5,1) * P(1)
     AB(3)=C(1/K-3)-FA * X(1),5,10X,P(1/K-1)-MATR * X(1),5,1,2=1,
     AB(4)=C(16),6(S)-MATR * X(1),12X,6,6,3X
     AB(5)=C(17),X(K/8)-MATR * X(1),11X,P(K/8)-MATR * X(1),5,3X,6,6,6,6,6,6)
(  WHITE )

```



```

5) TUNA
EHD)
SUBROUTINE FSHL3(BUJ,K,X,XB,P,TH,PHS)
DIMENSION X(6),P(6,6),XB(6),SUMPL(1800),SUMP2(1800),XAT(2),
SUMX1(SUMX2(1800)),SUMX2(1800),SUMS01(1800),SUMS02(1800)
REAL MEAN1,MEAN2
INTEGER BUJ
DATA SUMX1,SUMX2,SUMS01,SUMS02 /1800*0.,1800*0.,1800*0.,1800*0./
DATA SUMPL,SUMP2 /1800*0.,1800*0./
LEVELS=IE+1
IOUTP=IO
IF(BUJ.EQ.0) GO TO 30
K=AL(IKRS,9) XB1,XP2,XAT
EXP1=XP(1)-XB1
EXP2=XP(2)-XB2
DO I=1,X(1)-X(1)+XAT(1)
DO J=2,X(2)-X(2)+XAT(2)
IF(BUJ.NE.1) GO TO 20
SUMX1(K)=SUMX1(K)+EXP1*X1
SUMX2(K)=SUMX2(K)+EXP1*X2
SUMS01(K)=SUMS01(K)+EXP1*X1**2
SUMS02(K)=SUMS02(K)+EXP1*X2**2
SUMP1(K)=SUMP1(K)+P(1,1)
SUMP2(K)=SUMP2(K)+P(2,2)
CONTINUE
I=SUMPTOP(1,1)
J=SUMPTOP(2,2)
WRITE(IOUTP,3) BUJ,K,XB(1),XB(2),LXB1,EXR2,EFELX3,EXP1,X2,SJ,SP
RETURN
30
LEAD(IKRS,6)
WRITE(IOUTP,6)
DO I=1,N
REAL(IKRS,9) XB1,XP2,XAT
V=V01=SUMX1(I)/PHS
V=V02=SUMX2(I)/PHS
V=V01=SUMS01(I)/PHS-MEAN1*X2
V=V02=SUMS02(I)/PHS-MEAN2*X2
V=V01=SUMP1(I)/PHS
V=V02=SUMP2(I)/PHS
COSTAA=SGRT(V=V01/V=V02)
SIGMA=COST(V=V01+V=V02)
SUMPL=SGRT(SUMPL(I)/PHS+SUMP2(I)/PHS)
SUMP2=SGRT(SUMP2(I)+SIGMA**2)
CONTINUE

```

```

DAT04370
DAT04380
DAT04390
DAT04400
DAT04410
DAT04420
DAT04430
DAT04440
DAT04450
DAT04460
DAT04470
DAT04480
DAT04490
DAT04500
DAT04510
DAT04520
DAT04530
DAT04540
DAT04550
DAT04560
DAT04570
DAT04580
DAT04590
DAT04600
DAT04610
DAT04620
DAT04630
DAT04640
DAT04650
DAT04660
DAT04670
DAT04680
DAT04690
DAT04700
DAT04710
DAT04720
DAT04730
DAT04740
DAT04750
DAT04760
DAT04770
DAT04780
DAT04790
DAT04800
DAT04810
DAT04820
DAT04830
DAT04840

```


PAT04350
 PAT04350
 PAT04370
 PAT04380
 PAT04890
 PAT04900
 PAT04910
 PAT04920
 PAT04950
 PAT04960
 PAT04960
 PAT04970
 PAT04980
 PAT04990
 PAT05000
 PAT05010
 PAT05020
 PAT05030
 PAT05040
 PAT05050
 PAT05060

```

4  FUZZAT( K, 4X, 'SIGMAX', 9X, 'SIGMA', 5X, 'SIGMAF' )
5  FORCAT(10,3F20.5)
7  FFFFF(//)
8  FORCAT(214,3F9.5)
9  FORCAT(38,4F9.4)
  RETURN
  END

SUBROUTINE POISE(DSEED,Z,STD)
  DOUBLE PRECISION DSEED
  LOGZ=9
  RHO=606CF(DSEED)
  ZD=FKC*STDZ
  WRITE(CUTZ,9200) Z,ZN,RND
  Z=Z6
  DUECAT(5F70.8)
  RETURN
  END

```

CC
 9200

() 子程序名
 () 子程序名
 () 子程序名

PAT05070
 PAT05100
 PAT05110
 PAT05120
 PAT05130
 PAT05140
 PAT05170
 PAT05170
 PAT05190
 PAT05190
 PAT05200
 PAT05210
 PAT05220
 PAT05230
 PAT05240
 PAT05250
 PAT05260
 PAT05270
 PAT05280
 PAT05290
 PAT05300
 PAT05310
 PAT05320
 PAT05330
 PAT05340
 PAT05350
 PAT05360
 PAT05370
 PAT05380
 PAT05390
 PAT05400
 PAT05410
 PAT05420
 PAT05430
 PAT05440
 PAT05450
 PAT05460
 PAT05470
 PAT05480
 PAT05490
 PAT05500
 PAT05510
 PAT05520
 PAT05530
 PAT05540
 PAT05550
 PAT05560

SUBROUTINE GMP1(A,R,N,M)

```

DEFINITION A(N,M), R(M,N)
DO 10 I=1,N
DO 20 J=1,M
R(J,I)=A(I,J)
CONTINUE
10 RETURN
END

```

20
 10

SUBROUTINE GMP2(A,R,B,F,N,M)

```

DEFINITION A(I),B(I),F(I)
M=1*F
DO 10 I=1,M
F(I)=A(I)+B(I)
RETURN
END

```

10

SUBROUTINE GMP3(A,R,B,F,N,M)

```

DEFINITION A(I),B(I),F(I)
KN=N*B
DO 10 I=1,KN
F(I)=A(I)+B(I)
RETURN
END

```

10

SUBROUTINE GMP4(A,P,P,N,A,I)

```

DEFINITION A(I),B(I),C(I)
P=0
TR=1
DO 10 I=1,L
B=1+P
DO 20 J=1,N
C=J+I
J=J-K
10-1

```


DAT05570
 DAT05580
 DAT05590
 DAT05600
 DAT05610
 DAT05620
 DAT05630
 DAT05640
 DAT05650
 DAT05660
 DAT05670
 DAT05680
 DAT05690
 DAT05700
 DAT05710
 DAT05720
 DAT05730
 DAT05740
 DAT05750
 DAT05760
 DAT05770
 DAT05780
 DAT05790
 DAT05800
 DAT05810
 DAT05820
 DAT05830
 DAT05840
 DAT05850
 DAT05860
 DAT05870
 DAT05880
 DAT05890
 DAT05900
 DAT05910
 DAT05920
 DAT05930
 DAT05940
 DAT05950
 DAT05960
 DAT05970
 DAT05980
 DAT05990
 DAT06000
 DAT06010
 DAT06020
 DAT06030
 DAT06040

```

10 K(I,J)=C
    DO 10 I=1,M
      JI=JI+K
      JB=JB+I
      I(I,J)=I(I,J)+A(JI)+B(JB)
    K=10+M
  END

SUBROUTINE GMSPT(A,S,AS,N,M)
  DIMENSION A(M,M),AS(M,M)
  DO 10 I=1,N
    DO 20 J=1,M
      AS(I,J)=A(I,J)*S
    CONTINUE
  RETURN
  END

SUBROUTINE GMSPT(B,A,M)
  DIMENSION B(M,M),A(M,N)
  DO 6 JJ=1,N
    J=JJ-JJ
    JPI=J+1
    DO 7 II=1,N
      I=II-1
      IF(I,6) JJ GO TO 6
      IF(I,6) JJ GO TO 3
      AA=C
      IF(JI,CI,N) GO TO 2
      DO 1 L=JPI,M
        A=L+I,I)^A(J,I)
        A(L,J)=(B(I,J)-AA)/A(J,J)
      CONTINUE
    IFZ=0
    IF(JPI,CI,N) GO TO 5
    DO 4 K=JPI,M
      A(K)=A(K)+A(I,K)*AA
    A(I,1)=SQRT(B(I,1)-A(I,2))
    CONTINUE
  A(I,J)=C
  CONTINUE
  CONTINUE
  RETURN
  END
  
```


DAT06090C
 DAT06090C
 DAT06097C
 DAT06098C
 DAT06099C
 DAT06100C
 DAT06110C
 DAT06120C
 DAT06130C
 DAT06140C
 DAT06150C

C SETUP: ICUTP FOR ERRORS
 C 056 ICUTP FOR SPLIT
 C 057 ICUTP FOR SPLIT
 C 058 PPRINTS
 C IM=7
 C NRUNS=2
 C AVLL=180.
 C DATA X P11...-3...-5...
 C DATA X P21...-3.5...-5.5...
 C I(N+0)=C.
 C I(N+57)=.5


```

SUBROUTINE FTLTAL(BEY,U,ALT)
COMMON(50)
DIMENSION X(1),X(2),X(3),X(4),X(5),X(6),DTIME(1),U(2)
DATA BEY, U, DTIME, X /
K=0; RUCY=5
C INITIAL BUDDY DATA
DATA X(1)/-5.5,-5.5,-10.0,-10.0,-24.0,0.0/
DATA X(2)/-3.5,-3.5,-10.5,-10.5,-15.5,0.0/
DATA X(3)/0.0,1.0,2.0,2.0,4.0,3500.0/
C INITIAL BUDDY VELOCITY
U(1)=0(1)
U(2)=U(2)
C INITIAL VELOCITIES
U(1)=6E1/6076.115
U(2)=ALT/6076.115
U(3)=7.
U(4)=2.
C INITIAL BUDDY POSITION
U(1+4)=X(1)(BUDDY)
U(1+5)=X(2)(BUDDY)
C INITIAL TIME
U(1+6)=FTLTAL(BEY)
SUMUP=
END
EXT01450
EXT01460
EXT01470
EXT01480
EXT01490
EXT01500
EXT01510
EXT01520
EXT01530
EXT01540
EXT01550
EXT01560
EXT01570
EXT01580
EXT01590
EXT01600
EXT01610
EXT01620
EXT01630
EXT01640
EXT01650
EXT01660
EXT01670
EXT01680
EXT01690
EXT01700
EXT01710
EXT01720
EXT01730
EXT01740
EXT01750
EXT01760
EXT01770
EXT01780
EXT01790
EXT01800
EXT01810
EXT01820
EXT01830

```


SUBROUTINE DATA(REDY,S,X,J,T,F,REN)

 C(50)
 DIMENSION S(2),X(2),U(2)
 I=GET.POPY,T
 K=>FLUY-2
 IF (K7SK.GE.2) GO TO 2

 C(1)FIVE

 U(1)=U(1)
 U(2)=L(2)
 DO 10 I=1,2
 DO 10 J=1,2
 S(I,J)=L(N)
 N=I+J
 CONTINUE
 X(1)=L(N)
 X(2)=L(K+1)
 T=FIX(L(N+2))
 K=FIX(L(N+3)) + 1
 GO TO 50

 STORE

 U(1)=U(1)
 U(2)=U(2)
 DO 40 I=1,2
 DO 50 J=1,2
 U(N)=S(I,J)
 N=I+J
 CONTINUE
 U(N)=X(1)
 U(I+1)=X(2)
 U(I+2)=FLOAT(T)
 U(I+3)=FLOAT(K)

 K=I+J
 CONTINUE
 T=TOP
 F=0

EXT 01860
 EXT 01870
 EXT 01880
 EXT 01890
 EXT 01900
 EXT 01910
 EXT 01920
 EXT 01930
 EXT 01940
 EXT 01950
 EXT 01960
 EXT 01970
 EXT 01980
 EXT 01990
 EXT 02000
 EXT 02010
 EXT 02020
 EXT 02030
 EXT 02040
 EXT 02050
 EXT 02060
 EXT 02070
 EXT 02080
 EXT 02090
 EXT 02100
 EXT 02110
 EXT 02120
 EXT 02130
 EXT 02140
 EXT 02150
 EXT 02160
 EXT 02170
 EXT 02180
 EXT 02190
 EXT 02200
 EXT 02210
 EXT 02220
 EXT 02230
 EXT 02240
 EXT 02250
 EXT 02260


```

SUBROUTINE FILTER(S,P,X,U,Z,DELTA,XAI,ALTA,RH1,RR2,FR3,FRJY,K,H)
EXT02290
EXT02300
EXT02310
EXT02320
EXT02330
EXT02340
EXT02350
EXT02360
EXT02370
EXT02380
EXT02390
EXT02400
EXT02410
EXT02420
EXT02430
EXT02440
EXT02450
EXT02460
EXT02470
EXT02480
EXT02490
EXT02500
EXT02510
EXT02520
EXT02530
EXT02540
EXT02550
EXT02560
EXT02570
EXT02580
EXT02590
EXT02600
EXT02610
EXT02620
EXT02630
EXT02640
EXT02650
EXT02660
EXT02670
EXT02680
EXT02690
EXT02700
EXT02710
EXT02720
EXT02730
EXT02740
EXT02750
EXT02760
EXT02770

DIMENSION P(2,2),C(2),X(2),U(2),HT(2),XAI(2),
X(H(1,2),0(2,2)),I(2,2),S(2,2),XAI(2),
C(F(2,1),1(1,2)),FT(2,2),R(2,2),FITA(2,2),IFTA(2,2),
S(ST(2,2),ST(2,2)),SF(2,2),ZU(2),FSCT(2,2),
IIFGER,FUDY
RZ(1),IIFETA
DATA Q/4*C./
PAR1 I/1.C./0.,1./
IOUT=0

Q(1,1)=.001
Q(1,2)=.001
U(1,1)=1.0
L2=U(2)
X1=X(1)
X2=X(2)

C PROPAGATE
** X(K/R-1)**X

XAI(1)=X(1)+DELTA
XAI(2)=X(2)+DELTA

C ** S(K/R-1)**X

CALL GMTRA(S,ST,C)
CALL GPPRC(S,ST,CST,2,2)
CALL GNSFN(SST,PSLN,CST,2,2)
CALL GMAB(B,ST,0,2)
CALL GMSPT(B,ST,X,2)

C L X=XAI(1)-X(1)
L X2=XAI(2)-X(2)
DELTA=L/107.216
C L X=X1+DELTA**2+L X**2
C L X2=X2+DELTA**2+L X2**2
DELTA=X1+L X1+L X1+L X1+L X1+L X1
H(1,1)=(R1-0.1)*R1/R1/R1/R1/R1/R1/R1/R1/R1/R1
F(1,2)=(F12-0.1)*X1/R1/R1/R1/R1/R1/R1/R1/R1/R1/R1
F=.0007

```



```

SUMX2(N) = SUMX2(K) + D(LX2)
SUMS1(K) = SUMS1(K) + PDFLX1**2
SUMS2(K) = SUMS2(K) + PDFLX2**2
SUMI1(K) = SUMI1(K) + P(1,1)
SUMP2(K) = SUMP2(K) + P(2,2)
CONTINUE
S1 = SORT(P(1,1))
S2 = SORT(P(2,2))
WRITE(OUTPUT,3) BUOY, K, X1, X2, F01, X1, F02, LX2, S1, S2
RETURN
20
REAL (IMFES,6)
WRITE(OUTPUT,4)
DO 50 I=1,K
  REAL (IMFES,9) X3L, XR2, XAT
  MEAN1 = SUMX1(I)/FUNS
  MEAN2 = SUMX2(I)/FUNS
  VARX1 = SUMS1(I)/FUNS - MEAN1**2
  VARX2 = SUMS2(I)/FUNS - MEAN2**2
  VAN1 = SUMS1(I)/FUNS
  VAR2 = SUMS2(I)/FUNS
  SIGAX = SORT(VARX1 + VARX2)
  SIGMA = SORT(VAR1 + VAR2)
  SIGMAF = SORT(SIGX1(I)/FUNS + SIGX2(I)/FUNS)
  WRITE(OUTPUT,5) I, SIGMAX, SIGMA, SIGMAF
  CONTINUE
50
F01 = AT(  K', 4X, 'SIGMAX', +X, 'SIGMA', 5X, 'SIGMAF',
5  F02 = AT(10,2F10.5)
7  F03 = AT(//)
8  F04 = AT(2,14,3F9.5)
9  F05 = AT(3X,9F9.4)
  STOP
SUBSTITUTE F01,F2(0SEF),2,5TO)
2  F01 = POINT(0,0SEF)
3  F02 = 5
4  F03 = GBV(0,5)
5  F04 = N1*SIGMAF
6  F05 = AT(UTZ,02) ) Z, /N, *N)
7  Z = 1
8  F06 = AT(UTZ,0,2)
9  F07 = 1
  STOP

```

```

EXT03730
EXT03740
EXT03750
EXT03760
EXT03770
EXT03780
EXT03790
EXT03800
EXT03810
EXT03820
EXT03830
EXT03840
EXT03850
EXT03860
EXT03870
EXT03880
EXT03890
EXT03900
EXT03910
EXT03920
EXT03930
EXT03940
EXT03950
EXT03960
EXT03970
EXT03980
EXT03990
EXT04000
EXT04010
EXT04020
EXT04030
EXT04040
EXT04050
EXT04060
EXT04070
EXT04080
EXT04090
EXT04100
EXT04110
EXT04120
EXT04130
EXT04140
EXT04150
EXT04160
EXT04170
EXT04180
EXT04190
EXT04200
EXT04210

```


1 1. 本程序系由本所編譯，其內容與原程序無異，特此聲明。
 2 3. 本程序之編譯，係由本所編譯，其內容與原程序無異，特此聲明。
 3 4. 本程序之編譯，係由本所編譯，其內容與原程序無異，特此聲明。

```

EXT 04210
EXT 04220
EXT 04230
EXT 04240
EXT 04250
EXT 04260
EXT 04270
EXT 04280
EXT 04290
EXT 04300
EXT 04310
EXT 04320
EXT 04330
EXT 04340
EXT 04350
EXT 04360
EXT 04370
EXT 04380
EXT 04390
EXT 04400
EXT 04410
EXT 04420
EXT 04430
EXT 04440
EXT 04450
EXT 04460
EXT 04470
EXT 04480
EXT 04490
EXT 04500
EXT 04510
EXT 04520
EXT 04530
EXT 04540
EXT 04550
EXT 04560
EXT 04570
EXT 04580
EXT 04590
EXT 04600
EXT 04610
EXT 04620
EXT 04630
EXT 04640
EXT 04650
EXT 04660
EXT 04670
EXT 04680

```

```

SUBROUTINE GMTRZ(A, R, K, M)
  DIMENSION A(N, N), R(M, M)
  DO 10 I=1, N
    DO 20 J=1, M
      R(I, J)=A(I, J)
    GO TO 30
  ENDDO
  DO 40
    SUBROUTINE GMADD(A, B, P, R, M)
      DIMENSION A(I), B(I), R(I)
      PA=I*2
      DO 10 I=1, M
        R(I)=A(I)+B(I)
      ENDDO
    END
  ENDDO
  SUBROUTINE GMSUB(A, B, P, R, M)
      DIMENSION A(I), B(I), R(I)
      PA=I*2
      DO 10 I=1, M
        R(I)=A(I)-B(I)
      ENDDO
    END
  ENDDO
  SUBROUTINE GMP3(A, P, R, M, I)
      DIMENSION R(I), P(I), P(I)
      IF=0
      IF=-M
      DO 10 I=1, I
        IF=IF*M
      ENDDO
      DO 10 J=1, M
        IF=IF+1
      ENDDO
      IF=J-1
      IF=J-1
    END
  ENDDO

```


XT 04690
 XT 04700
 XT 04710
 XT 04720
 XT 04730
 XT 04740
 XT 04750
 XT 04760
 XT 04770
 XT 04780
 XT 04790
 XT 04800
 XT 04810
 XT 04820
 XT 04830
 XT 04840
 XT 04850
 XT 04860
 XT 04870
 XT 04880
 XT 04890
 XT 04900
 XT 04910
 XT 04920
 XT 04930
 XT 04940
 XT 04950
 XT 04960
 XT 04970
 XT 04980
 XT 04990
 XT 05000
 XT 05010
 XT 05020
 XT 05030
 XT 05040
 XT 05050
 XT 05060
 XT 05070
 XT 05080
 XT 05090
 XT 05100
 XT 05110
 XT 05120
 XT 05130
 XT 05140
 XT 05150
 XT 05160
 XT 05170

```

K(I)=V
DO 70 I=1,M
  J1=J1+N
  J2=J2+1
  K(I)=A(I)+A(J1)*B(I)
  CONTINUE
END

SUBROUTINE GMSIP(A,S,AS,N,I)
  DIMENSION A(N,I),AS(N,M)
  DO 70 I=1,N
    DO 70 J=1,M
      AS(I,J)=A(I,J)*S
  CONTINUE
END

SUBROUTINE GMSIT(I,A,N)
  DIMENSION B(N,I),A(N,M)
  DO 70 JJ=1,N
    J=J+1-JJ
    JPJ=J+1
    DO 70 II=1,N
      I=I+1-II
      B(I,II)=A(JP,II)
    CONTINUE
  END

  AA=C
  B(CPI,C)=B(C)
  DO 70 L=J+1,N
    AA=L+A(L,I)*A(L,I)
    B(L,I)=(B(L,I)-AA)/L(J,J)
  CONTINUE
  AA=0
  B(CPI,C)=B(C)
  DO 70 K=J+1,N
    A(K)=A(K,I)*A(L,I)
    B(L,I)=B(L,I)-A(K,I)*A(K,I)
  CONTINUE
  B(L,I)=C
  CONTINUE
  CONTINUE
  END
  
```


EXT05170
EXT05180
EXT05190
EXT05200
EXT05210
EXT05220
EXT05230

STUP:
C 58 ICONF FOR SPLOT
C 57 ICONF FOR SPLIT
C 56 PRINTS
C 10=7
C 100=5-20
C DATA XBL1...=3..5..5..5...
C DATA XBL2...=3..5..5..5...
C

APPENDIX B
COMPUTER PROGRAM FOR DATA GENERATION

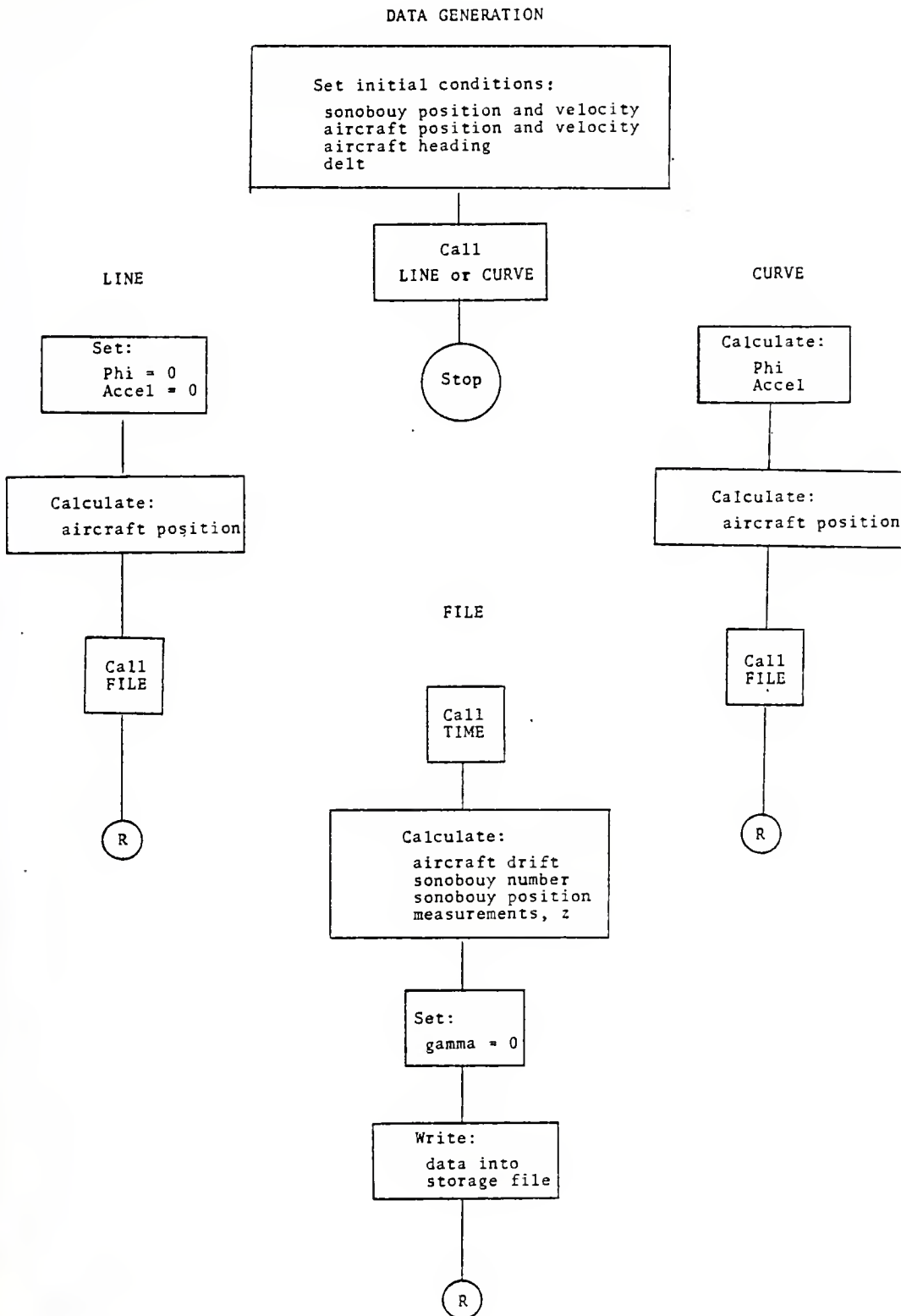


Figure 37. Flow chart: data generation program.

GLOSSARY OF COMPUTER VARIABLES

DATA GENERATION PROGRAM

A	Vector of aircraft accelerations
AL	Altitude in nautical miles
ALT	Altitude
ANT	Antenna
AVEL	Initial aircraft velocity
AX1	Amplitude of Schuler cycle, A_{X1}
AX2	Amplitude of Schuler cycle, A_{X2}
B	Intercept on N-S axis of straight track
BANG	Sonobuoy drift direction
BOUY	Sonobuoy RF channel or number
BVEL	Sonobuoy drift direction
CKL	Rate of change of nautical miles for a change in degrees of longitude
D	Length of straight track
DELT	Interval between measurements, Δt
DELV1	Relative velocity, Δv_1
DELV2	Relative velocity, Δv_2
DELX1	Relative position, Δx_1
DELX2	Relative position, Δx_2
DH	Total change in heading while on curved track
DSEED	Seed for the random number generator
END	Indicator of EOF
G	Gravitational acceleration
GAMMA	Aircraft pitch angle, γ

GR	Gamma in radians
H	Aircraft heading
HNEW	Final heading on curved track
HOUR	Time in hours
HR	Heading in radians
IOUT	Device on which print is made
IOUTP	File in which results are written
IOUTR	File in which true sonobuoy positions are written
IOUTZ	File in which random vectors are inspected
ITIME	Time from aircraft clock in seconds
KX1	Rate of linear navigational drift, K_{x1}
KX2	Rate of linear navigational drift, K_{x2}
LAT	Latitude
LATI	The latitude of the origin of the local earth fixed coordinate system
LONG	Longitude
LONGI	The longitude of the origin of the local earth fixed coordinate system
LTIME	Array of initial drop times for the sonobuoy
M	Slope of straight track
MARK	Indicates the first time a buoy is to be processed
MIN	Time in minutes
N	Index
NBOUY	Total number of sonobuoys
NSTOP	End of line or curve series
PHI	Aircraft roll angle, ϕ
PI	π
PI2	2π

PR Phi in radians
 R Radius of curved track
 RB1 Unit vector component of antenna baseline
 RB2 Unit vector component of antenna baseline
 RB3 Unit vector component of antenna baseline
 S Distance aircraft travels in time Δt
 SEC Time in seconds
 SKL Rate of change of nautical miles for a change in
 degrees of latitude
 TRACK Direction of aircraft travel over the ground
 U Direction to center of curved track
 V Direction from center of curved track to aircraft
 VA1 Velocity of aircraft
 VA2 Velocity of aircraft
 VB1 Sonobuoy drift
 VB2 Sonobuoy drift
 WANG Wind direction
 WVEL Wind velocity
 XAI Aircraft inertial position, X_a^I
 XAT Aircraft true position, \bar{X}_a
 XB1 True geographical location of sonobuoy, x_1
 XB2 True geographical location of sonobuoy, x_2
 XC1 Location of the center of the curved track
 XC2 Location of the center of the curved track
 XX1 Incremental change in X_1
 XX2 Incremental change in X_2
 Z Measurement vector

CRI00520
 CRI00530
 CRI00540
 CRI00550
 CRI00560
 CRI00570
 CRI00580
 CRI00590
 CRI00600
 CRI00610
 CRI00620
 CRI00630
 CRI00640
 CRI00650
 CRI00660
 CRI00670
 CRI00680
 CRI00690
 CRI00700
 CRI00710
 CRI00720
 CRI00730
 CRI00740
 CRI00750
 CRI00760
 CRI00770
 CRI00780
 CRI00790
 CRI00800
 CRI00810
 CRI00820
 CRI00830
 CRI00840
 CRI00850
 CRI00860
 CRI00870
 CRI00880
 CRI00890
 CRI00900
 CRI00910
 CRI00920
 CRI00930
 CRI00940
 CRI00950
 CRI00960
 CRI00970
 CRI00980
 CRI00990

4 CALL CUPVEL(XAT,3.5,H,00C.,S,MARK)
 5 CALL LINE(XAT,H,21.,S,MARK)
 6 CALL CUPVEL(XAT,3.5,H,27C.,S,MARK)
 7 CALL LINE(XAT,H,21.,S,MARK)
 8 CALL CUPVEL(XAT,3.5,H,18C.,S,MARK)
 9 CALL LINE(XAT,H,22.,S,MARK)
 10 CALL CUPVEL(XAT,3.5,H,09C.,S,MARK)
 11 CALL LINE(XAT,H,22.,S,MARK)
 12 CALL CUPVEL(XAT,3.5,H,0.,S,MARK)
 13 CALL LINE(XAT,H,23.,S,MARK)
 14 CALL CUPVEL(XAT,3.5,H,27C.,S,MARK)
 15 CALL LINE(XAT,H,23.,S,MARK)
 16 CALL CUPVEL(XAT,3.5,H,18C.,S,MARK)
 17 CALL LINE(XAT,H,24.,S,MARK)
 18 CALL CUPVEL(XAT,3.5,H,09C.,S,MARK)
 19 CALL LINE(XAT,H,24.,S,MARK)
 20 CALL CUPVEL(XAT,3.5,H,00C.,S,MARK)
 21 CALL LINE(XAT,H,25.,S,MARK)
 22 CALL CUPVEL(XAT,3.5,H,27C.,S,MARK)
 23 CALL LINE(XAT,H,25.,S,MARK)
 24 CALL CUPVEL(XAT,3.5,H,18C.,S,MARK)
 25 CALL LINE(XAT,H,26.,S,MARK)
 26 CALL CUPVEL(XAT,3.5,H,09C.,S,MARK)
 27 CALL LINE(XAT,H,26.,S,MARK)

CR101006
 CR101010
 CR101020
 CR101030
 CR101040
 CR101050
 CR101060
 CR101070
 CR101080
 CR101090
 CR101100
 CR101110
 CR101120
 CR101130
 CR101140
 CR101150
 CR101160
 CR101170
 CR101180
 CR101190
 CR101200
 CR101210
 CR101220
 CR101230
 CR101240
 CR101250
 CR101260
 CR101270
 CR101280
 CR101290
 CR101300
 CR101310
 CR101320
 CR101330
 CR101340
 CR101350
 CR101360
 CR101370
 CR101380
 CR101390
 CR101400

```

END=92555.9
IEND=55
WRITE(ICLU,9001) IEND
WRITE(ICUTP,5000) IEND
9000  FORMAT(10X,F10.4)
9001  FORMAT(12)

STOP
END

SUBROUTINE LIFE(XAT,H,D,S,MARK)
DIMENSION XAT(2),A(2)
REAL M
NSTOP=IFIX(D/S)
PHI=C.
A(1)=0.
A(2)=C.
IF(H.EG.0.) GO TO 20
IF(H.EC.180.) GO TO 40
HR=H*3.1415926/180.
M=CC TAN(HR)
b=XAT(1)-M*XAT(2)
XAZ=5*SIN(HR)

10  I=1,NSTOP
XAT(2)=XAT(2)+XAZ
XAT(1)=M*XAT(2)+b
CALL FILE(XAT,H,PHI,A,MARK)
GO TO 55

20  M=30  K=1,NSTOP
XAT(1)=XAT(1)+C
CALL FILE(XAT,H,PHI,A,MARK)
GO TO 55

40  M=50  N=1,NSTOP
XAT(1)=XAT(1)-C
CALL FILE(XAT,H,PHI,A,MARK)
GO TO 55

50  CALL FILE(XAT,H,PHI,A,MARK)
55  RETURN
END
  
```



```

SURFCURVE CURVE(XAT,R,H,HNFW,S,MARK)
DIMENSION XAT(2),A(2)
DATA PI,PI2,G /3.1415926,6.2831852,32.2/
AVFL=180.
U=(H-SC.)*PI/180.
XC1=F*CCS(U)+XAT(1)
XC2=P*SIN(U)+XAT(2)
V=(H+SC.)*PI/180.
DH=H+360.-HNFW
IF(DH.CT.360.) DH=DH-360.
NSTOP=FIX(DH*PI/180.*E/S)
PHI=-ATAN(AVFL*1.6878)**2/(G*R*607(.115))*180./PI

```

```

DO 10 N=1,NSTOP
V=V-S/R
IF(V.GT.PI2) V=V-PI2
IF(V.LT.C.) V=V+PI2
A(1)=CCS(V)*AVFL**2/P
A(2)=-SIN(V)*AVFL**2/P
H=V*180./PI-90.
IF(DH.LT.C.) H=H+360.
XAT(1)=F*CCS(V)+XC1
XX2=SGRT(R**2-(XAT(1)-XC1)**2)
IF(V.LT.PI) XAT(2)=X(2)+XX2
IF(V.GT.PI) XAT(2)=X(2)-XX2
CALL FILL(XAT,H,PHT,A,MARK)
ENDPHW
RETHEN
END

```

10

```

SURFCURVE CURVE(XAT,R,H,HNFW,S,MARK)
DIMENSION XAT(2),A(2)
DATA PI,PI2,G /3.1415926,6.2831852,32.2/
AVFL=180.
U=(H+SC.)*PI/180.
XC1=F*CCS(U)+XAT(1)
XC2=P*SIN(U)+XAT(2)
V=(H-SC.)*PI/180.
DH=H+360.-HNFW
IF(DH.CT.360.) DH=DH-360.
NSTOP=FIX(DH*PI/180.*E/S)
PHI=ATAN(AVFL*1.6878)**2/(G*R*607(.115))*180./PI
DO 10 N=1,NSTOP
V=V+S/R

```

0101430
0101440
0101450
0101460
0101470
0101480
0101490
0101500
0101510
0101520
0101530
0101540
0101550
0101560
0101570
0101580
0101590
0101600
0101610
0101620
0101630
0101640
0101650
0101660
0101670
0101680
0101690
0101700
0101710
0101720
0101730
0101740
0101750
0101760
0101770
0101780
0101790
0101800
0101810
0101820
0101830
0101840
0101850
0101860
0101870
0101880
0101890
0101900


```

IF(V,GT,PI?) V=V-PI?
IF(V,LT,0.) V=V+PI?
A(1)=-((S(V)*AVF1**2/F
A(2)=-SIN(V)*AVFL**2/R
P=V*16C./PI+90.
IF(H,Cf,360.) H=H-360.
XAT(1)=P*CD5(V)+XC1
XAL=5CRT(R**2-(XAT(1)-XC1)**2)
IF(V,LT,PI) XAT(2)=XC2+XX2
IF(V,GT,PI) XAT(2)=XC2-XX2
CALL FILE(XAT,H,PHI,A,MARK)
F=H*Fw
P*TURN
STOP
SUBROUTINE FUL(XAT,H,PHI,A,MARK)
DIMENSION Z(3),XAL(2),XAT(2),A(2)
REAL LAT,LENG
I47,C7F,FCUR,SIC,BURV,AHT
LTP=PI/2.14159267
LUT=7
LUTR=HUT+1
LUTP=10
AVH=16C.
WVL=0.
MARK=0.
IF(ARK,NO,1) GOTO 1
DETF(FCUT,5094)
WRTT(IUTP,5095)
WRTT(IUTR,9096)
CALL TIME(FCUR,MIN,SEC,MARK)
TIME=360*FCUR+60*MIN+SEC
CALL ACERF(XAT,XAT,TIME)
CALL BURV(BURV,MARK)
CALL BUYPD(BURV,TIME,XB1,XB2,VE1,VE2,MARK)
TIME=1
ALT=36C.
M=PI/6C/76.115
GAP=A=C.
LX>1=XAL-XAT(1)
LX2=XE2-XAT(2)
L
G(1) - (LX(1)+LX2) *Z
CALL PAF(CALF0,6095,PHI,CPI,PR2,263)
Z(1) - (PI*XAL+PI*FCUR+PI*3)/SORT(D_LX1*2+DEL_C2*2+AV**2)

```

10

1

2

L

30


```

15  H(G)5(Z(L)).L1=.366) GO TO 20
20  IF(GNR.FC.0) GO TO 15
    AUT=C
    GT TC 15
    WRITE(IUCT,5CR2)
    IF(NPRK.CO.1) DSFFD=7654321

C    ** Z(2) - VELOCITY RELATIVE TO WATER SURFACE **
    VAL=AVEL* $\cos(\text{H*PI}/180.)$  + WVFL* $\cos(\text{WANG*PI}/180.)$ 
    VAL=AVEL* $\sin(\text{H*PI}/180.)$  + WVFL* $\sin(\text{WANG*PI}/180.)$ 
    DELV1=VAL-VAI
    DELV2=VP2-VA2
    Z(I)=SQRT(DELV1**2+DELV2**2)

C    ** Z(3) - POINT ANGLE **
    IF(DELV2.NE.0.) GO TO 30
    IF(DELV1.GE.0.) TRACK=0.
    IF(DELV1.LT.0.) TRACK=180.
    GO TO 31
30  TRACK=ATAN(DELV2/DELV1)*180./PI
    IF(DELV2.LT.0.) TRACK=90.-TRACK
    IF(DELV2.GT.0.) TRACK=270.-TRACK
    Z(I)=TR/CR-H
    IF(Z(3).GT.180.) Z(3)=Z(3)-360.
    IF(Z(3).LT.-180.) Z(3)=Z(3)+360.

    WRITE(IUCTP,9081) PAK,XAI,XAT
    WRITE(IUCTE,9083) MAPK,XP1,XP2,XAT,DELV1,DELV2,TRACK
    CALL TATECP(XAI(1),XAI(2),LAT,LONG)
    WRITE(IUCT,9080)RUCY,PHUP,ATN,SEC,Z,LAT,LONG,ALT,H,G5,113,PHI,A,ANT,510,700
    WRITE=NAFK+1

9080  TUBAT(11),312,17.3,16.3,15.3,14.5,13.5,12.0,16.1,14.5,1
    3,17.0,12)
9081  TUBAT(110,4E10,4)
9082  TUBAT(100,FAE,BLAP,MC)
9083  TUBAT(13,4E9,4,3E10,4)
9084  TUBAT(17,1EAT,12: RUM 9/09, DLT=90, //, H A 5,
    3X, Z(3), 2X, Z(3), 2X, Z(3), 3X, XAI(1), 3X, XAI(2), 2X,
    3X, XP1, 2X, XP2, 2X, PH1, 3X, XAI, 3X, AX2, 1A, A10)
9085  TUBAT(17, DAT,17: PUP 9/09, DLT=90, //,
    3X, XAI(1), 3X, XAI(2), 3X, XAT(1), 3X, XAT(2))
9086  TUBAT(17, DAT,17: RUM 9/09, DLT=90, //, 090-2, 5, 0, 1,
    //, 3X, XP1, 3X, XP2, 3X, XAT(1), 3X, XAT(2), 3X, DELV1, 5X, D-1
    V2, 5X, TRACK)
    15, 5X, TRACK)

```



```

SUBROUTINE BUYPD(BUCY,IA,K)
  INTEGER BU
  REAL Y=4
  IF(IA.K.CT.64) GO TO 10
  C9602 NBUY=3
  C9603 NBUY=3
  C9604 IF(IA.K.GT.42) GO TO 10
  C9605 NBUY=2
  C9606 IF(IA.K.CT.21) GO TO 10
  NBUY=1
  C8 IF(IA.K.LC.1) BY=0
  C9 BUY=MBKBUY
  C11 IF(BCCY.LC.NBUY) GO TO 20
  C12 BY=BY-MBUY
  C13 GO TO 20
  C14 CONTINUE
  C15 RETURN
  END

```

00103350
 00103360
 00103370
 00103380
 00103390
 00103400
 00103410
 00103420
 00103430
 00103440
 00103450
 00103460
 00103470
 00103480
 00103490
 00103500
 00103510
 00103520
 00103530
 00103540
 00103550
 00103560
 00103570
 00103580
 00103590
 00103600
 00103610
 00103620
 00103630
 00103640
 00103650
 00103660
 00103670
 00103680
 00103690
 00103700
 00103710
 00103720
 00103730
 00103740
 00103750
 00103760
 00103770
 00103780
 00103790
 00103800
 00103810
 00103820

```

SUBROUTINE BUYPD(BUCY,TIME,X1,X2,X3,X4,X5,IA,K)

```

```

DIMENSION XRI(31),XRP(31),TIME(31)
INTEGER BU
REAL Y=4
IF(IA.K.NE.1) GO TO 2
XRI(1)=3
XRI(2)=4
XRI(3)=5
XRI(4)=6
XRI(5)=7
XRI(6)=8
XRI(7)=9
XRI(8)=10
XRI(9)=11
XRI(10)=12
XRI(11)=13
XRI(12)=14
XRI(13)=15
XRI(14)=16
XRI(15)=17
XRI(16)=18
XRI(17)=19
XRI(18)=20
XRI(19)=21
XRI(20)=22
XRI(21)=23
XRI(22)=24
XRI(23)=25
XRI(24)=26
XRI(25)=27
XRI(26)=28
XRI(27)=29
XRI(28)=30
XRI(29)=31
XRI(30)=32
XRI(31)=33
XRP(1)=XRI(1)
XRP(2)=XRI(2)
XRP(3)=XRI(3)
XRP(4)=XRI(4)
XRP(5)=XRI(5)
XRP(6)=XRI(6)
XRP(7)=XRI(7)
XRP(8)=XRI(8)
XRP(9)=XRI(9)
XRP(10)=XRI(10)
XRP(11)=XRI(11)
XRP(12)=XRI(12)
XRP(13)=XRI(13)
XRP(14)=XRI(14)
XRP(15)=XRI(15)
XRP(16)=XRI(16)
XRP(17)=XRI(17)
XRP(18)=XRI(18)
XRP(19)=XRI(19)
XRP(20)=XRI(20)
XRP(21)=XRI(21)
XRP(22)=XRI(22)
XRP(23)=XRI(23)
XRP(24)=XRI(24)
XRP(25)=XRI(25)
XRP(26)=XRI(26)
XRP(27)=XRI(27)
XRP(28)=XRI(28)
XRP(29)=XRI(29)
XRP(30)=XRI(30)
XRP(31)=XRI(31)
TIME(1)=XRI(1)
TIME(2)=XRI(2)
TIME(3)=XRI(3)
TIME(4)=XRI(4)
TIME(5)=XRI(5)
TIME(6)=XRI(6)
TIME(7)=XRI(7)
TIME(8)=XRI(8)
TIME(9)=XRI(9)
TIME(10)=XRI(10)
TIME(11)=XRI(11)
TIME(12)=XRI(12)
TIME(13)=XRI(13)
TIME(14)=XRI(14)
TIME(15)=XRI(15)
TIME(16)=XRI(16)
TIME(17)=XRI(17)
TIME(18)=XRI(18)
TIME(19)=XRI(19)
TIME(20)=XRI(20)
TIME(21)=XRI(21)
TIME(22)=XRI(22)
TIME(23)=XRI(23)
TIME(24)=XRI(24)
TIME(25)=XRI(25)
TIME(26)=XRI(26)
TIME(27)=XRI(27)
TIME(28)=XRI(28)
TIME(29)=XRI(29)
TIME(30)=XRI(30)
TIME(31)=XRI(31)

```


1. 日期與時間
 2. 日期與時間
 3. 日期與時間
 4. 日期與時間
 5. 日期與時間
 6. 日期與時間
 7. 日期與時間
 8. 日期與時間
 9. 日期與時間
 10. 日期與時間
 11. 日期與時間
 12. 日期與時間
 13. 日期與時間
 14. 日期與時間
 15. 日期與時間
 16. 日期與時間
 17. 日期與時間
 18. 日期與時間
 19. 日期與時間
 20. 日期與時間
 21. 日期與時間
 22. 日期與時間
 23. 日期與時間
 24. 日期與時間
 25. 日期與時間
 26. 日期與時間
 27. 日期與時間
 28. 日期與時間
 29. 日期與時間
 30. 日期與時間
 31. 日期與時間
 32. 日期與時間
 33. 日期與時間
 34. 日期與時間
 35. 日期與時間
 36. 日期與時間
 37. 日期與時間
 38. 日期與時間
 39. 日期與時間
 40. 日期與時間
 41. 日期與時間
 42. 日期與時間
 43. 日期與時間
 44. 日期與時間
 45. 日期與時間
 46. 日期與時間
 47. 日期與時間
 48. 日期與時間
 49. 日期與時間
 50. 日期與時間
 51. 日期與時間
 52. 日期與時間
 53. 日期與時間
 54. 日期與時間
 55. 日期與時間
 56. 日期與時間
 57. 日期與時間
 58. 日期與時間
 59. 日期與時間
 60. 日期與時間
 61. 日期與時間
 62. 日期與時間
 63. 日期與時間
 64. 日期與時間
 65. 日期與時間
 66. 日期與時間
 67. 日期與時間
 68. 日期與時間
 69. 日期與時間
 70. 日期與時間
 71. 日期與時間
 72. 日期與時間
 73. 日期與時間
 74. 日期與時間
 75. 日期與時間
 76. 日期與時間
 77. 日期與時間
 78. 日期與時間
 79. 日期與時間
 80. 日期與時間
 81. 日期與時間
 82. 日期與時間
 83. 日期與時間
 84. 日期與時間
 85. 日期與時間
 86. 日期與時間
 87. 日期與時間
 88. 日期與時間
 89. 日期與時間
 90. 日期與時間
 91. 日期與時間
 92. 日期與時間
 93. 日期與時間
 94. 日期與時間
 95. 日期與時間
 96. 日期與時間
 97. 日期與時間
 98. 日期與時間
 99. 日期與時間
 100. 日期與時間

CRI00040
 CRI00050
 CRI00060
 CRI00070
 CRI00080
 CRI00090
 CRI00100
 CRI00110
 CRI00120
 CRI00130
 CRI00140
 CRI00150
 CRI00160
 CRI00170
 CRI00180
 CRI00190
 CRI00200
 CRI00210
 CRI00220
 CRI00230
 CRI00240
 CRI00250
 CRI00260
 CRI00270
 CRI00280
 CRI00290
 CRI00300
 CRI00310
 CRI00320
 CRI00330
 CRI00340
 CRI00350
 CRI00360
 CRI00370
 CRI00380
 CRI00390
 CRI00400
 CRI00410
 CRI00420
 CRI00430
 CRI00440
 CRI00450
 CRI00460
 CRI00470
 CRI00480
 CRI00490
 CRI00500
 CRI00510

```

C IC ALTF, (CFCK:
C IOUT=7
C IOUTP=10
C IOUTZ=5
C XAT(1)=-3.
C XAT(2)=-5.
C AVFL=180.
C F=IRG.
C DELT=9C.
C ALT=3000.
C GAMMA=6.
C ELLIP=7654221.000
C AXI,AX2,KX1,KX2 IN ACDFIF
C WVFL=0.
C WANG=0.
C PULL=2.
C BANG=0.50.
C LINE ATLC CURVE CALLS
C FOR INITIAL BUOYS-ADJUST 'C98' IN BUOYNO
C AND INITIAL BUOY POSITIONS IN BUOYPO
C
C *** WARNING: H CANNOT BE GREATER THAN 360. ***
C DIMENSION XAT(2)
C IOUT=7
C IOUTF=10
C IOUTZ=5
C MAPK=1
C XAT(1)=-3.
C XAT(2)=-5.
C H=100.
C AVFL=100.
C DELT=9C.
C SEVIF=PI*ELL/3600.
C CALL LINE(XAT,H,7.5,S,MAPK)
C CALL CURVE(XAT,5.5,H,0.9C,S,MAPK)
C CALL LINE(XAT,H,10.,S,MAPK)
  
```


APPENDIX C
Range Analysis

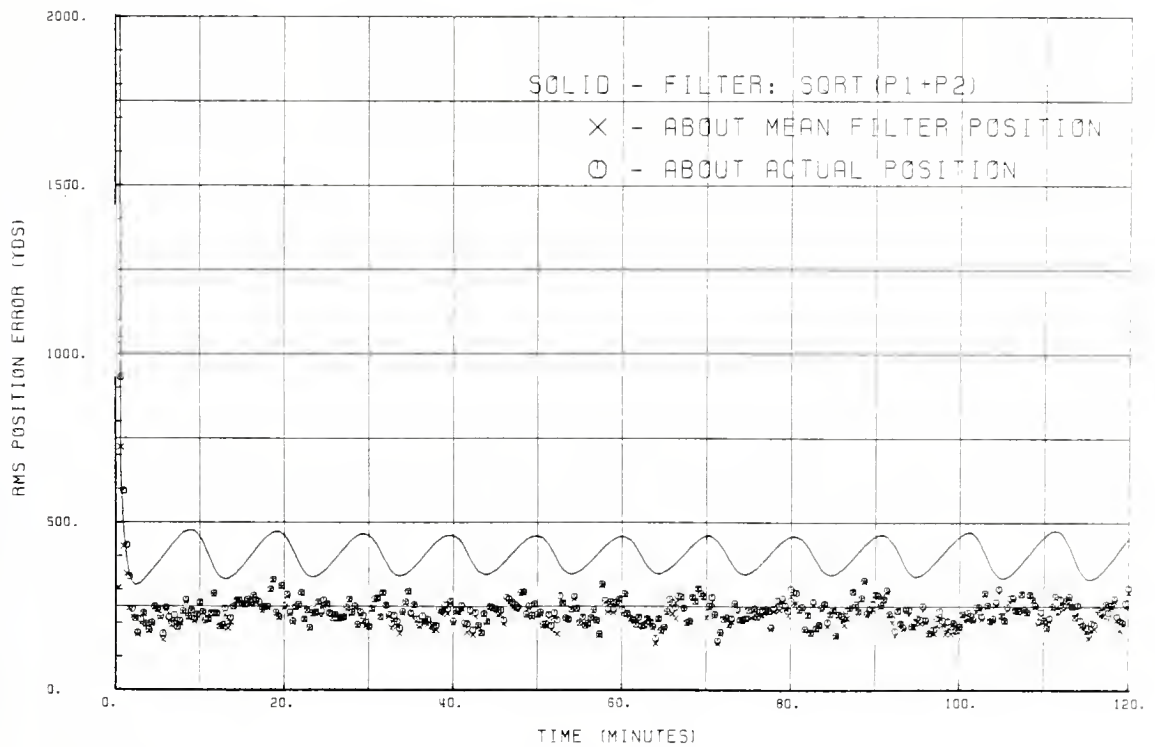
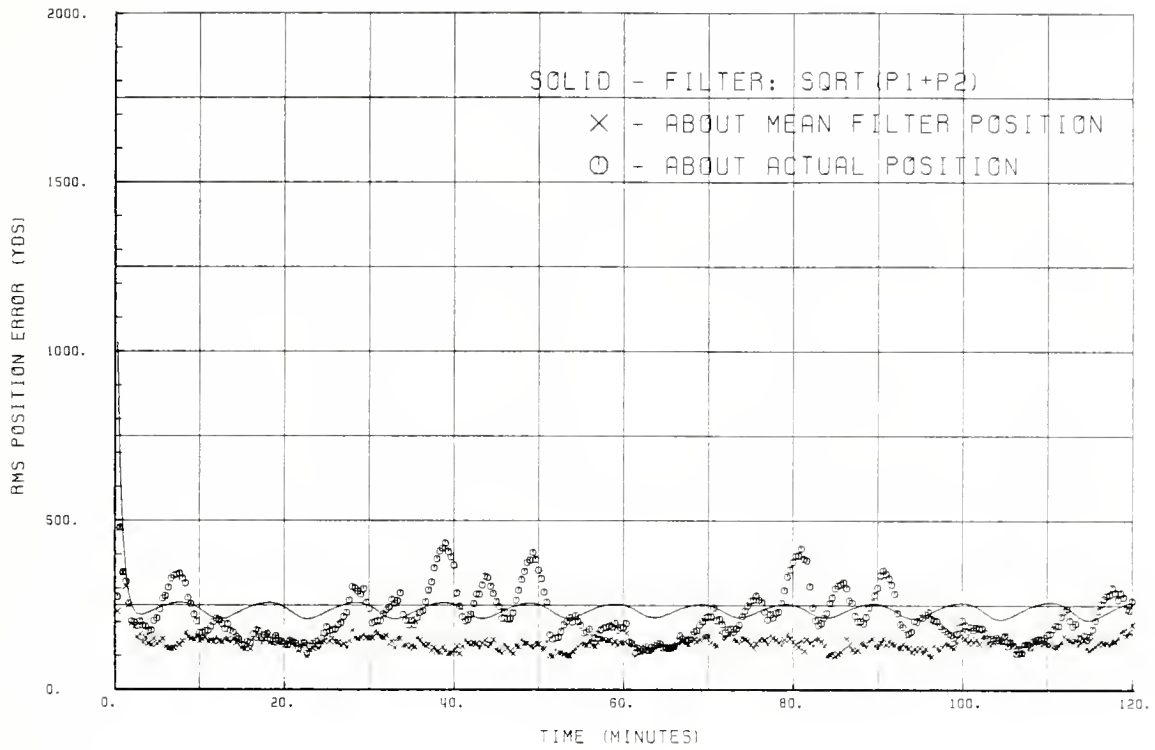


Figure 38. RMS errors for two-state system (top) and six-state system (bottom) using circular pattern at 5 NM.

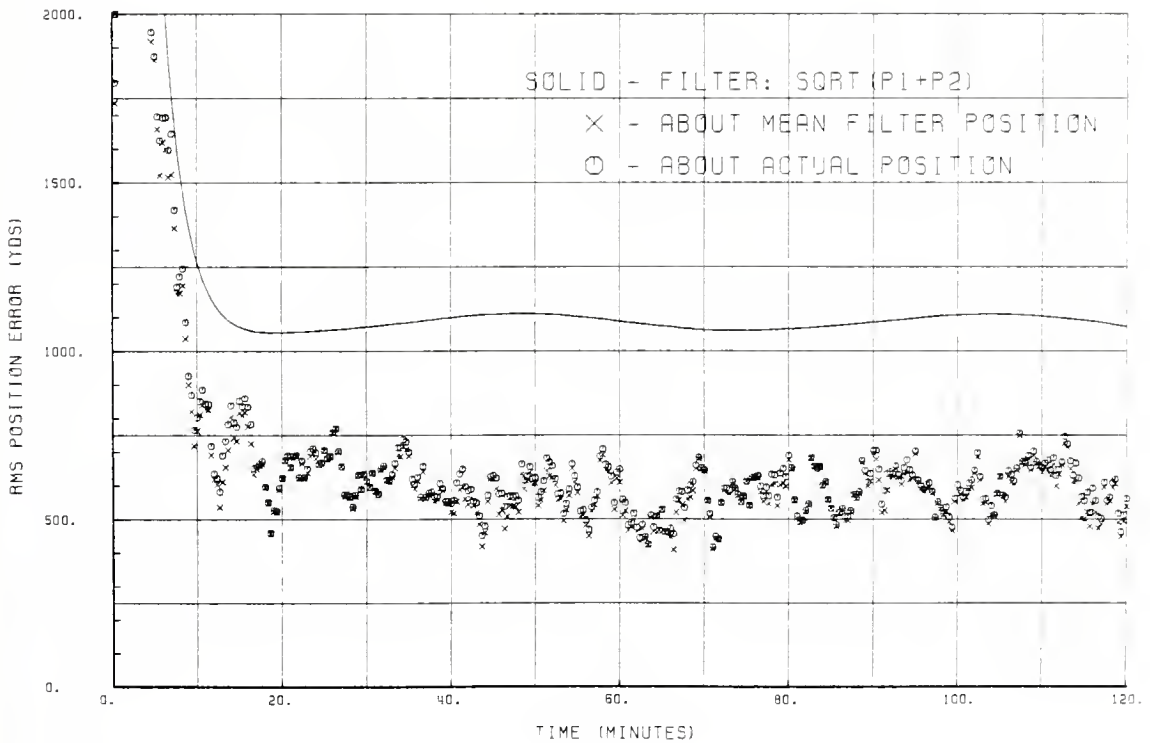
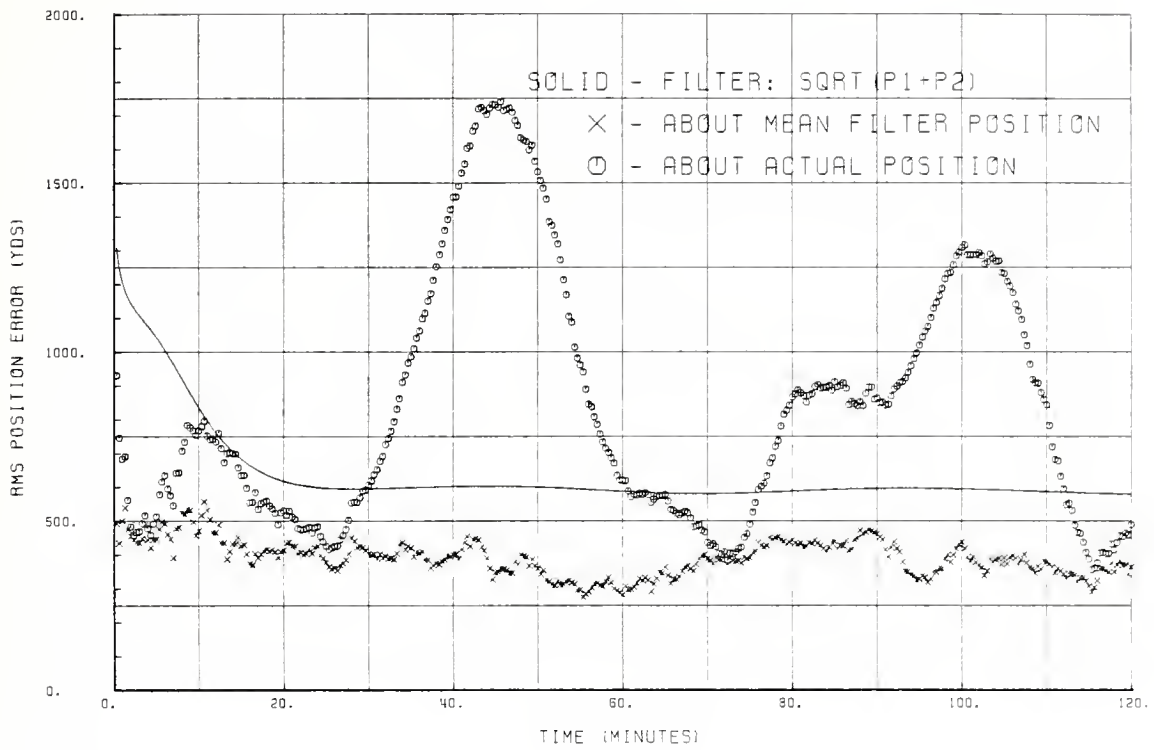


Figure 39. RMS errors for two-state system (top) and six-state system (bottom) using circular pattern at 30 NM.

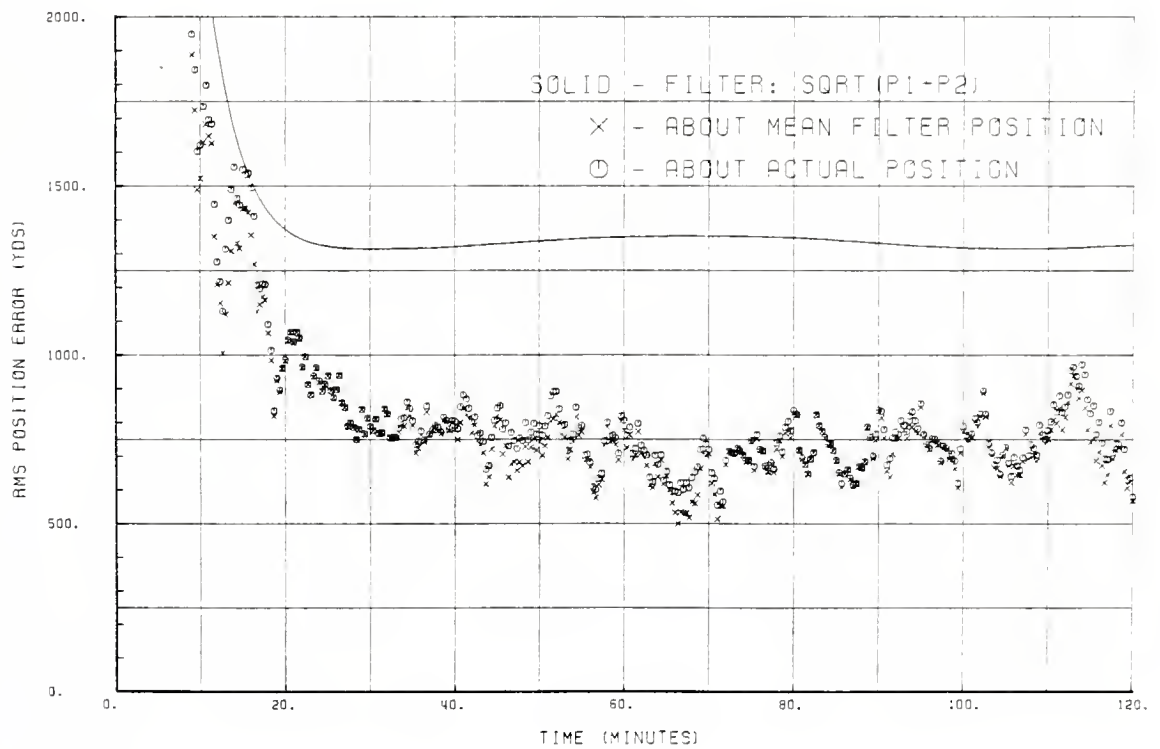
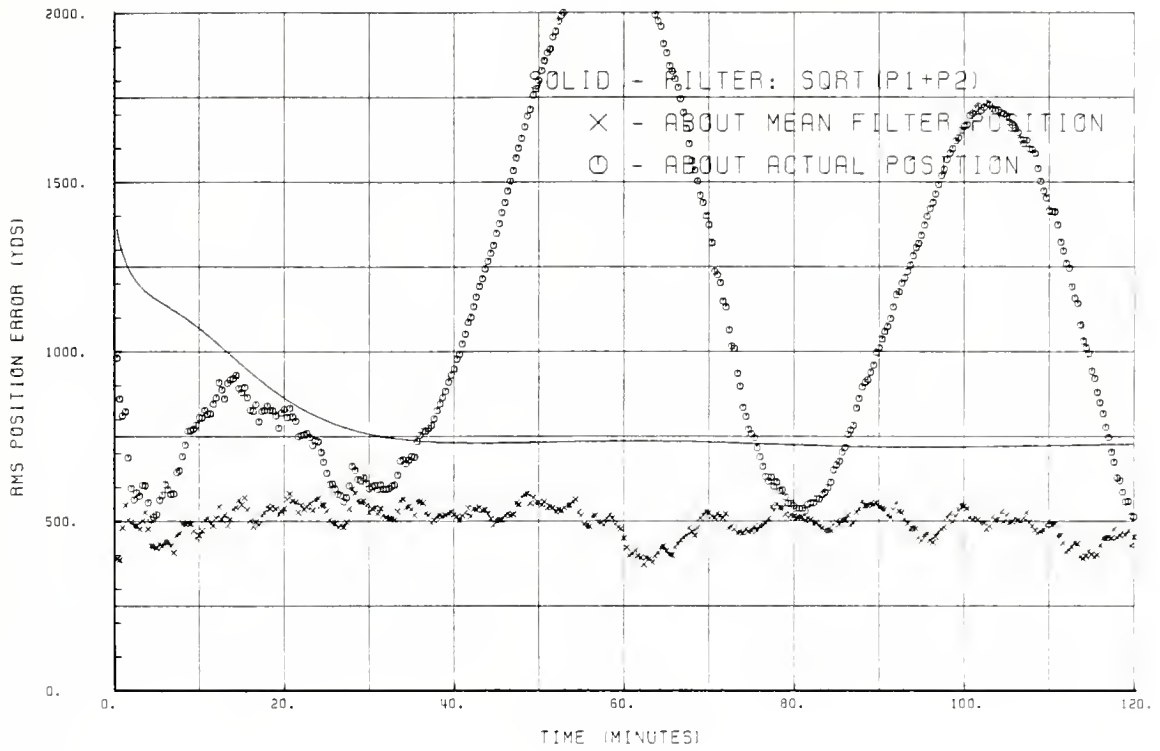


Figure 40. RMS errors for two-state system (top) and six-state system (bottom) using circular pattern at 45 NM.

Frequency Analysis

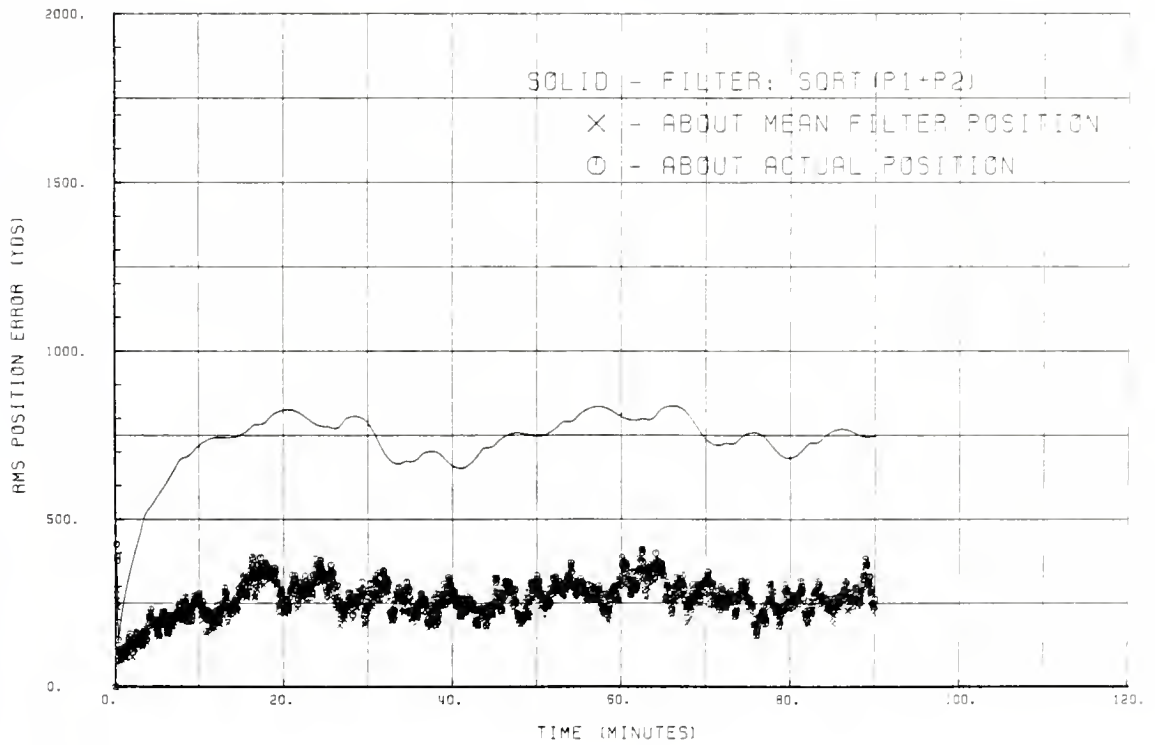
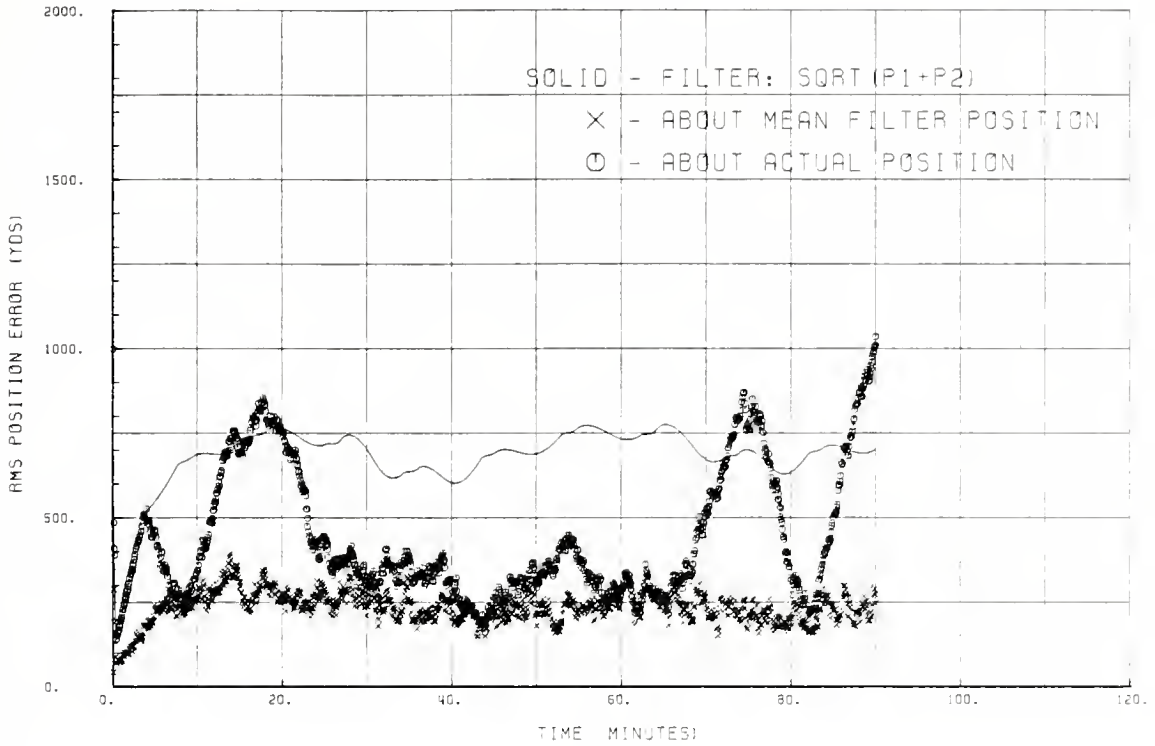


Figure 41. RMS errors for two-state system (top) and six-state system (bottom) using square pattern with $t=4$ sec.

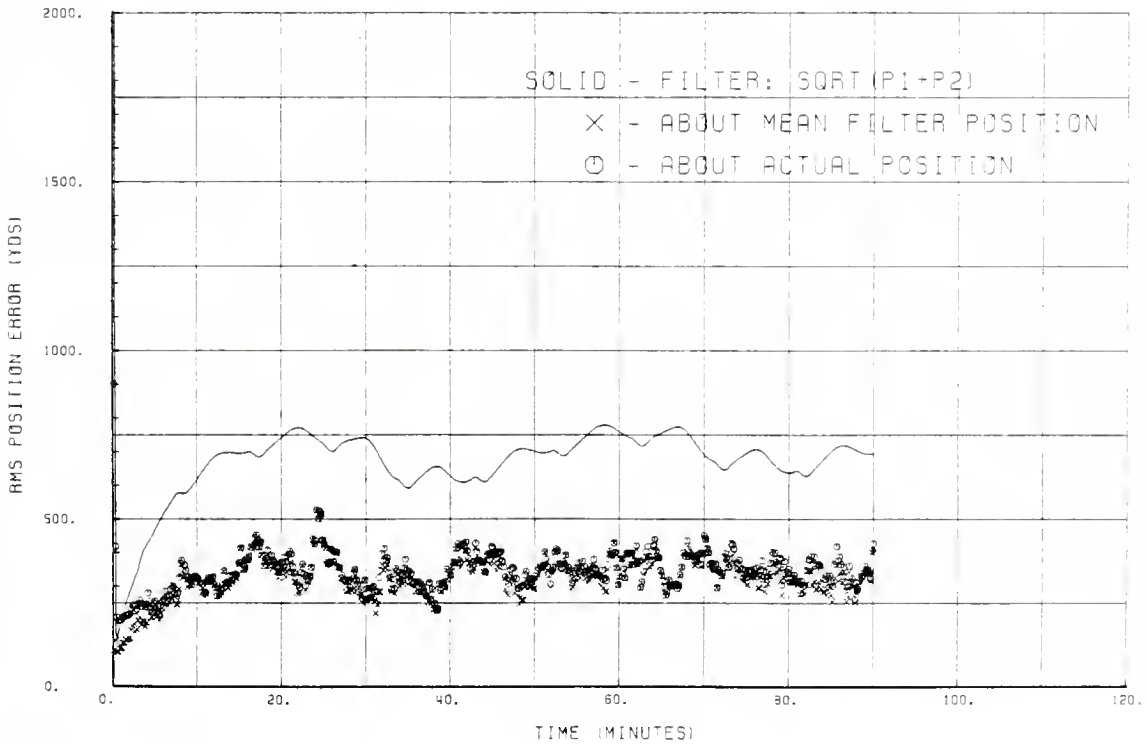
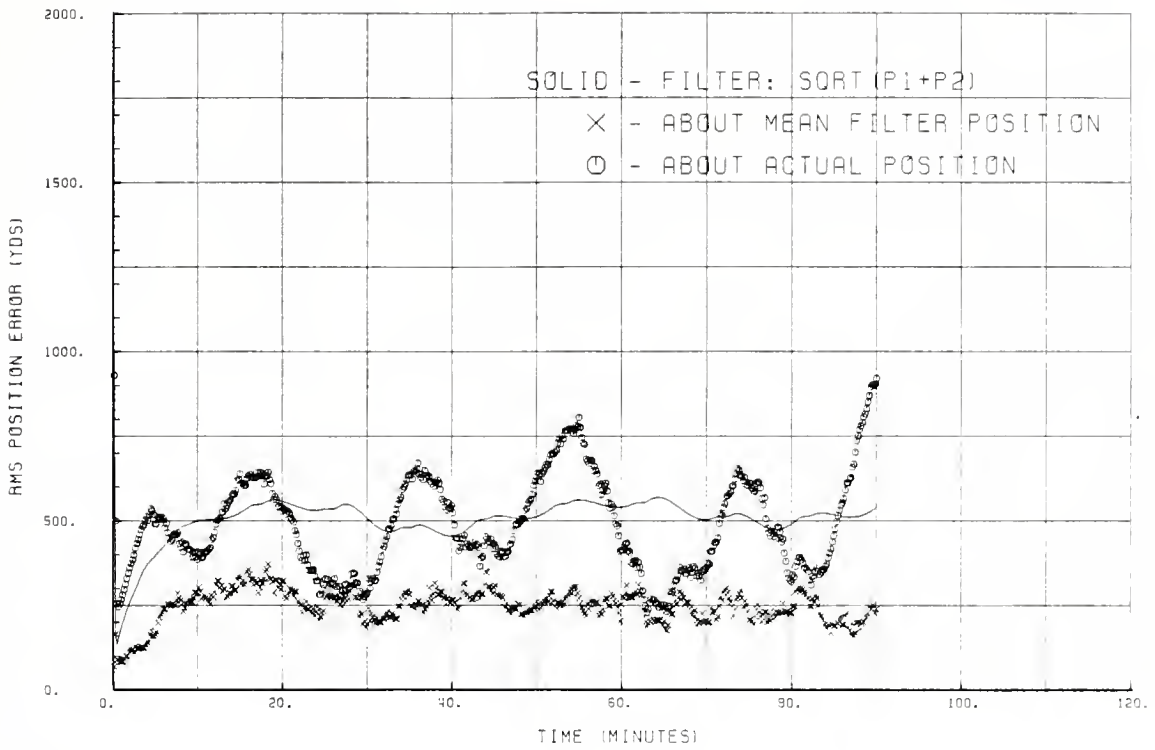


Figure 42. RMS errors for two-state system (top) and six-state system (bottom) using square pattern with $t=10$ sec.

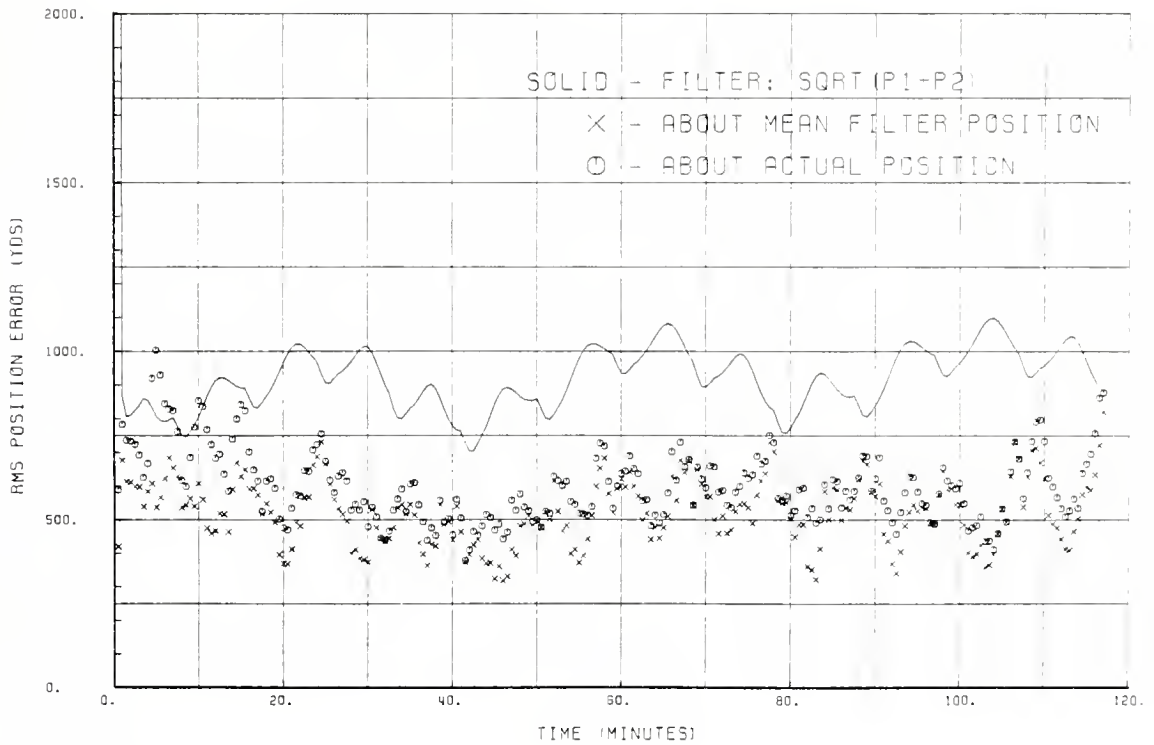
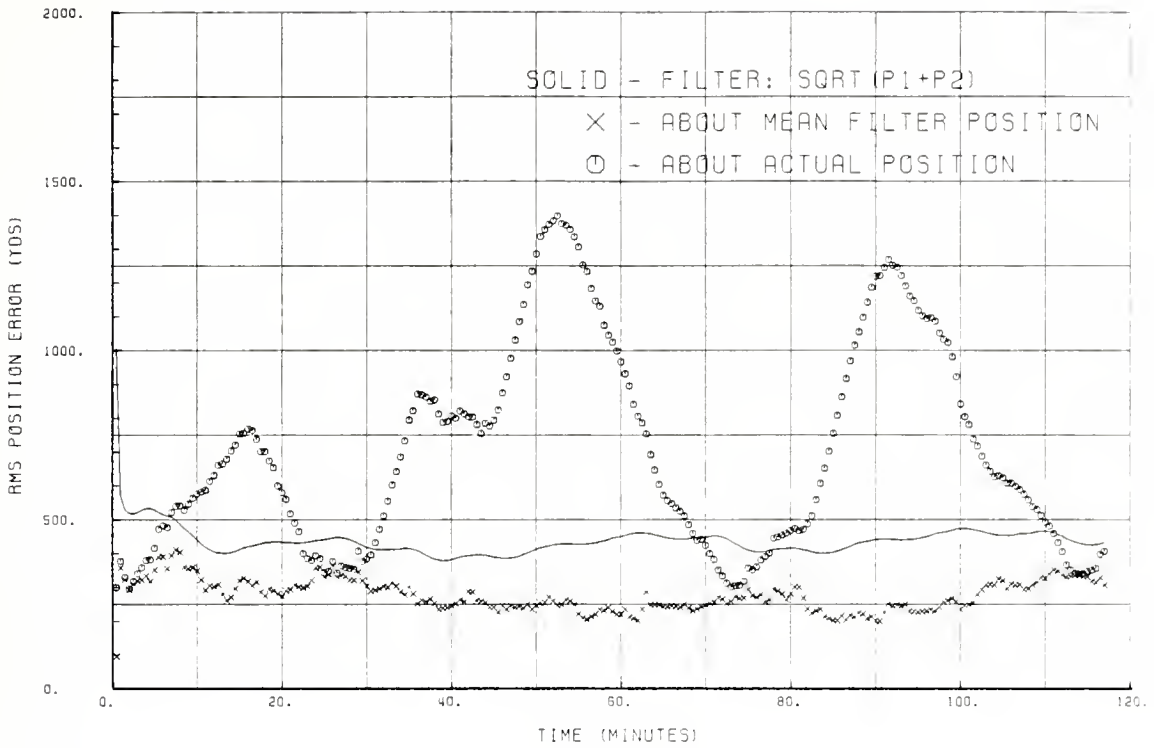


Figure 43. RMS errors for two-state system (top) and six-state system (bottom) using square pattern with $t=30$ sec.

Altitude Analysis

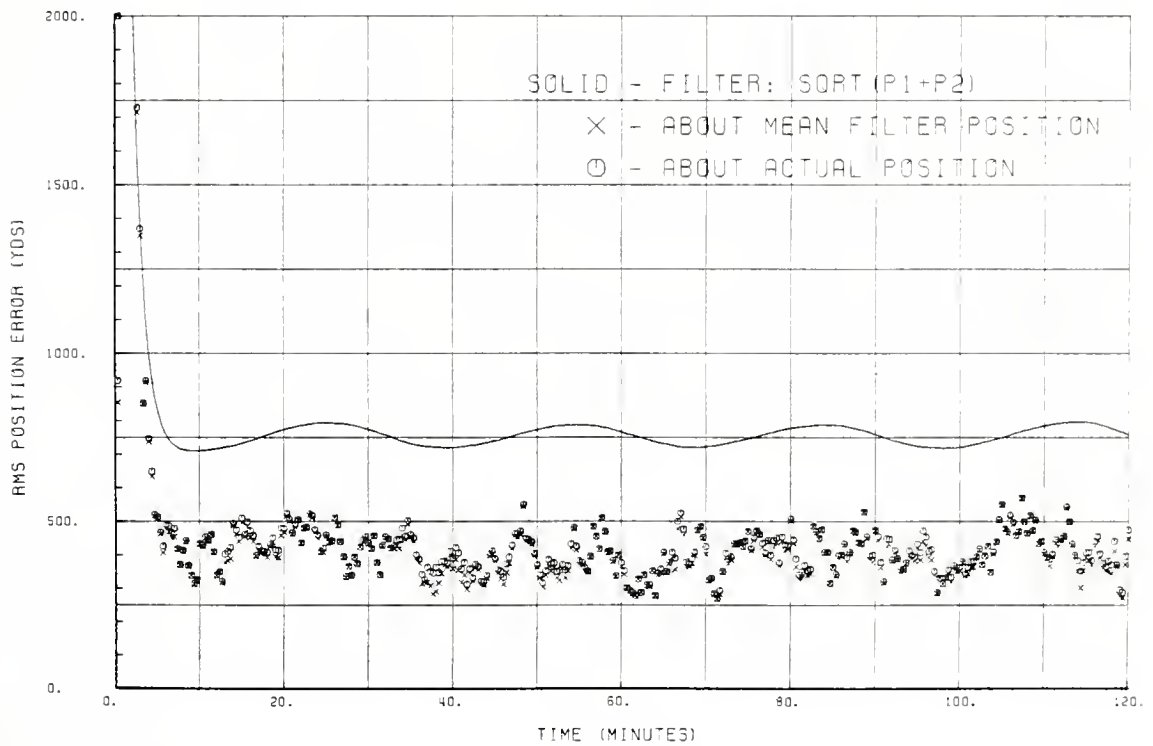
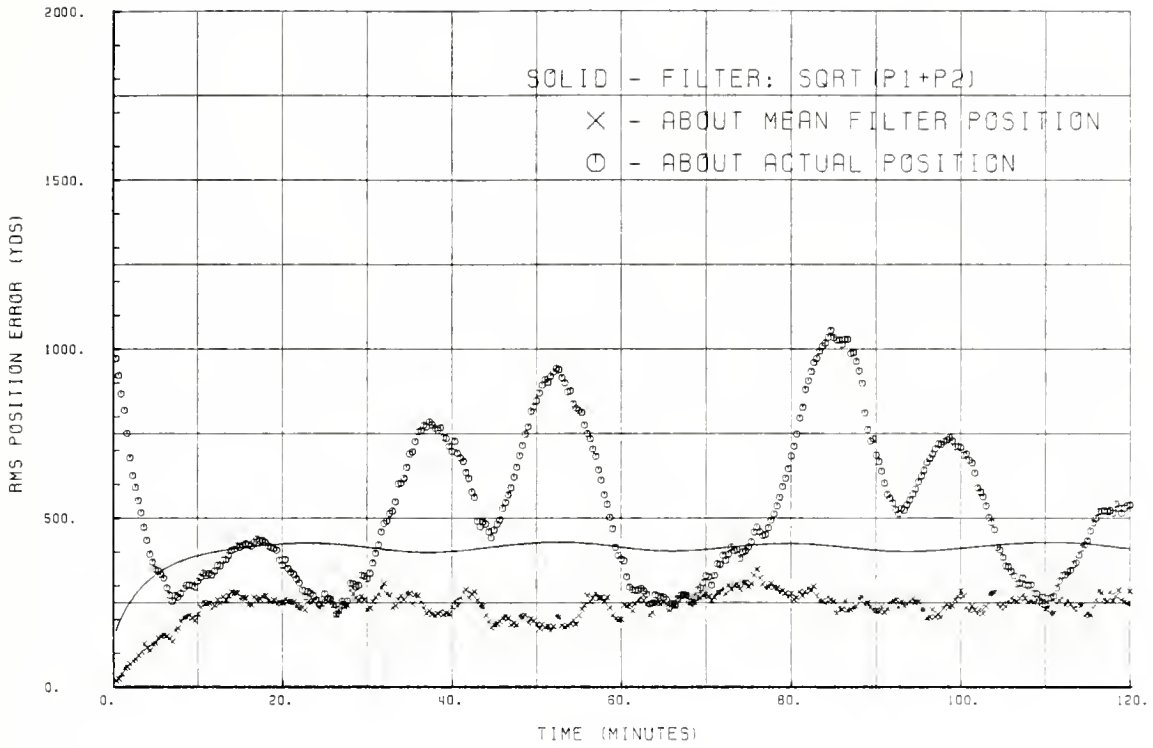


Figure 43. RMS errors for two-state system (top) and six-state system (bottom) using circular pattern, Alt=300'.

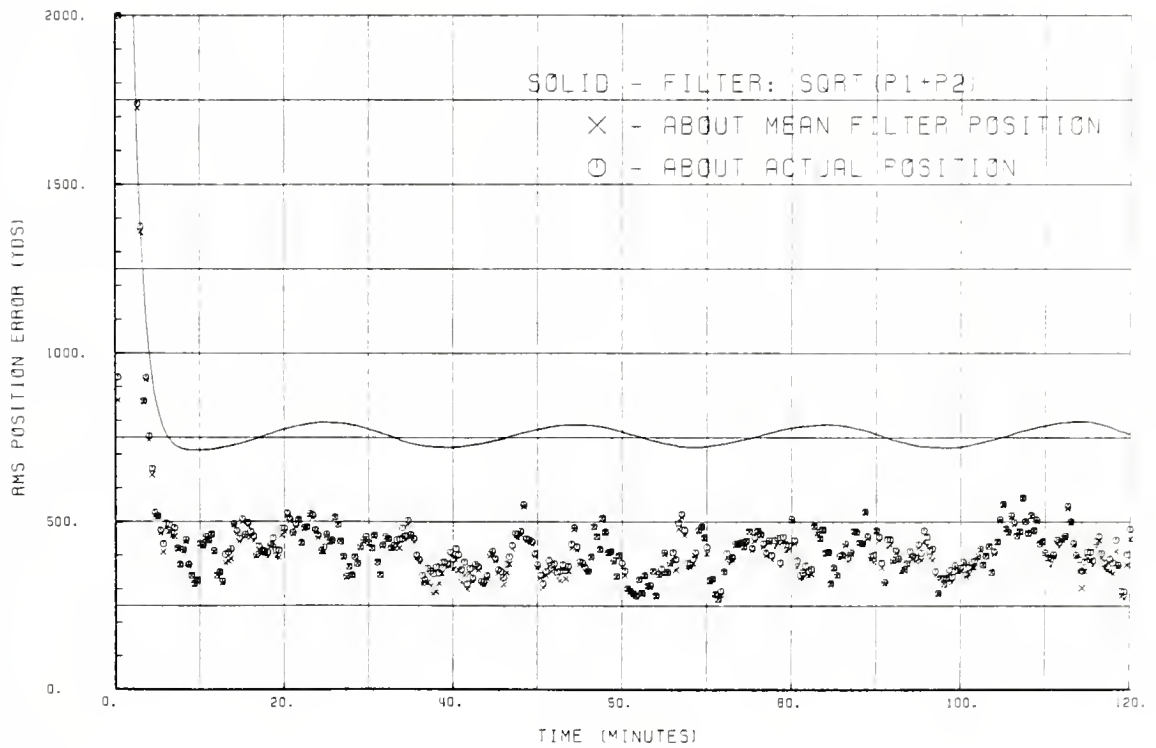
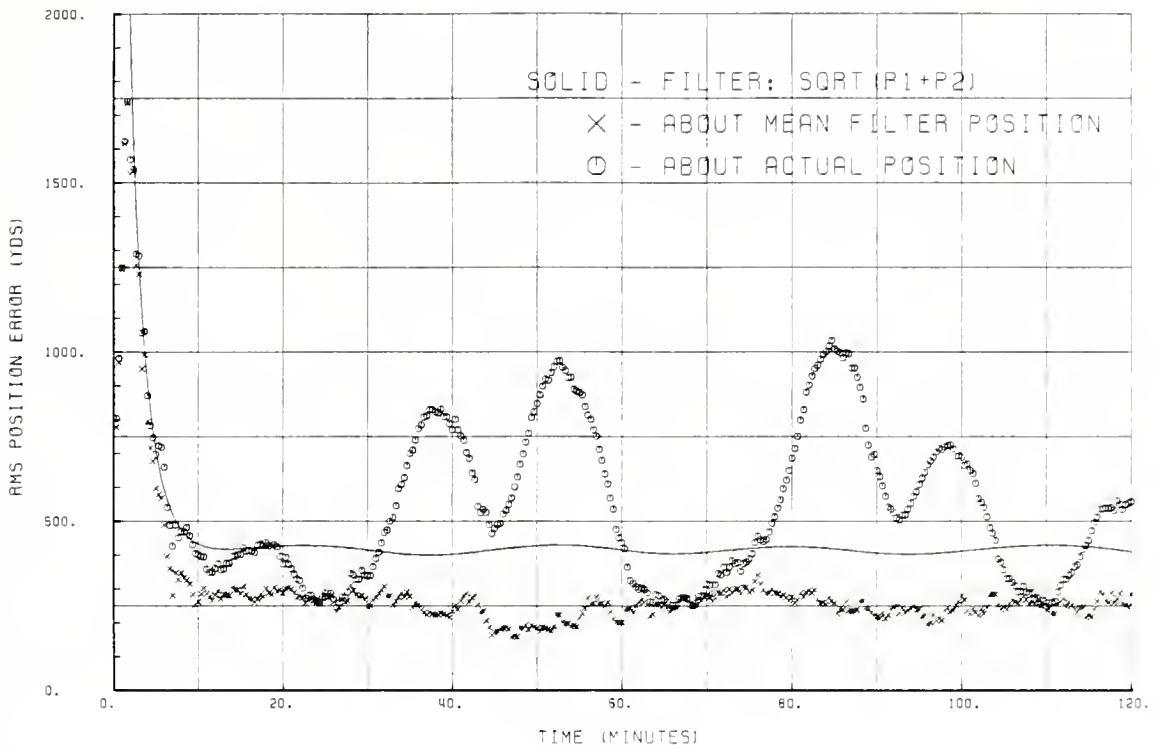


Figure 45. RMS errors for two-state system (top) and six-state system (bottom) using circular pattern, Alt=10,000'.

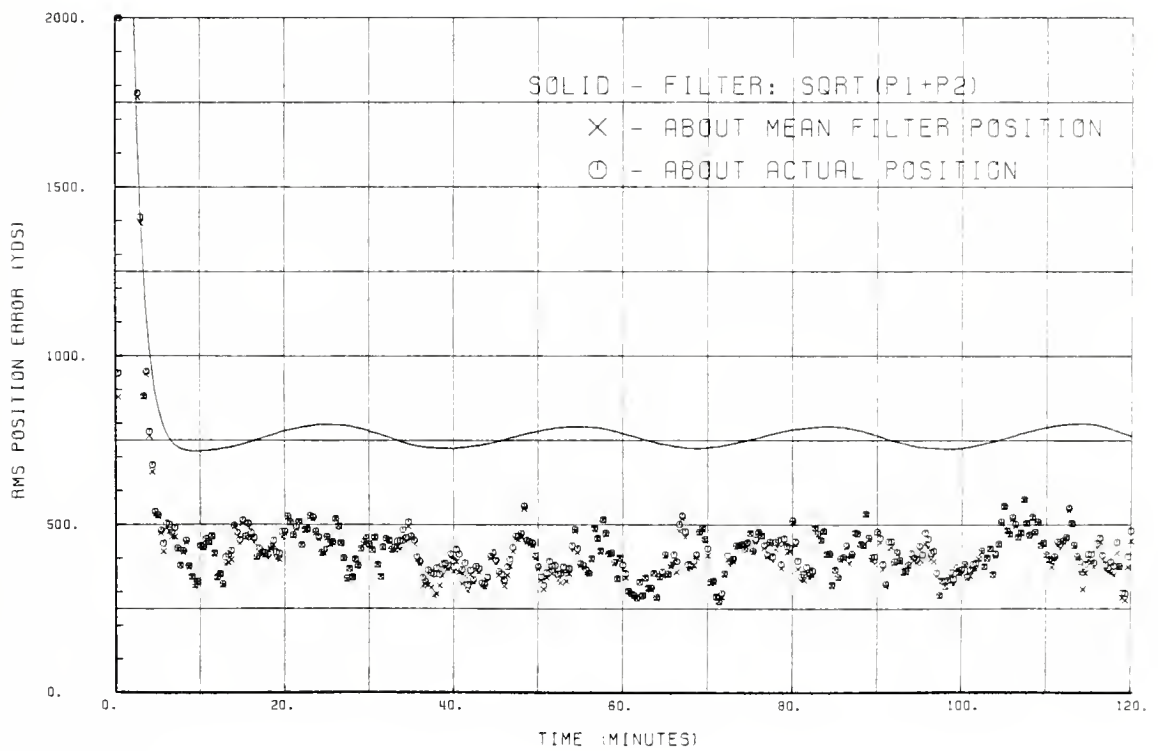
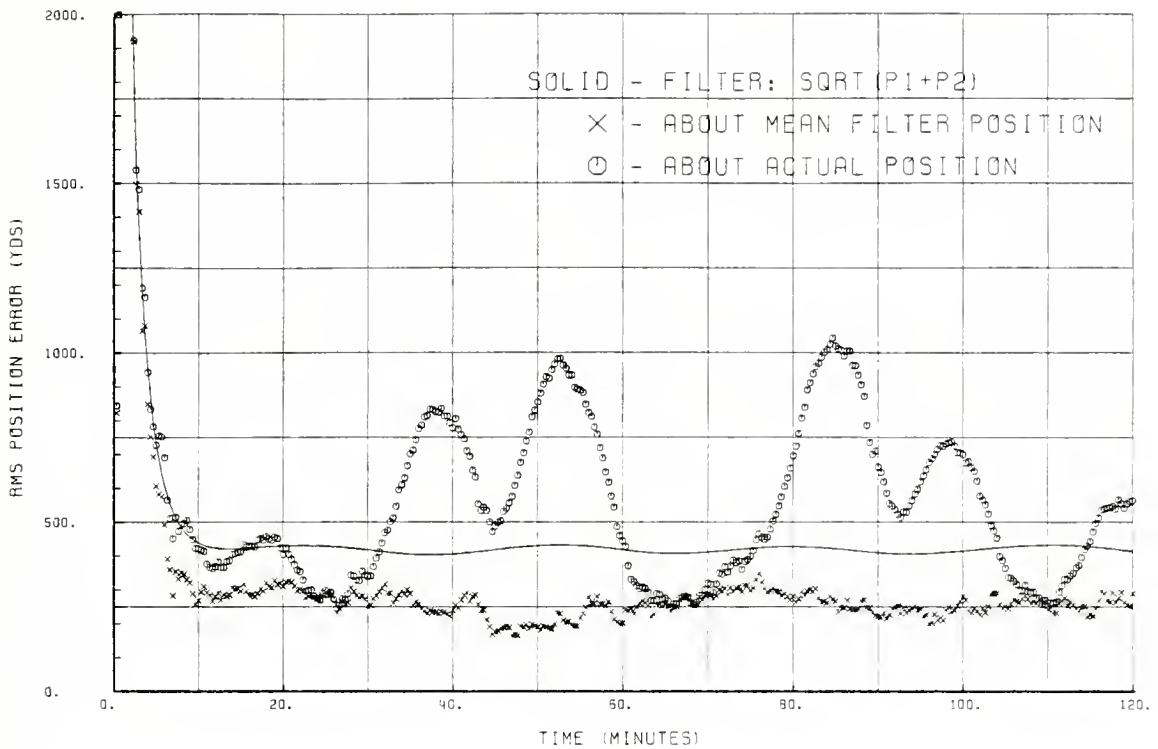


Figure 46. RMS errors for two-state system (top) and six-state system (bottom) using circular pattern, Alt=20,000'.

BIBLIOGRAPHY

- Bryson, Jr., A. E. and Yu-Chi Ho, Applied Optimal Control, Hemisphere Publishing Corp. 1975.
- Carlson, N. A., Fast Triangular Formulation of the Square Root Filter, Vol. II, No. 9, AIAA Journal, September 1973.
- Demetry, J. S., Notes on the Theory and Applications of Optimal Estimation, Naval Postgraduate School, Monterey, California 1970.
- Gelb, A. and others, Applied Optimal Estimation, M.I.T. Press 1974.
- Leondes, C. T. Editor, Control and Dynamic Systems, Vol. 12, Academic Press, 1976.
- Orincon Corporation Report OC-R-78-A003-1 Sonobuoy Reference System, by Asher, R. M., Judge, R., and Sorenson, H. W., December 1978.
- System Functional Description for Sonobuoy Reference System, FD-17 (I 4.3), Naval Air Development Center, June 1978.
- System Functional Description for Navigation, FD-9 (I 3/4.2) Naval Air Development Center, November 1977.

INITIAL DISTRIBUTION LIST

	No. Copies
1. Defense Documentation Center Cameron Station Alexandria, Virginia 22314	2
2. Library, Code 0142 Naval Postgraduate School Monterey, California 93940	2
3. Department Chairman, Code 62 Department of Aeronautics Naval Postgraduate School Monterey, California 93940	1
4. Prof. D. J. Collins, 67Co Department of Aeronautics Naval Postgraduate School Monterey, California 93940	3
5. LT N. M. Brownsberger 3802 La Miranda Pl Pittsburg, California 94565	2
6. Dr. D. Birnbaum, Code 2031 Naval Air Development Center Warminster, Pennsylvania 18974	1

Thesis 184310
B8243 Brownsberger
c.1 Estimation of
sonobuoy position
relative to an aircraft
using extended kalman
filters.

10 JUN 91

57778

Thesis 184310
B8243 Brownsberger
c.1 Estimation of
sonobuoy position
relative to an aircraft
using extended kalman
filters.

thesB8243

Estimation of sonobuoy position relative



3 2768 002 08054 1

DUDLEY KNOX LIBRARY